COLLISION COMPLEXES OF INTERMEDIATE LIFETIME

by

Suresh Chandra Khandelwal

A Dissertation Submitted to the Faculty of the

DEPARTMENT OF CHEMISTRY

In Partial Fulfillment of the Requirements
For the Degree of

DOCTOR OF PHILOSOPHY

In the Graduate College

THE UNIVERSITY OF ARIZONA

1 9 7 4

THE UNIVERSITY OF ARIZONA

GRADUATE COLLEGE

I hereby recommend that this dissertation prepared under my direction by SURESH CHANDRA KHANDELWAL

entitled Collision Complexes Of Intermediate Lifetime.

be accepted as fulfilling the dissertation requirement of the degree of Doctor Of Philosphy

Walter B. Miller III — Dissertation Director

10 Jan 1974 — Date

After inspection of the final copy of the dissertation, the following members of the Final Examination Committee concur in its approval and recommend its acceptance:*

W. R. Salzman	15 Jan 74
G. K. Vemulapalli	15 Jan 74
M F Bunker	15 Jan 74
Anton Fenander	Jan 15th 1974

*This approval and acceptance is contingent on the candidate's adequate performance and defense of this dissertation at the final oral examination. The inclusion of this sheet bound into the library copy of the dissertation is evidence of satisfactory performance at the final examination.

STATEMENT BY AUTHOR

This dissertation has been submitted in partial fulfillment of requirements for an advanced degree at The University of Arizona and is deposited in the University Library to be made available to borrowers under rules of the Library.

Brief quotations from this dissertation are allowable without special permission, provided that accurate acknowledgment of source is made. Requests for permission for extended quotation from or reproduction of this manuscript in whole or in part may be granted by the head of the major department or the Dean of the Graduate College when in his judgment the proposed use of the material is in the interests of scholarship. In all other instances, however, permission must be obtained from the author.

SIGNED: Suresh C. Khandelwal

ACKNOWLEDGMENTS

The author wishes to express his sincere appreciation and gratitude to Dr. Walter B. Miller, his dissertation director, for his patience, encouragement, and guidance throughout his doctoral program; and to the other members of his committee, Drs. W. R. Salzman, G. K. Vemulapalli, M. F. Burke, and Q. Fernando, whose assistance and support was always readily available.

The author is grateful to his colleague, Gary Pippin, for his suggestions during these studies.

The author wishes to express his admiration and appreciation to Kusum, his wife, whose enthusiasm, patience, and inspiration made completion of this manuscript possible. To her and to our children this work is dedicated.

The financial support received from the Department of Chemistry through research and teaching assistantships, from The University of Arizona through a predoctoral fellowship, and from the Office of Coordinator of Research during the past four and a half years is gratefully acknowledged.

To these and all others who supported him in this work, the author is grateful.

TABLE OF CONTENTS

TABLE OF CONTENTS--Continued

LIST OF ILLUSTRATIONS

LIST OF ILLUSTRATIONS--Continued

LIST OF ILLUSTRATIONS--Continued

LIST OF TABLES

ABSTRACT

The crossed molecular beam reactions of barium with the chloride and iodide of potassium, and the chloride of cesium have been studied experimentally. The product alkali atoms in these reactions were detected with a Pt-W filament, surface ionization detector. We have shown that these reactions proceed through an osculating complex. Calculations of the total cross section and angular distribution of products in the reactions of barium with potassium chloride, potassium iodide, cesium chloride, and cesium iodide have been done on the basis of the statistical theory. Computer programs have been developed to implement these calculations and to transform them from the center of mass coordinate frame to the laboratory frame.

CHAPTER 1

INTRODUCTION

The crossed molecular beam investigations of bimolecular reactions offer the most direct means of studying the individual steps of chemical reactions. Following the first report by Datz and Taylor (1), a large number of reactions have been studied using this technique. Most of the reactions studied involve either an alkali atom or an alkali halide molecule as one of the reactants because of the availability of suitably sensitive detectors for these chemical species. Investigators have been able to explain a number of reaction mechanisms using this technique. For example, the intense luminescence from atomic sodium D-lines observed by Polanyi (2) in his classical studies of (Na,Cl_2) using diffusion flames has long provoked questions about its origin (3, 4). In this reaction the principal mechanistic question was whether the Na^* atoms come (a) directly from $Cl + Na_2 \rightarrow NaCl + Na^*$, or (b) indirectly from $Cl + Na_2 \rightarrow NaCl^\dagger + Na$, followed by $NaCl^\dagger + Na \rightarrow NaCl + Na^*$. Struve, Kitagawa, and Herschbach (5) showed that route (a) was responsible for the formation of Na^* atoms, by crossing beams of Na_2 and Cl atoms, and observing the chemiluminescence. Thus the main

advantage of the molecular beam technique is that it allows one to look at the reaction product after a single encounter of the reactants, thus providing information about the elementary processes of classical kinetics.

The reactions in the beams can be characterized by the lifetime of the intermediate complex which is formed during the reaction. If the intermediate complex has a lifetime greater or equal to five rotational periods, then the reaction intermediates are called long-lived complexes. If the intermediate complex has a lifetime less than or equal to one rotational period, it is called a short-lived complex. The intermediate cases where the lifetime is of the order of 2-3 rotational periods are generally referred to as osculating complexes. It has been observed that if the exothermicity of the reaction is large (say $\geq$ 20 kcal.) then these reactions belong to the short-lived category. If the exothermicity of the reaction is small ($\leq$ 6 kcal.) then they belong to the long-lived category. The short-lived complexes show either a forward peaking (stripping) or a backward peaking (rebound) with respect to one beam (say the atomic beam), whereas long-lived complexes show two peaks of the same intensity in the forward and backward region.

A qualitative criterion for the formation of a long-lived intermediate has been suggested by the RRK (6) formula which relates the lifetime of a collision complex,

τ, to the total available energy ϵ and the strength or well depth E^* of the complex by the expression

$$\tau \cong \tau_o \left(\frac{\epsilon - E^*}{\epsilon}\right)^{(1-s)}$$

where s is the number of "active" vibrational modes in the complex and τ, a characteristic vibrational period of $\sim 10^{-13}$ sec. Factors that increase E^* and s will tend to favor formation of long-lived intermediates while increased ϵ will decrease the lifetime of the collision complex. ϵ is directly related to ΔD^o, the difference in dissociation energies or exothermicity of the reaction. If the exothermicity is large, τ will be small. Generally it has been observed that with severe bonding changes in a reaction (for example covalent $\rightarrow$ ionic), the exothermicity is large, and complexes formed are short-lived (7). If the exothermicity of the reaction is small, the collision complexes formed will be long-lived. For the intermediate cases, where the lifetime of the complex is $\sim 10^{-12}$ sec., these reactions belong to the osculating category.

Not many reactions have been reported in the literature which belong to the osculating category. The characteristic angular distribution in such reactions is two peaks of different intensity in the angular distribution. The reactions of cesium with the chloride and iodide of thallium, reported by Fisk, McDonald, and Herschbach (8) belong to this category. Later, Kwei, Lees, and Silver (9)

reported another set of osculating complexes in the reactions of lithium with the fluoride and bromide of potassium. No further work has been reported in the literature on reactions whose exothermicity lies in the intermediate region and which have been characterized as belonging to osculating category. For this reason we have chosen to study the reactions of barium with the chlorides and iodides of potassium and cesium. The exothermicity of these reactions lies in the intermediate range, from 6.5 kcal. for Ba + CsI reaction to 14.5 kcal. for Ba + KCl reaction. Moreover, in order to estimate a reasonable value for the cross section of these reactions and the expected angular distribution of products, we have followed the statistical approach suggested by Pechukas, Light, and Rankin (10) and White and Light (11). The angular distribution of products predicted by this theory is in good agreement with the experimental results for the reactions which proceed via long-lived collision complexes (11). We have applied this theory to test whether it can be extended to explain the angular distribution of products of the reactions which belong to the osculating category.

Chapter 2 of this dissertation gives a description of the apparatus, devices used to obtain low pressures, ovens for the production of beams of the reactants, the surface ionization detector for the measurement of the signal, and experimental procedures.

Chapter 3 includes the kinematic analysis, some discussion of the conversion of data from the center of mass (CM) coordinate system to the laboratory (LAB) coordinate system and experimental results on the barium reactions. An attempt has been made to fit these experimental results (angular distribution of alkali atoms) with an assumed simple analytic function in the CM with three adjustable parameters.

Chapter 4 explains in fair detail the calculations of total reactive and non-reactive cross sections of these reactions on the basis of the statistical theory. It also discusses the dependence of the total cross section on initial vibrational energy, rotational energy, and relative translational energy of the reactants.

The formalism for the calculation of the angular distribution of products in the CM and conversion of these data to the LAB system has been developed in Chapter 5. Dependence of the differential cross section on vibrational energy and final translational energy are also described here in detail. The calculations have been carried out for four systems--the reactions of barium with KCl, KI, CsCl, and CsI.

Finally, Chapter 6 presents a brief discussion of the experimental results of these beam studies. It also compares the experimental results with those obtained from the statistical model.

CHAPTER 2

APPARATUS AND PROCEDURE

Experiments were performed by crossing beams of barium atoms and alkali halide molecules at right angles and observing the direction in which the molecules fly from the region of intersection. When molecules of one beam are deflected by collision with the molecules of the other beam, it is termed elastic scattering. Elastic scattering does not contribute to the chemical reaction. The chemically reactive scattering is given by the angular distribution of the product molecules formed in some of the collisions. The angular distribution of the products in reactive scattering provides the information regarding reaction cross section, the partitioning of the total available energy between internal (rotational and vibrational) and external (translational) degrees of freedom, and other details of the collision dynamics. The elastic scattering gives information about the inter-molecular forces between the colliding molecules, while reactive scattering helps one to understand the detailed mechanics of the chemical reaction.

Apparatus

The molecular beam apparatus consists of one vacuum chamber of thick pyrex glass. It has three large brass flanges on three sides to permit easy access to the equipment inside. The lower part of the vacuum chamber rests on a thick aluminum table.

The geometrical arrangement of this system is shown in Fig. 1. One of the flanges on the side of the chamber contains (a) an ion gauge for the measurement of pressure, (b) a support for the detector, and (c) a needle valve which is used to introduce small amounts of oxygen or propane into the vacuum chamber. To ensure that molecules in the beam collide only at the scattering center, it is necessary that the mean free path of the background gas be greater than the dimensions of the apparatus. To achieve this, pressure in the apparatus was maintained at $\sim 1 \times 10^{-6}$ torr. These pressures are far lower than those of the ordinary experiments in gas phase kinetics. The low pressure required was obtained by using an oil diffusion pump in combination with a mechanical pump and a liquid nitrogen baffle. These were connected to the lower part of the vacuum chamber.

Each of the two beams was formed by heating the substance in an oven and letting the vapor effuse out of a slit. These molecules were then collimated into a beam by a second slit. The two beams intersect at an angle of 90 degrees. The upper flange contains a rotatable lid, which

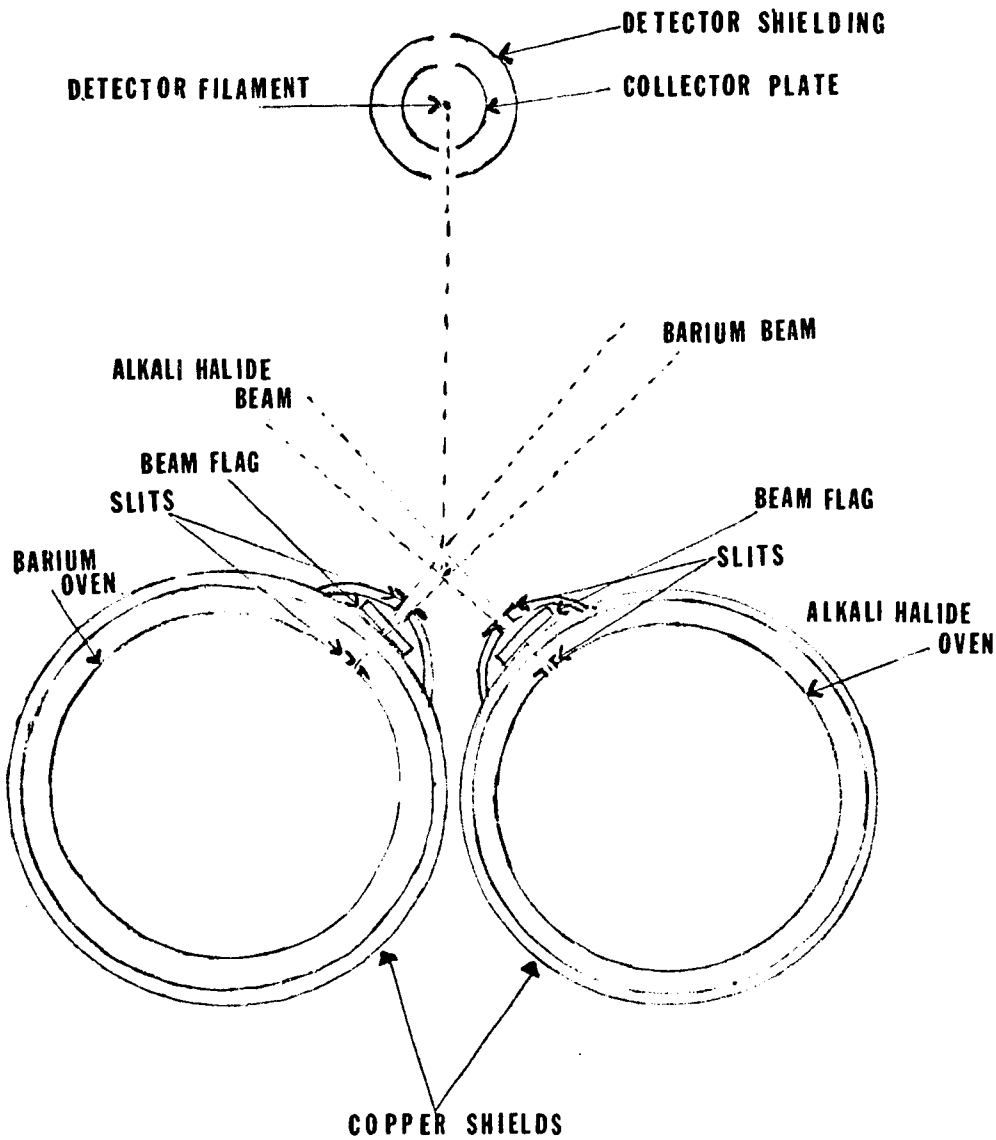

Fig. 1. Geometrical arrangement of the ovens and detector.

turns about an axis through the center of the interaction volume. The ovens were mounted on supports which were hung from the rotatable lid. The elastic and reactive scattering was observed at various laboratory angles, Θ, with a fixed detector, by rotating the ovens.

The molecules, which come out of the interaction volume, were measured with a surface ionization detector. The angular position of the lid was determined to within $\pm$ 1 degree by means of markings on the lid. The essential parts of the apparatus are described below.

Vacuum System

A vacuum of the order of 10^{-6} torr in the beam apparatus was produced by an oil diffusion pump (NRC VHS 6, 500 cc) backed by a mechanical pump (Welch Duo Seal Vacuum Pump Model 1397) and a liquid nitrogen baffle (NRC 316-6 Cryotrap). The pressure was monitored by a thermocouple gauge down to a pressure of 10^{-2} torr and by an ionization gauge (NRC 507) down to a pressure of 10^{-7} torr. The pressure from both the gauges was read on a NRC High Vacuum Gauge Control (NRC 831). Rubber O-rings were used as vacuum seals. The seal between the rotating lid and the top flange was a special Teflon O-ring, which allowed the rotating lid to turn smoothly in a low pressure system. These O-rings were well coated with high vacuum grease. To

make electrical contacts amphenol plugs were soldered to the flanges.

Ovens

Both ovens were made in a cylindrical shape from chemically resistant stainless steel. These ovens were closed by stainless steel lids of the same cross section. They were heated by passing a current through tantalum wire, insulated with ceramic rods. The tantalum wire passes through shafts drilled in the oven walls. Each oven position was fixed by placing it inside a copper shield. Two ceramic rods at right angles pass through the bottom of the copper shield and the bottom side of the oven to provide support for it. There were two slits, one outside the oven hole and the other outside the copper shield. Each slit was made from two thin pieces of stainless steel sheet. The copper shields were also cylindrical in shape, closed at the top and open at the bottom. Each copper shield was fused to a hollow copper tube in the top central part of the shield. These copper tubes supported the copper shield by the O-ring type vacuum seals on the rotating lid.

Cold water was circulated through these copper tubes continuously in order to keep the copper shields at a lower temperature than the oven. Two beam flags were provided outside the second slits, which were supported by O-ring type vacuum seals on the rotating lid. These flags were

manually controlled to close and open the second slit at the copper shield. The temperature was measured using a chromel-alumel thermocouple placed at the bottom of the oven and was read with a millivoltmeter. The alkali halide oven was heated directly with alternating current whereas the barium oven was heated with a direct current and was biased at + 9 volts in order to prevent electron emission, which otherwise leads to a large negative current as a background.

Detector

The molecules scattered out from the interaction volume in the direction of the detector were ionized by the surface ionization detector. In surface ionization the molecules and atoms strike the electrically heated metal filament and only those molecules and atoms of low ionization potential form positive ions. This allows an immediate discrimination against the background molecules of high ionization potential. These ions are collected and measured as a current.

The filament, made of 92% Pt- 8% W wire of .076mm diameter, is used as a differential surface ionization detector. The detector was constructed by spot welding the Pt-W wire to the two nickel wires which were electrically insulated from the collector by two ceramic rods. A stainless steel cylinder was placed around the wire which serves as a collector. This entire filament-detector was surrounded

by another stainless steel cylinder. Two rectangular openings were cut in these cylinders, one for allowing the beam to impinge on the filament and the other for allowing that part of the beam not intercepted by the wire to pass through the cylinders. These cylinders were kept at ground potential to protect the filament from external sources of noise.

This detector was used in two different modes to distinguish between elastically scattered alkali halides and alkali atoms formed in the reactive scattering. We have followed the technique suggested by Touw and Trishka (12). According to this technique the filament can be used in two conditions, one with a low work function which is termed a methanated mode and the other with a high work function which is termed an oxygenated mode. In the methanated mode the filament can ionize only alkali atoms whereas in the oxygenated mode the filament can ionize both alkali atoms and alkali halide molecules. In order to prepare the filament in the methanated mode, propane was admitted to the vacuum chamber by a variable leak to bring the pressure to 1-3 x 10^{-5} torr. The Pt-W filament is run at 2000^{o}K (0.35 amp). After some time the propane was shut off. This treatment gave a reproducible filament condition in which no alkali halide was detected. In our apparatus the normal mode is the methanated mode. For the oxygenated mode, oxygen was admitted to the vacuum chamber near the

filament by a needle valve and through a Tygon tubing to reach a pressure of 1-3 x 10^{-5} torr. The Pt-W filament is run at 0.35-0.40 amp. In order to maintain the oxygenated mode, oxygen must be continuously let into the chamber. This treatment gives a surface condition to the filament in which both alkali atoms and alkali halide molecules were detected. Thus we could use the same filament in two different modes to measure reactive as well as elastic scattering with good efficiency

The filament was biased to +30 volts which helped to repel the positive ions toward the surrounding stainless steel cylinder. The cylinder which surrounds the filament does not preferentially attract the positive ions but only intercepts them. The current formed by these ions, ~ 10^{-8} - 10^{-12} amp, was measured on an electrometer (Keithley 610 CR Solid State Electrometer). The filament was heated by the current (0.30-0.40 amp) from a regulated power supply (Lambda Solid State Power Supply Model LP 410 FM). The current was measured on an ammeter.

Experimental Procedure

One of the ovens was loaded with a solid piece of barium metal (supplied by Ventron Corporation, Alfa Products, Catalog #00038 Rod, 23mm., 99.5% pure) and the other with alkali halide crystals (CsCl, supplied by Kawecki Chemical Co., Lot 1061-119, HP; KCl, supplied by Matheson

Coleman & Bell, A.C.S. Reagent; KI, Baker Analyzed Reagent). They were sealed by tightening their lids with screws. A copper gasket was used between the lid and the oven to prevent leakage from the ovens at high temperature. It was found that the barium beam corrodes the copper gasket and that there was a large leakage of barium at that location. In order to check this leak the barium oven lid was replaced by a thick stainless steel cork-shaped lid, which was tightly screwed to the oven. These ovens were placed inside the copper shields. In order to prevent heat losses from the ovens, another internal heat shield was used. This was made of a thin shiny stainless steel sheet and was placed along inner walls of the copper shield. The lower part of the copper shield was covered with thin aluminum foil to prevent heat loss. Electrical connections were made for heating the ovens. All these adjustments were done outside the vacuum chamber.

After these preparations the top flange was put on the vacuum chamber. All the three flanges were sealed. The mechanical pump was then turned on. When the pressure reached 0.1 torr as measured on thermocouple gauge, the diffusion pump heater was turned on. It takes about 10-15 minutes to reach a pressure of 10^{-5} torr. A current of $\sim$ 2 amp was passed through the oven heaters and the entire apparatus was left for 14-16 hours for getting rid of any adsorbed gases in the ovens.

After 14-16 hours liquid nitrogen was added to the baffle to bring the pressure down into 10^{-6} torr range. The current in the ovens was increased gradually by increasing the voltages in steps of 2-3 volts and allowing the ovens to thermalize at that temperature for about half an hour. This process was continued until the operating temperatures were attained. When pressure in the chamber reached about 10^{-5} torr, the current in the filament was turned on and set to a value of 0.3 amp.

When the operating temperatures of the ovens were reached, the filament was prepared in the oxygenated mode by introducing oxygen at a pressure of 5×10^{-5} torr. The filament was biased at -30 volts and the negative current in the electrometer was observed. The negative current gradually decreased and reached a small value $\sim 10^{-13}$ amp. The filament was then biased to +30 volts. The filament was now ready to measure the alkali halide beam signals. The parent alkali halide beam intensity was measured by bringing the alkali halide oven behind the detector and opening the flag. We tried to measure the barium beam intensity in the same way, but this always gave a small ion current due to the poor response of the detector toward barium atoms. We could, however, see a small attenuation in the parent alkali halide beam signal by opening the barium beam flag. The alkali halide beam signal was usually $\sim 10^{-8}$ amp. The oxygen flow was stopped and

propane was introduced in the chamber to convert the filament to the methanated mode. In this mode the negative current increases and reaches a value of ~ 10^{-7} amp. All measurements in the methanated mode were taken by biasing the filament at +30 volts and by setting the current at 0.30 amp.

In these experiments a "signal" is the difference in the collector ion currents (a) and (b), where (a) is the sum of the ion currents read (i) when both flags are open and (ii) when both flags are closed, and (b) is the sum of the ion currents contributed by individual beams of alkali halide and barium.

The first angular scan was done in the methanated mode at intervals of 5° from -20° to 110°. At each angle the ion currents were measured with the four combinations of the two flags: (a) both flags open, (b) only barium beam flag open, (c) only alkali halide beam flag open, and (d) both flags closed. These currents were recorded twice at each of the combinations of the flags. Data recorded at 45° were taken as reference. Between the readings at two different angles, a reading at the reference point was recorded. This was done to normalize the data taken at different times. The drift with time of this normalization signal was used to correct the data for slow changes in beam intensities due to the temperature drifts of the ovens. This signal measures only alkali atoms formed in reactive

scattering. After finishing the measurements in the methanated mode, the filament was prepared in the oxygenated mode. The signal was recorded again in a similar way. This signal gives a measure of alkali atoms and alkali halide molecules. The elastic scattering data found were not very interesting, probably due to wide oven slits and we have made no attempt to make the slit width small to obtain good elastic scattering data.

CHAPTER 3

ANALYSIS

A chemical reaction of the type

$$A + BC \longrightarrow AB + C$$

where A, B, and C can be atoms or molecules, when studied in the gas phase by conventional bulb techniques, is characterized by its rate constant. Moreover one can predict whether this reaction will occur or not for a given set of conditions from thermodynamics. However, these studies do not show any dependence on the internal state (characterized by its rotational quantum number and vibrational quantum number) of an individual molecule. The rate constant measured by conventional techniques is actually the superposition of all microscopic events which lead to a chemical reaction. Each reactant molecule in the reaction vessel is possibly in a different internal state and accordingly, it will react differently. The crossed molecular beam technique allows the observation of the product after a single reactive collision. One can in principle consider this reaction as

$$A(j) + BC(k) \longrightarrow AB(\ell) + C(m)$$

where j,k,ℓ,m characterize the internal state of the

molecule concerned. Since these reactions take place through collision, the reaction is also dependent on the relative velocity V. One expects a given initial system $(V_i,j,k,...)$ to lead to many final states $(V_f,\ell,m,...)$. It is possible to analyze the states of the product molecules generated in collisions of reactants in selected states. However, in the experiments discussed here there is no internal state selection or analysis. Therefore it is necessary to work with distributions over states. Furthermore, the direction of the initial relative velocity V_i can be taken as fixed, by defining a kinematic coordinate system and the final relative velocity V_f measured with respect to it. Thus, after summing over final states and averaging over the initial states, we characterize the dynamics of a chemical reaction by a distribution function $I_{V_i}(V_f)$. Thus $I_{V_i}(V_f)\, dV_f$ gives the probability of finding the products between velocities V_f and $V_f + dV_f$ for an initial velocity V_i.

A primary aim in reactive scattering experiments is the determination of the angular distribution of products and partitioning of the total available energy in the product molecules. In order to analyze the experimental results, we require a center of mass (CM) distribution function. If a CM distribution is assumed, it may be transformed to the laboratory (LAB) coordinate system by averaging over initial experimental conditions.

Entemann (13) has developed a stochastic approach to obtain a CM distribution consistent with experimental data. The relationship (13, 14) between various quantities in the CM system to those in the LAB system can be easily derived by a Newton diagram (Fig. 2). This is a vector diagram in which V_A and V_{BC} represent the parent beam velocities, γ their angle of intersection, C the velocity of their center of mass, O the origin in the LAB system, and c the origin in the CM system. Θ is the angle at which product recoils after collision in the LAB system whereas in the CM system the product recoils at an angle θ with a velocity u. Thus a point (v, Θ) in the LAB space corresponds to (u, θ) in the CM space.

If we consider the distribution of products in the center of mass system then the distribution function takes the form $I_{V_i}(u)$ or $I_{E_i}(u)$ which characterizes the reaction. E_i is the initial translational energy and is proportional to V_i^2. Since the product is measured as a function of angle θ, we have $I_{E_i}(u, \theta)\, du \sin\theta\, d\theta$ as the probability that product will recoil in the CM system at an angle between θ and $\theta + d\theta$ and at a velocity between u and u+du. Since all these experiments involve non-velocity selected beams, there is a distribution in E_i which must be taken into account for the probability distribution, so that the probability density will become $I(u, \theta, E_i)$. In order to get a function $I(u, \theta)$ we must consider the velocity

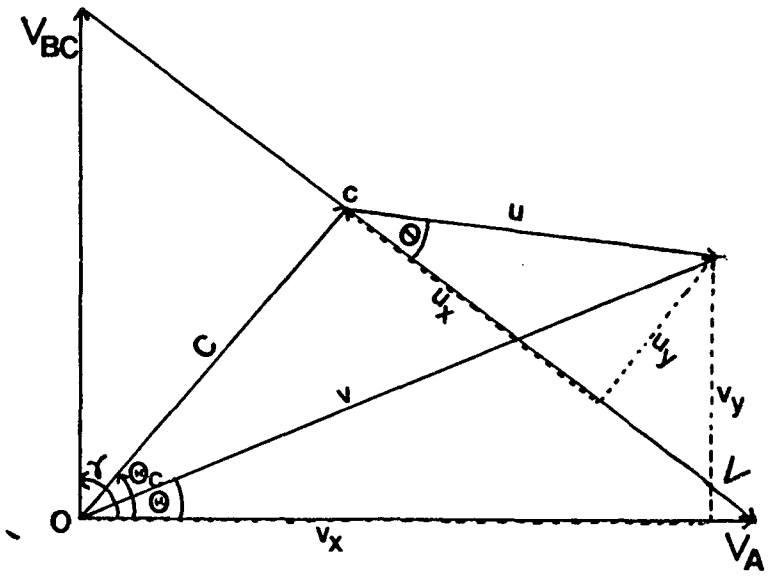

for $\gamma = 90^{o}$

$$\Theta_c = \tan^{-1} \left(\frac{m_{BC}V_{BC}}{m_A V_A}\right)$$

$$C = \frac{(m_A^2 V_A^2 + m_{BC}^2 V_{BC}^2)}{m_A + m_{BC}}$$

$$V = (V_A^2 + V_{BC}^2)^{\frac{1}{2}}$$

$$u_x = \frac{v_x V_A - v_y V_{BC} + V_{BC}^2}{V} - \frac{m_A \cdot V}{m_A + m_{BC}}$$

$$u_y = \frac{v_x V_{BC} + v_y V_A - V_A V_{BC}}{V}$$

Fig. 2. Newton diagram representing kinematics of reaction A + BC $\longrightarrow$ Products.

averaged distribution

$$I(u, \theta) = \int I(u, \theta, E_i)\ P\ (E_i)\ dE_i.$$

Now we are left with a CM distribution $I(u, \theta)$. This is called the CM differential cross-section and is the most important parameter in characterizing the dynamics of a chemical reaction. This can be correlated with a LAB distribution $I(v, \Theta)$. The kinematic analysis is used to correlate these two functions.

$$I_{LAB}(v, \Theta) \longleftrightarrow I_{CM}(u, \theta).$$

Kinematic Analysis

The kinematic analysis, which is based solely on conservation laws, gives results that are independent of the model used to describe the reaction dynamics.

The Conservation of Energy

Let E_i, E_f denote the kinetic energies of the relative motion of the reactants and the products, respectively, and W, W' the internal energies of the reactants and products. If ΔD_o denote the difference in the dissociation energies of AB and BC (measured from zero point level) then the total energy, E, is given by

$$E = E_i + W + \Delta D_o$$

$$= E_f + W'$$

where

$$E_i = \frac{1}{2} \mu_i V_i^2$$

and

$$E_f = \frac{1}{2} \mu_f V_f^2.$$

V_i and V_f are the initial and final relative velocities, μ_i and μ_f are the initial and final reduced masses of the atom-diatomic systems.

The Conservation of Intensity

The intensity of the product beam is measured in the LAB system. The transformation for the intensities in the CM system or vice versa, is determined by the following equations.

All the particles which emerge in a specified element $du\ d\omega$ in the CM system appear in the corresponding element $dv\ d\Omega$ in the LAB system; i.e., flux of particles must be conserved (particles can not be created or destroyed). This requires for the in-plane case

$$I_{LAB}\ (v, \Theta)\ dv\ d\Omega = I_{CM}\ (u,\ \theta)\ du\ d\omega \qquad (3.1)$$

where $d\Omega$, $d\omega$ are the solid angle elements in the LAB space and in the CM space, respectively. Since the LAB and CM systems are related by a linear transformation, the differential volume elements corresponding to these solid angle elements must be equal;

$$v^2 \, dv \, d\Omega = u^2 \, du \, d\omega. \qquad (3.2)$$

On combining equations (3.1) and (3.2), we get

$$I_{LAB}(v, \Theta) = I_{CM}(u, \theta) \frac{v^2}{u^2} , \qquad (3.3)$$

as the relationship between LAB and CM intensities. The factor v^2/u^2 is referred to as the "Jacobian" for the CM $\longrightarrow$ LAB transformation (13). The Jacobian is often a dominant factor in the kinematic analysis of the reactive scattering and strongly weights the scattering at small recoil velocities.

In the derivation of equation (3.3), it is assumed that there is a continuous distribution of CM recoil velocities u. It can be easily shown that for the case in which the product CM velocity is fixed, e.g., elastic scattering, the proper Jacobian becomes (15)

$$v^2/[u^2 \cos(u,v)].$$

Since there is a distribution in CM points (u, θ) due to the distribution in parent beam velocities that can contribute to intensity at a LAB point (v, Θ), equation (3.3) must be averaged over the distribution of beam velocities. Under our conditions the proper expression relating the observed intensity at (v, θ) to the CM intensity is

$$I_{LAB}(v, \Theta) =$$

$$\int_0^\infty dV_A \int_0^\infty dV_{BC}\; n_A(V_A)\; n_{BC}(V_{BC})\; V\frac{v^2}{u^2}\; I_{CM}(u, \theta), \qquad (3.4)$$

where $n_A(V_A)$, $n_{BC}(V_{BC})$ are the number density distributions of the parent beam velocities and are proportional to $V_i^2 \exp(-V_i^2/\alpha^2)$, where α is the most probable velocity of the beam. V is the relative velocity of the reactants for a given V_A and V_{BC}.

Conservation of Momentum

In a collision which yields two particles AB and C, their recoil momenta in the CM system must be equal in magnitude and opposite in direction,

$$m_{AB}u_{AB} = - m_C u_C.$$

Thus if AB appears at an angle θ, C appears at $\pi - \theta$. m_{AB} and m_C denote the masses of AB and C respectively and u's their velocities. The recoil velocities are related to the final relative velocity V_f and to the translational energy, E_f, released by

$$m_{AB}\; u_{AB} = m_C\; u_C = \mu_f V_f = (2\mu_f\; E_f)^{\frac{1}{2}}$$

where μ_f is the reduced mass of (AB + C) system.

Computational Factors

We assume for ease in computing the intensities that $I_{CM}(u,\theta)$ can be separated in two factors as follows

$$I_{CM}(u,\theta) = T(\theta)\, U(u)$$

where $T(\theta)$ depends only on θ and $U(u)$ gives the distribution of u and is independent of θ. The functional form of $U(u)$ used in our calculations is

$$U(u) = (u/u^*)^2 \exp[1.0 - (u/u^*)^2],$$

where u^* is one of the parameters which has to be adjusted in order to fit experimental data from the assumed CM function.

The function $T(\theta)$ is given by the product of two functions as

$$T(\theta) = T_1(\theta,a)\, T_2(\theta,b). \tag{3.5}$$

$T_1(\theta,a)$ is a simple exponential function and is given by

$$\begin{aligned} T_1(\theta,a) &= \exp(-\theta/a) && (0^\circ < \theta \leq 90^\circ), \\ &= \exp(-(180 - \theta)/a) && (90^\circ < \theta \leq 180^\circ). \end{aligned} \tag{3.6}$$

This factor in angular part is taken mainly from geometric considerations as this will give a symmetric distribution about 90°.

The second factor $T_2(\theta,b)$ is related to the decaying characteristic of the intermediate complex, since reaction prodeeds via an intermediate complex, which

decomposes to give products. The life of this intermediate complex is expressed in terms of the number of rotations it makes before decomposition. So the intensity at an angle is the sum of the intensities contributed by the intermediate after it completes one rotation, two rotations, and so on, depending on its lifetime. This is expressed mathematically as

$$T_2(\theta,b) = e^{-\theta/b} + e^{-(360-\theta)/b} + e^{-(360+\theta)/b} + e^{-(720-\theta)/b} + e^{-(720+\theta)/b} + \dots .$$

where $0^\circ < \theta \leq 180^\circ$. The sum can be rearranged as

$$\begin{aligned} T_2(\theta,b) &= e^{-\theta/b}[1+e^{-(360/b)} + e^{-(720/b)} + \dots] \\ &\quad + e^{\theta/b}[e^{-(360/b)} + e^{-(720/b)} + \dots] \\ &= e^{-\theta/b}(1-X)^{-1} + e^{\theta/b}[(1-X)^{-1} - 1], \end{aligned}$$

where $X = e^{-360/b}$.

On normalizing this functio: at $\theta = 0^\circ$ and simplifying, we get

$$T_2(\theta,b) = \frac{e^{-(\theta/b)} + X\, e^{(\theta/b)}}{1 + X} . \qquad (3.7)$$

Thus $T(\theta)$ is a function of the parameters a and b. In this function b gives a measure of the lifetime of the intermediate complex. These parameters are to be adjusted for a given system in order to get good agreement with the LAB distribution.

The procedure used for the transformation of the assumed $T(\theta)\ U(u)$ to the LAB system was the same as employed by Entemann (13). The main features are as follows.

1. A set of points in LAB space is chosen to compare with available experimental data. For each point (v,Θ), from a given contributing Newton diagram (defined by parent beam velocities V_A and V_{BC} and angle of intersection γ--in this case $\gamma = 90^{o}$) the corresponding point in CM space (u, θ) is determined.
2. The assumed CM intensity (flux density) at point $I(u, \theta, V)$ is weighted by the probability associated with the kinematic diagram and multiplied by the Jacobian v^2/u^2 to obtain contribution to $I(v,\Theta)$ from that kinematic diagram. In Equation (3.4) $n_A(V_A)n_{BC}(V_{BC})V$ represents the probability associated with the kinematic diagram. This computation is repeated for all the combinations (V_{Ai} and V_{BCj}) that one wishes to consider and the contributions added, resulting in a value of $I(v,\Theta)$. Typically $I(v,\Theta)$ is calculated for 30 values of v: 50, 100, 150, ..., 1500 meters/sec and at 10^{o} intervals in Θ.
3. An integration $\int I(v,\Theta)\ dv$ is performed to obtain the total flux $I(\Theta)$ at an angle Θ, which is compared to experimental angular distributions measured without velocity analysis.

These calculations were done on a CDC 6400 computer with the program written by Entemann (13) and modified by Siska (16).

Results and Discussion

Figure 3 shows the laboratory distribution of K in the barium-potassium chloride reaction. The smooth curve is obtained by transforming the assumed CM differential cross section to the LAB system and averaging the set of Newton diagrams arising from the thermal velocities distribution in the parent beam. The temperatures at which beams are prepared are given in Table 1. One can observe that the angular distribution of the K atoms shows two peaks, one in the forward direction and the other in the backward direction with respect to KCl beam. A better idea of this analysis can be obtained by looking at the Newton diagram of the system (Fig. 3). The two vectors V_{KCl} and V_{Ba} represent the most probably velocities of the two beams, respectively. The two peaks are observed at $\sim 20^{o}$ and $\sim 85^{o}$, having almost the same intensity.

Table 1. Beam Temperatures

Element	Oven Temperature (^{o}K)
Ba	1000
KCl	975
KI	950
CsCl	950

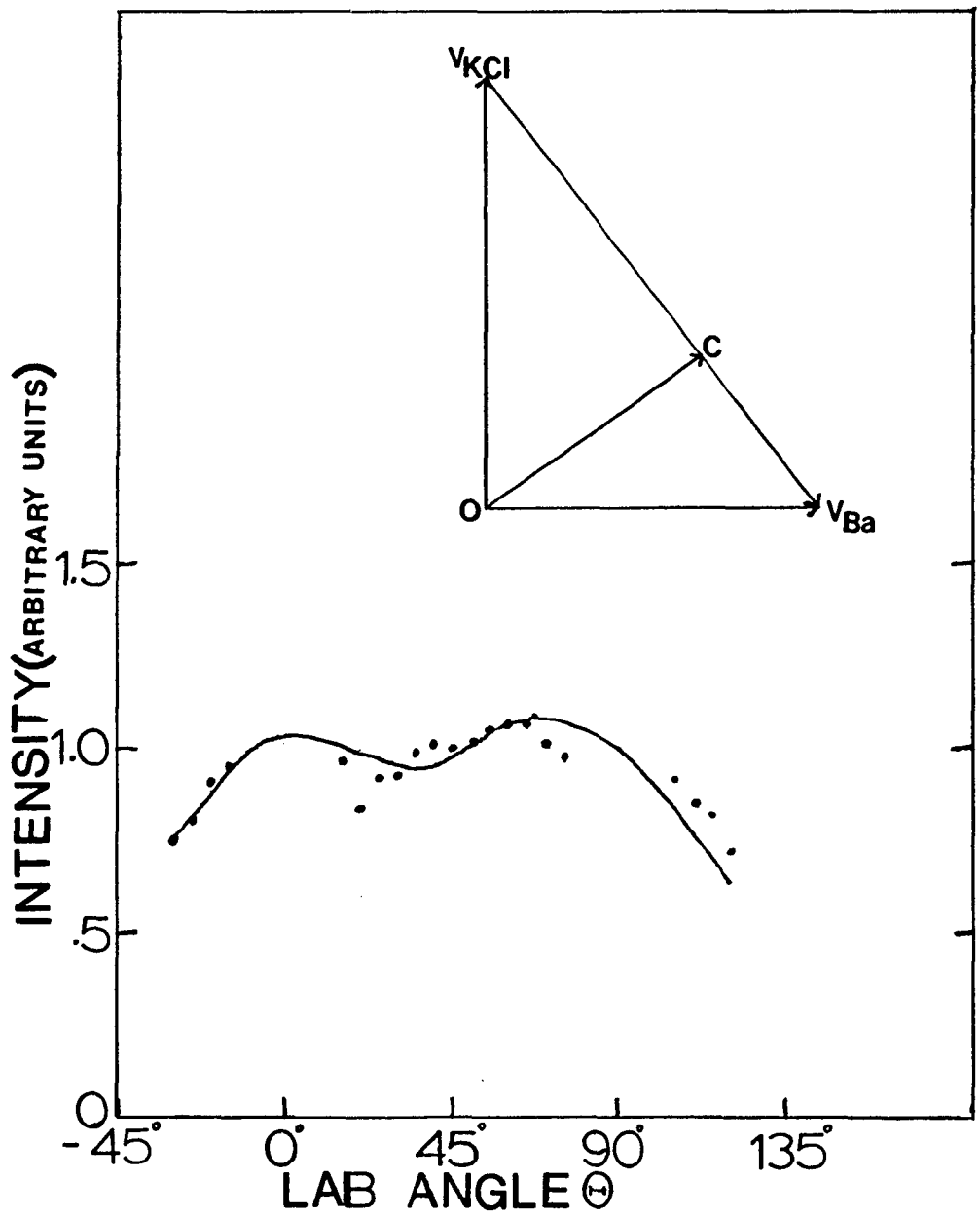

Fig. 3. Intensity of scattering of K atoms as a function of LAB angle; experimental (indicated by dots), from CM function (smooth curve), for the Ba + KCl reaction.

The angular distribution of the Cs atoms measured in the laboratory in the reaction of barium-cesium chloride is shown in Fig. 4. The smooth curve is obtained by converting assumed CM angular-distribution to the LAB system. This angular distribution of the Cs atoms also shows two peaks; one in the forward direction is stronger than the one in the backward direction. The two peaks are observed at $\sim 0^{o}$ and 85^{o}.

For the barium-potassium iodide system, angular distribution of K atoms is shown in Fig. 5. The smooth curve is calculated by converting assumed CM differential cross section to the LAB system. In this case, also, the angular distribution of K atoms shows two peaks, one at $\sim 0^{o}$ and the other at $\sim 75^{o}$. Moreover this reaction is also dominated by the forward peaking of K atoms with respect to the KI beam.

In these reactions it is assumed that reactants form an intermediate complex. Thus the shape of the angular distribution for the reactively scattered alkali atoms in each case depends on the lifetime of this intermediate complex. The formation of an intermediate complex and its dissociation to products is completely determined by initial conditions and the three adjustable parameters a, b, and u^{*} in the assumed CM angular distribution function. The comparison of the angular distribution of the alkali atoms calculated from the assumed function with

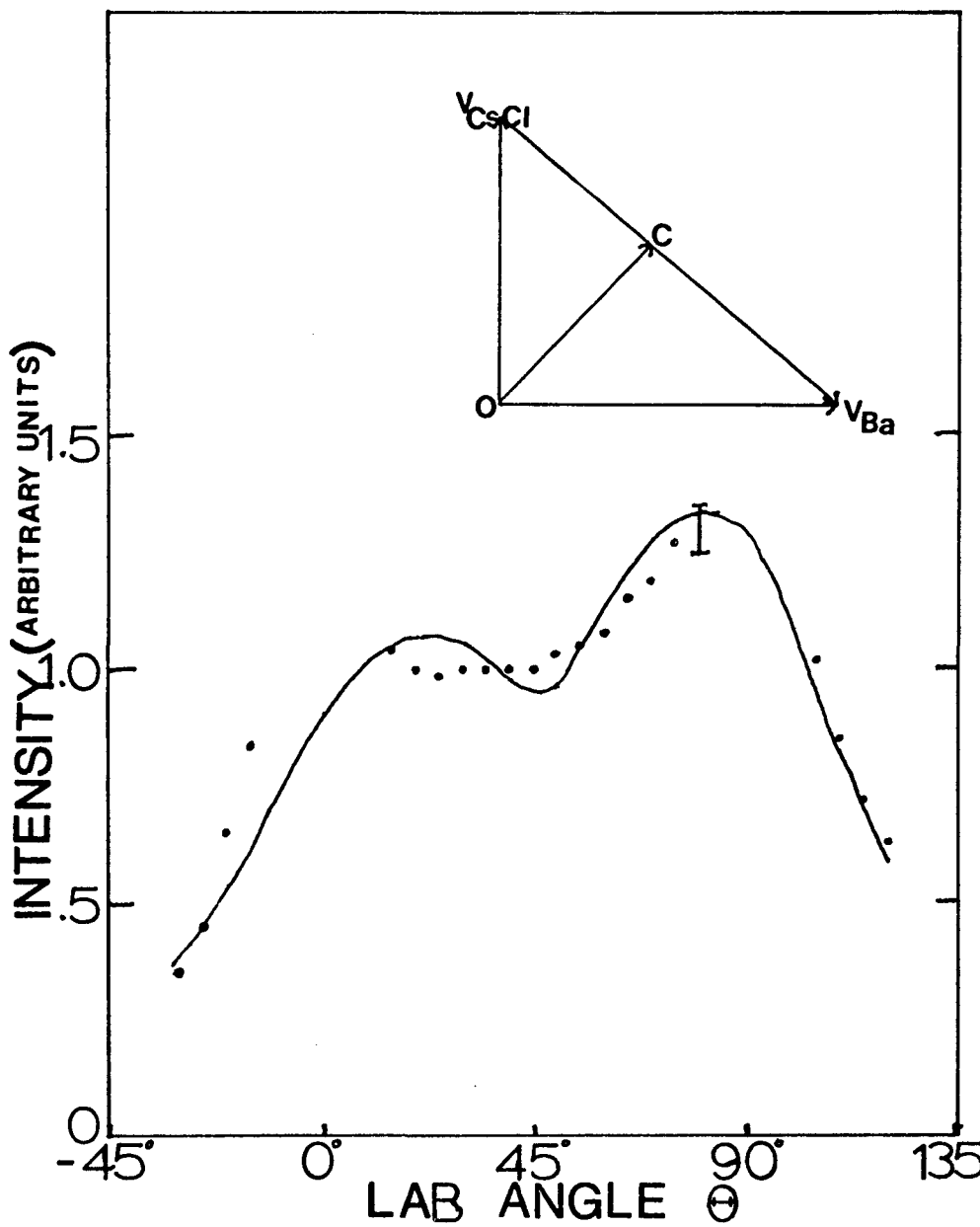

Fig. 4. Intensity of scattering of Cs atoms as a function of LAB angle; experimental (indicated by dots), from CM function (smooth curve).

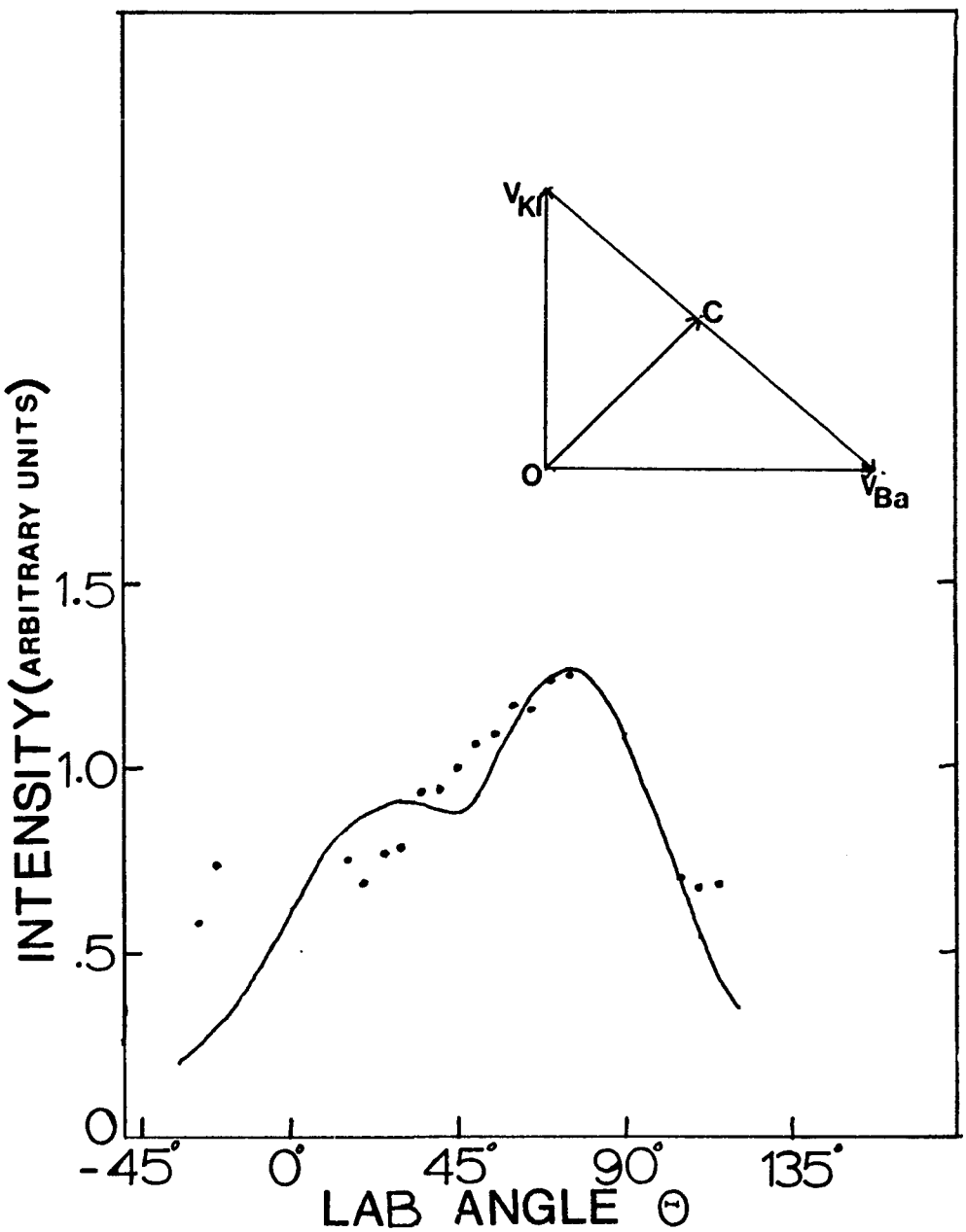

Fig. 5. Intensity of scattering of K atoms as a function of LAB angle; experimental (indicated by dots), from CM function (smooth curve), for the Ba + KI reaction.

the data gave fairly good results. Table 2 lists the best-fit values of a, b, and u^*. Parameter b in this function gives a measure of lifetime of the intermediate complex formed during the reaction. The value of b indicates that lifetimes of the intermediate complexes formed in these reactions follow the order:

$$[BaKCl]^\dagger > [BaCsCl]^\dagger > [BaKI]^\dagger$$

which can also be inferred from angular distribution data. This type of angular distribution which shows two peaks, where one peak is more intense than the other, is considered to follow osculating behavior (8). In the osculating model it is assumed that the intermediate complex $[Ba\ MX]^+$ rotates and during the rotation about its total angular momentum vector, the complex decomposes. If the lifetime of the intermediate complex is greater than five rotational periods, the angular distribution of the product will show forward backward symmetry with respect to the initial relative velocity vector. This is the characteristic of a long-lived complex (17). Moreover, these reactions do not follow the pattern of the reactions which proceed via a very short-lived intermediate complex. Short-lived complexes are characterized by their peaking either in the forward direction with the stripping mechanism (7) or in the backward direction with the rebound mechanism (18). The three reactions investigated here follow the pattern of the

Table 2. Cross Section Parameters

System	a (in degrees)	b (in degrees)	u^* (x 10^4 cm/sec)	E_f (kcals)
Ba + KCl	160	350	8	3.7
Ba + CsCl	100	180	4	4.5
Ba + KI	100	150	3	0.5

Cs + TlX reactions which have been characterized as osculating reactions (8).

The values of final translational energy, E_f, of the product atom were calculated by assuming that the product atom recoils with the peak velocity. This velocity is given by the parameter u^* in the function U(u). The exothermicity of the reactions of Ba with CsCl and KI is the same, but there is an appreciable difference in the values of E_f of the product atom in these two reactions. This implies greater internal excitation of the BaI product.

CHAPTER 4

TOTAL CROSS SECTIONS

General Formulation of the Statistical Theory

Let us consider that reaction between an atom A and a molecule BC takes place as

$$A + BC \rightleftharpoons [ABC] \longrightarrow AB + C \ .$$

Reactants Reaction Complex Products

A strongly coupled "reaction complex" is formed which then dissociates among various products. The statistical assumption is that the probability of dissociation of the complex to a given state depends only on the dynamical quantities conserved in the complex (which in this case are total angular momentum and energy), i.e., all attainable states are equally probable.

To define a reaction complex for collisions with strong attractive forces, we assume that reactive scattering can occur only when the relative energy of translation exceeds the hump in the effective potential for radial motion. The hump in the potential curve results from the addition of the $1/r^2$ orbital angular momentum term and atom-molecule attraction term. The effective radial potential

$U_{\ell_i}(r_i)$ is given by

$$U_{\ell_i}(r_i) = -\frac{C_i}{\gamma_i^6} + \frac{\ell_i(\ell_i+1)\hbar^2}{2\,\mu_i\,r_i^2}\,, \tag{4.1}$$

where first term is due to dispersion and second term is due to orbital angular momentum. The other symbols in Equation (4.1) are:

C = interaction constant (spherically averaged sum of dipole-induced dipole and dispersion contributions),

ℓ = angular momentum quantum number,

μ = three body reduced mass of atom-molecule,

$$[\mu_i = (m_A\, m_{BC})/(m_A + m_{BC})],$$

and the subscripts i and f refer to initial and final states. To find $\ell_{i\ max}$ we use the equation

$$E_i \geq \text{Maxumum } (U_{\ell_i}(r_i))$$

and for Maximum $(U_{\ell_i}(r_i))$,

$$\frac{dU_{\ell_i}}{dr_i} = 0.$$

This leads to the condition

$$\ell_i(\ell_i+1)\hbar^2 \leq 6\,\mu_i\,C_i^{1/3}(\tfrac{1}{2}\,E_i)^{2/3} \tag{4.2}$$

where E_i is the initial translational energy. Equation (4.2) determines the value of maximum orbital angular

momentum quantum number, $\ell_{i\ max}$, which allows complex formation.

The other symbols that will be used are:

v = vibrational quantum number,

J = rotational angular momentum quantum number,

$\mathcal{J}$ = total angular momentum quantum number,

I = two body moment of inertia,

$\mathcal{J}_z$ = zth component of $\mathcal{J}$

E = total energy.

The energies are considered to be so low that complete dissociation can not occur. The reaction complex is defined completely as far as the statistical theory is concerned by $\mathcal{J}$, $\mathcal{J}_z$, and E. The probability of forming a complex (E, $\mathcal{J}$, $\mathcal{J}_z$) from initial state (v_i, J_i, ℓ_i) is

$$\frac{1}{(2\ell_i+1)(2J_i+1)}, \text{ if } |\ell_i - J_i| \leq \mathcal{J} \leq |\ell_i + J_i|,$$

otherwise zero.

The probability of decomposition of the complex (E, $\mathcal{J}$, $\mathcal{J}_z$) to a given state is the same for all states accessible under conservation of total energy and angular momentum. Conservation of energy requires

$$E = E_i + E_{v_i} + \left[\frac{J_i(J_i+1)\hbar^2}{2\ I_i}\right] \tag{4.3}$$

$$= E_f + E_{v_f} + \left[\frac{J_f(J_f+1)\hbar^2}{2\ I_f}\right] + Q \tag{4.3a}$$

where Q is the zero-zero exothermicity of the reaction $i \rightarrow f$. Conservation of angular momentum implies that each intersection in the (ℓ_f, J_f) plane is such that

$$|\ell_f - J_f| \leq \mathcal{J} \leq |\ell_f + J_f| \tag{4.4}$$

contains one and only one state accessible from $(\mathcal{J}, \mathcal{J}_z)$. Moreover the complex must be able to dissociate over the final state orbital angular momentum barrier, which restricts ℓ_f by

$$\ell_f(\ell_f+1)\hbar^2 \leq 6\,\mu_f\, C_f^{1/3}[\tfrac{1}{2}\, E_f(J_f)]^{3/2}. \tag{4.5}$$

For a given v_i, J_i, v_f, and $\mathcal{J}$, Equations (4.4) and (4.5) define a bounded region in the (ℓ_f, J_f) plane; the number of states of reaction products in the vibrational level v_f accessible from the reaction complex $(E, \mathcal{J}, \mathcal{J}_z)$ is the number of integer pair points (ℓ_f, J_f) within or on the boundary of the region. The equation of the boundary curve, which can be easily obtained from Equations (4.3) and (4.5), is

$$\left(\frac{\ell}{\ell_o}\right)^3 + \left(\frac{J}{J_o}\right)^2 = 1$$

and equations for the other three sides of the cross-hatched area as shown in Fig. 6 can be obtained from conservation of angular momentum. Let $\overline{n}(v_f;\, E, \mathcal{J}, \mathcal{J}_z)$ be the number of integer pair points (ℓ_f, J_f) in this area, and

$$N(E, \mathcal{J}, \mathcal{J}_z) = \sum_{v_f} \overline{n}(v_f;\, E, \mathcal{J}, \mathcal{J}_z)$$

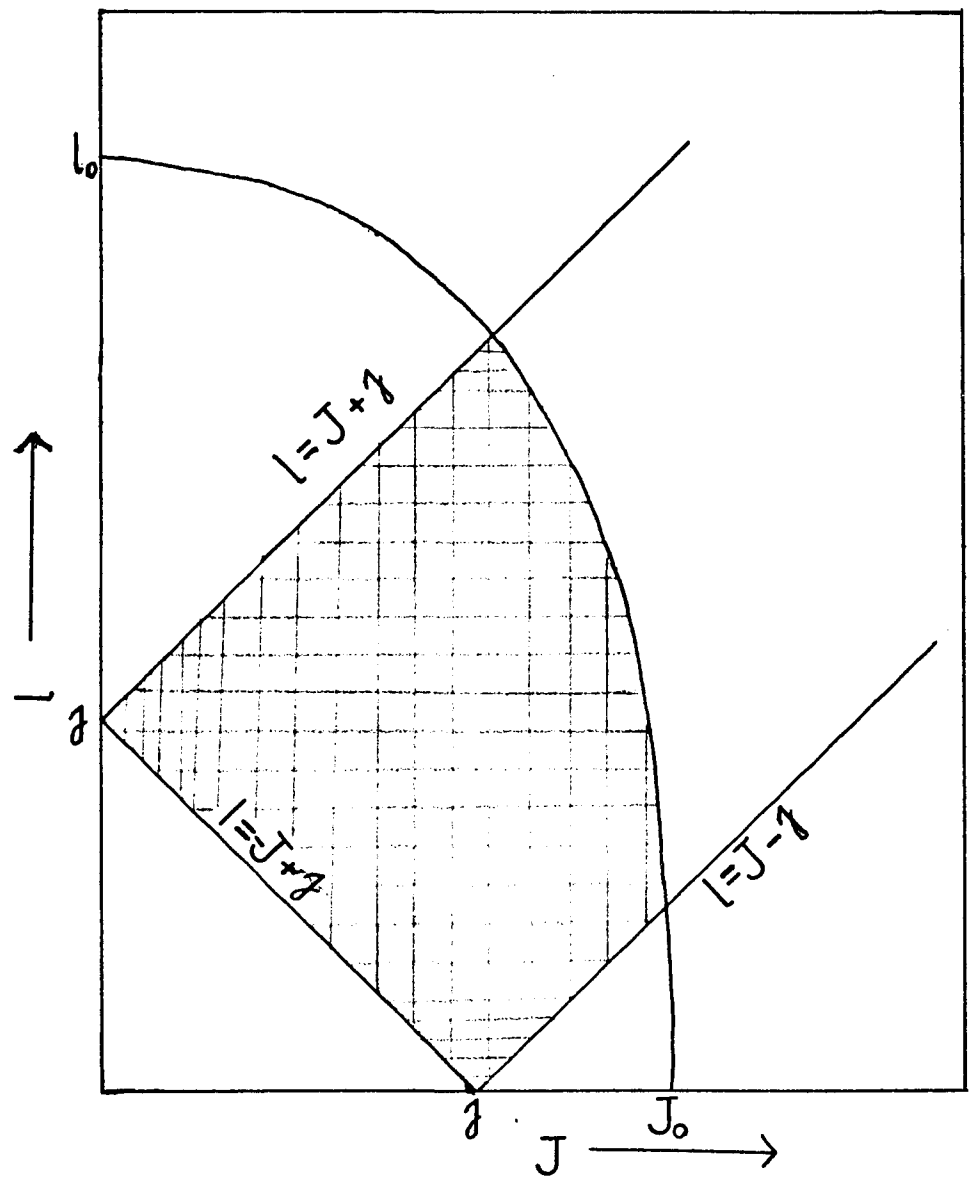

Fig. 6. Region of allowed (J,ℓ) space for a given $\mathcal{J}$ and E (shown by the cross-hatched area).

where $N(E, \mathcal{J}, \mathcal{J}_z)$ is the total number of integer pair points for all possible vibrational states. The probability of dissociation of the complex to a given state (v_f, E_f, ℓ_f, J_f) is then given by

$$P(v_f,E_f,J_f,\ell_f;E,\mathcal{J},\mathcal{J}_z) = \frac{1}{N(E,\mathcal{J},\mathcal{J}_z)} . \tag{4.6}$$

In the above derivation of probability, we have assumed that the reaction takes place only via reaction complex and there is no direct product formation. One can show (19) using *S*-matrix properties that

$$p_i + \sum_j P^o_{ij} = 1 \tag{4.7}$$

where p_i is the probability that a complex is formed from reactants i and P^o_{ij} is the probability of a direct transition to products j from reactants i (or vice versa) without going through the intermediate complex. Equation (4.7) can be considered as a conservation of probability; i.e., either the system goes directly to some product states or else to complex. Moreover, Miller (19) has obtained an expression of overall transition probability in terms of direct transition probabilities:

$$|S_{ij}|^2 = P^o_{ij}+(1-\sum_k P^o_{ik})(1-\sum_k P^o_{kj})/(N-\sum_{kk'} P^o_{kk'})$$

where N is the number of channels. The simplest possible assumption is that $P_{ij} = 0$; i.e., there is no direct transition and with this assumption one sees that $p_i = 1$ for all

i, and

$$\langle |S_{ij}|^2 \rangle = \frac{1}{N} , \tag{4.8}$$

which is the usual form of the statistical model.

The maximum cross section for a given partial wave (20) is

$$\frac{\pi(2\ell_i + 1)\hbar^2}{2\mu_i E_i} .$$

The partial cross section, $\overline{\sigma}$, for the reaction is then given by

$$\overline{\sigma}(v_f,J_f,\ell_f,E_f;v_i,J_i,\ell_i,E_i) = \left(\frac{\pi\hbar^2(2\ell_i+1)}{2\mu_i E_i}\right) \times \sum_{\mathcal{J}} \sum_{\mathcal{J}_z=-\mathcal{J}}^{+\mathcal{J}} \frac{P(v_f,J_f,\ell_f,E_f;E,\mathcal{J},\mathcal{J}_z)}{(2\ell_i+1)(2J_i+1)} , \tag{4.9}$$

$$= \frac{\pi\hbar^2}{2\mu_i E_i(2J_i+1)} \sum_{\mathcal{J}} (2\mathcal{J}+1)P(v_f,J_f,\ell_f E_f;E,\mathcal{J},\mathcal{J}_z) \tag{4.10}$$

and the total cross-section of the reaction, σ, is given by

$$\sigma(v_f,J_f,E_f;v_i,J_i,E_i) = \frac{\pi\hbar^2}{2\mu_i E_i(2J_i+1)} \sum_{\ell_i=0}^{\ell_{imax}} (2\mathcal{J}+1) \times \sum_{\ell_f} P(v_f,J_f,E_f;E,\mathcal{J},\mathcal{J}_z) \tag{4.11}$$

and

$$\sigma(v_f;v_i,J_i,E_i) = \sum_{J_f} \sigma(v_f,J_f,E_f;v_i,J_i,E_i). \tag{4.12}$$

Since the free atom of the initial state in our experiments was relatively heavy, the mean orbital angular momentum was

large compared to the rotational angular momentum so J_i has been taken as equal to zero and our expression for total cross-section reduces to

$$\sigma(v_f,J_f,E_f;v_i,0,E_i) = \frac{\pi\hbar^2}{2\mu_i E_i} \sum_{\ell_i=0}^{\ell_{imax}} (2\ell_i+1)$$

$$\times \sum_{\ell_f} P(v_f,J_f,\ell_f,E_f;E,\ell_i) \qquad (4.13)$$

(since $|\ell_i-J_i| \leq \mathcal{J} \leq |\ell_i+J_i|$; when $J_i=0$, $\mathcal{J}=\ell_i$).

Calculations

In the calculations described here a diatomic molecule is considered as a rigid rotor. The main part of these calculations was to estimate N, the total number of states. A number of quantities are required for the estimation of N (e.g., C, α, r_e).

The dipole-induced dipole interaction constant C (erg-Cm^6) was calculated for an $(Atom)_1$ + $(Molecule)_2$ system using the London formula (21):

$$C = \frac{3\ E_1\ E_2}{2(E_1+E_2)}\ \alpha_1\alpha_2 + d_2^2\ \alpha_1$$

where

E_1 = energy for atom

E_2 = energy for molecule

α_1 = polarizability of atom

α_2 = polarizability of molecule

d_2 = dipolemoment of molecule.

E_1 is usually of the order of ionization potential. For alkali metals, however, it is the energy of the resonance ($S \longrightarrow P$) transition. E_2 is determined as the sum of the first ionization potential of metal atom and ½ dissociation energy of molecule.

The polarizability of molecule BaCl was estimated as $\alpha_{BaCl} = \alpha_{Ba^+} + \alpha_{Cl^-}$. For this we need polarizability of Ba^+ ion, which was calculated as discussed in Appendix A.

The dipole moment of BaCl was calculated using the following formula (22):

$$d = e\, r_e - \frac{r_e^4\, e(\alpha_+ + \alpha_-) + 4\, r_e\, e\alpha_+\alpha_-}{r_e^6 - 4\alpha_+\alpha_-},$$

where α_+, α_- are polarizabilities of positive and negative ions which form the molecule. The equilibrium internuclear distance, r_e, for BaCl was determined by the relationship (23),

$$r_e = a_{ij} - b_{ij} \log F_2,$$

where $F_2 = 5.8893 \times 10^{-7}\, \mu\, \omega_e$ dynes/cm.

In the above relationship μ is the reduced mass and ω_e is the vibrational frequency of diatomic. a_{ij} and b_{ij} are parameters in the function. In this case $a_{ij} = 2.71$; $b_{ij} = 1.09$. The vibrational energy was calculated by using a two term formula

$$E_v = (v+\tfrac{1}{2})\omega_e - (v+\tfrac{1}{2})^2 \omega_e X_e,$$

where ω_e is the vibrational spacings in cm^{-1} and $\omega_e X_e$ the anharmonicity. The vibrational energy used in these calculations was the energy above the zero level. For the values of physical quantities used in the calculations, see Table 3.

Table 3. Parameters Used in the Calculations on the Ba + KCl Reaction

	r_e(Å)	d(D)	Resonance Emerge E as Used in London Formula	α ($Å^3$)	C(10^{-60}) erg-cm^6	w_e* (cm^{-1})	$w_e X_e$ (cm^{-1})
K	--	--	1.6 eV	37.0	--	--	--
KCl	3.0	10.48	6.55 eV	3.0	--	280.0	0.9
Ba	--	--	4.04 eV	34.0	--	--	--
BaCl	2.588	9.21	7.75 eV	5.74	--	279.3	0.89
Ba + KCl	--	--	--	--	4344.4	--	--
K + BaCl	--	--	--	--	3814.0	--	--

*Ref. (24).

The general procedure of calculation is as follows. First one assumes some values for E_i, v_i, J_i and calculates E, the total energy by using Equation (4.3). Using this value of E and for a given value of v_f and J_f, one finds out E_f, the final energy of translation using Equation (3.3a). After knowing $E_f(J_f)$, one calculates an upper

limit on ℓ_f; i.e., $\ell_{f\ max}$, using Equation (3.5) and then consequently the number of states $n(v_f;E,\mathcal{J},\mathcal{J}_z)$ for all $\mathcal{J}$ involved. The probabilities and cross sections follow directly.

A lot of time has been spent on the development of a computer program to calculate N, the total number of states. All calculations have been done on the CDC 6400. In the program all summations have been replaced by integrals and were calculated using the Gaussian quadrature method (25). Six points were found to be sufficient to evaluate the integrals.

Results and Discussion

The total number of states for any given reactive channel N_r and for any given non-reactive channel N_{nr} increases as the initial translational energy increases and, for a given E_i, are dependent on total angular momentum $\mathcal{J}$. The change in total number of states as a function of $\mathcal{J}$, the total angular momentum quantum number at E_i = 0.085 eV is shown in Fig. 7. This theory predicts that as the initial translational energy is increased the fraction of total states available for reactive scattering $N_r/(N_r+N_{nr})$ decreases. Since the reactive cross section is dependent on this fraction, the reactive cross section also decreases. The reactive cross section, σ_r, drops to almost half when translational energy is increased from 0.06 eV to 0.40 eV

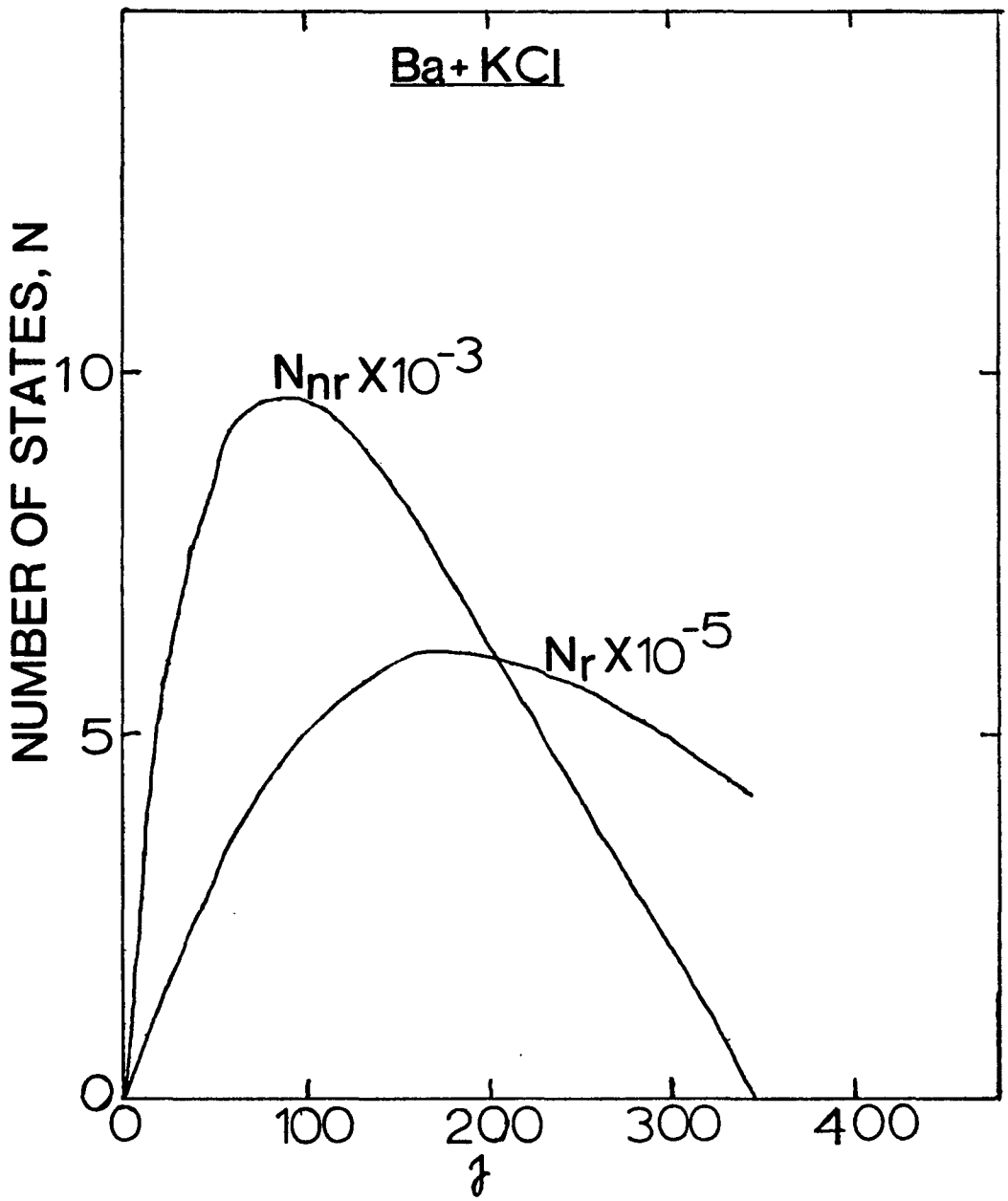

Fig. 7. Total number of states as a function of total angular momentum for the Ba + KCl reaction -- For the case $E = E_i = .085$ eV and $\ell_{i\ max} = 343$.

(Fig. 8). The initial translational energy plays a very important role in deciding the value of total energy E since the vibrational and rotational contributions to E are very small. Moreover the value of $\ell_{i\ max}$ also depends only on E_i, and not on E, the total energy. The effect of initial vibrational energy is small and this does not produce a marked change in the value of the reactive cross section (Fig. 9). Since the final translational energy, E_f, is determined by the final vibrational and rotational energies, their contributions affect the value of the cross section. The effects of the final vibrational energy and the final rotational energy are shown in Figs. 10 and 11. As the vibrational energy is increased, the final translational energy decreases (Equation 4.3a) and therefore the cross section decreases. The cross section increases with the increase in rotational angular momentum quantum number and then falls off rapidly as J_f approaches J_o, the value of rotational angular momentum when $\ell_f = 0$. At this value of J_f, E_f becomes zero.

It is possible to calculate the total reactive cross section for this model by a much simpler method (19). According to this model it is assumed that there is a critical impact parameter b_o such that collisions with $b < b_o$ lead to complex formation and collisions with $b > b_o$ do not; b_o is determined by the criterion that the particles be able to cross over the effective radial potential

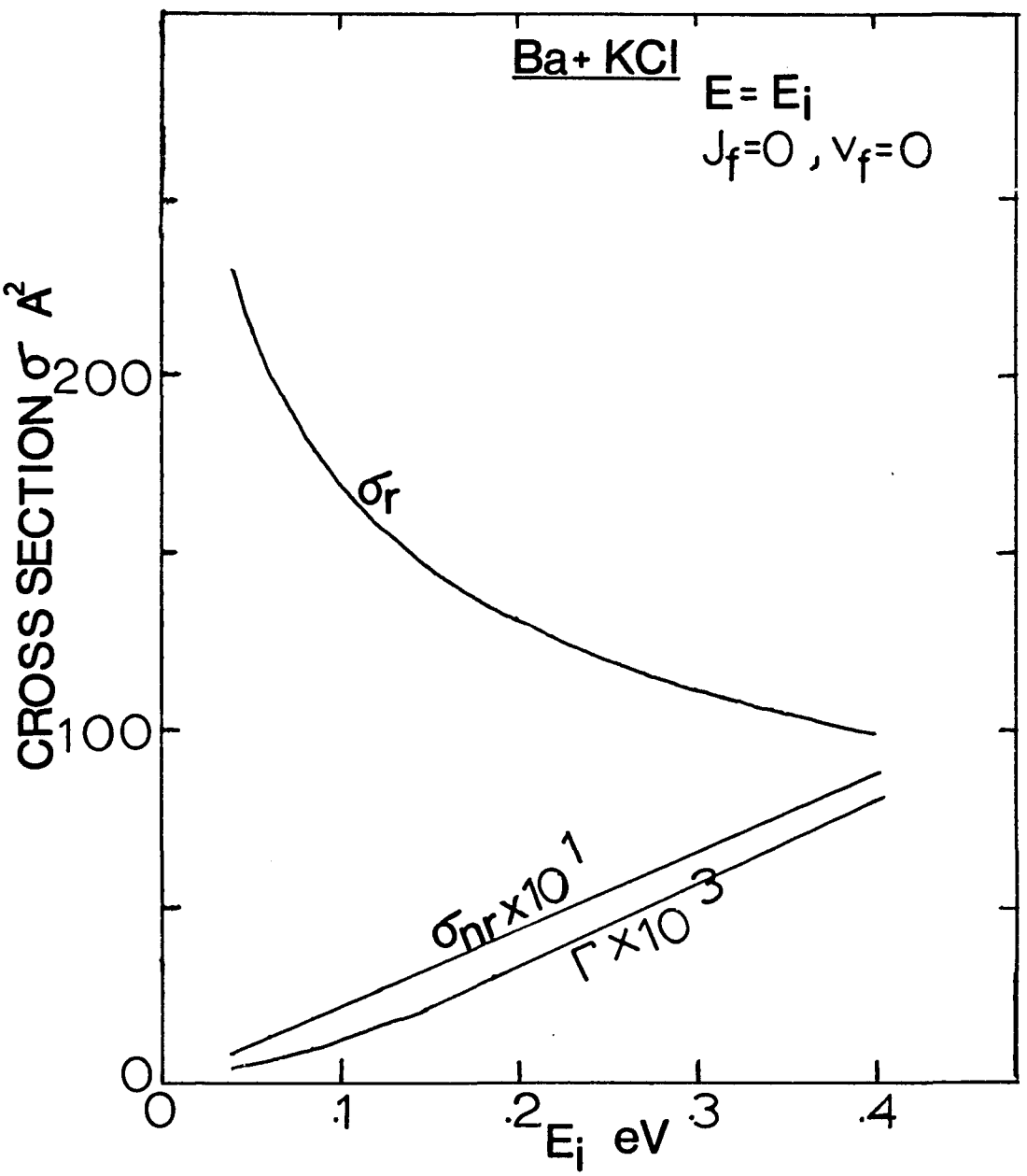

Fig. 8. Cross section as a function of initial translational energy for the Ba + KCl reaction -- Γ, the ratio of $\frac{\sigma_{\text{no reaction}}}{\sigma_{\text{reaction}}}$, is plotted as a function of E_i.

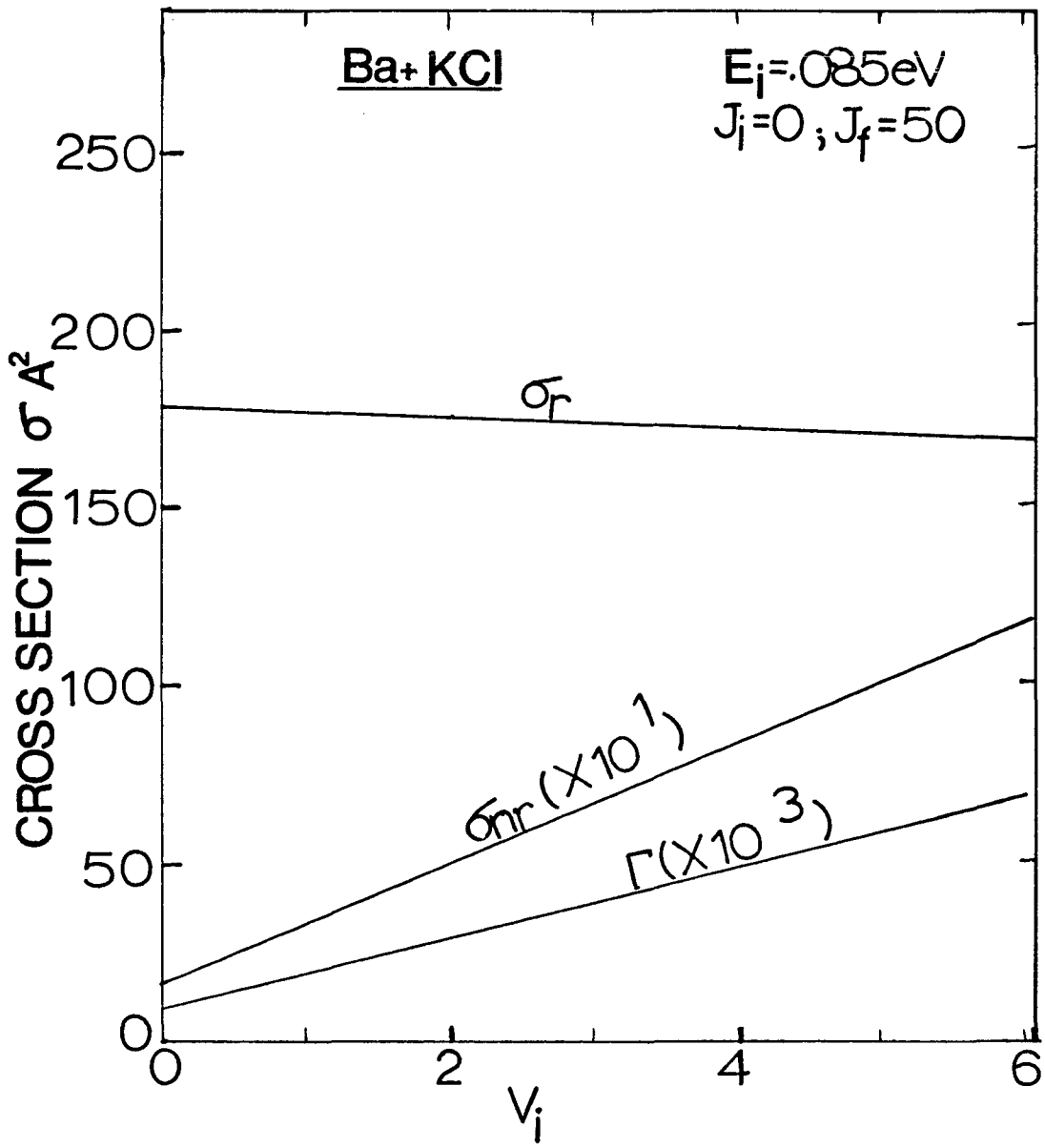

Fig. 9. Effect of initial vibrational energy on the cross section for the Ba + KCl reaction -- For the case E_i = .085 eV; v_f = 0. Γ is plotted as a function of V_i.

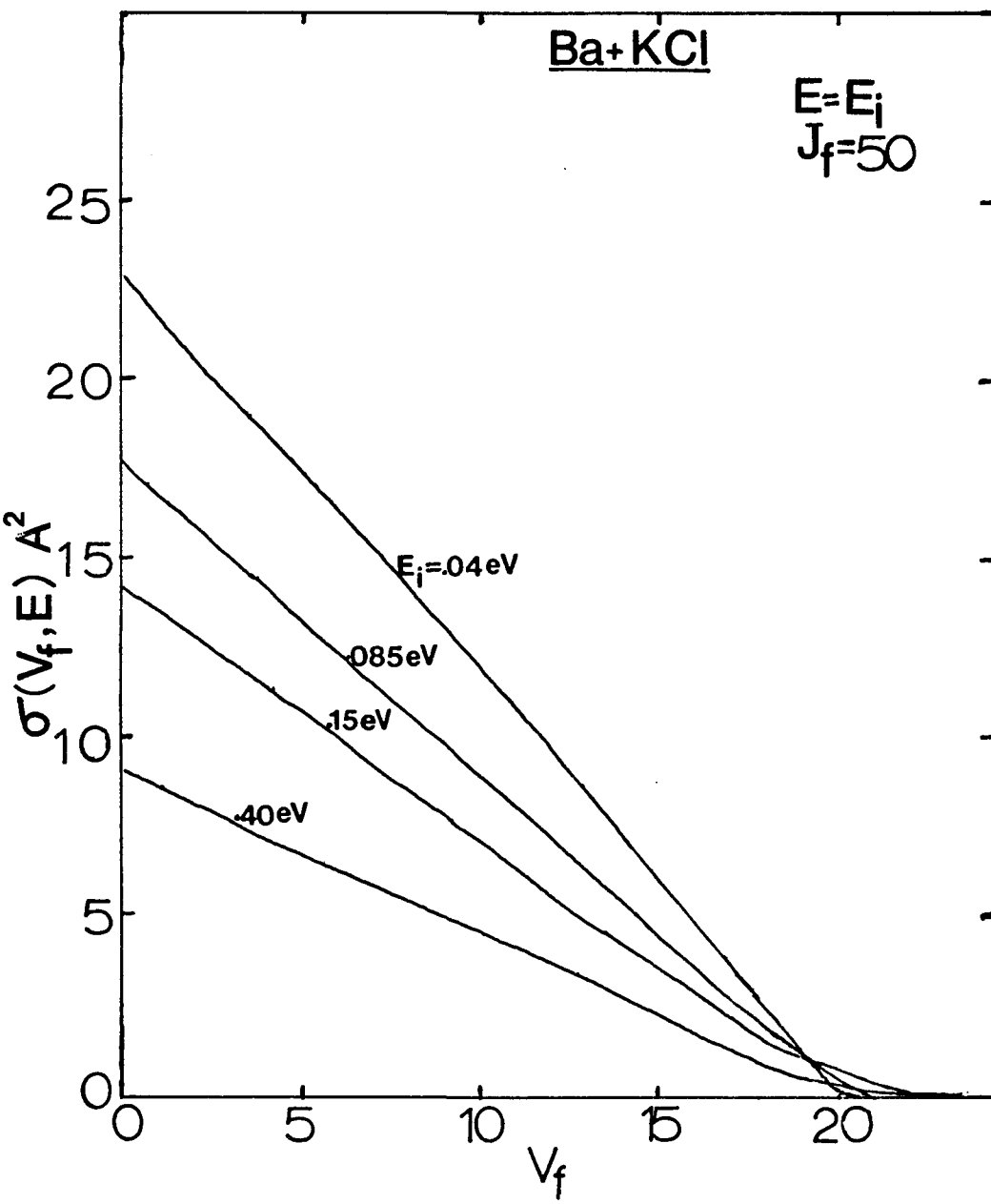

Fig. 10. Effect of final vibrational energy on the cross section for the Ba + KCl reaction.

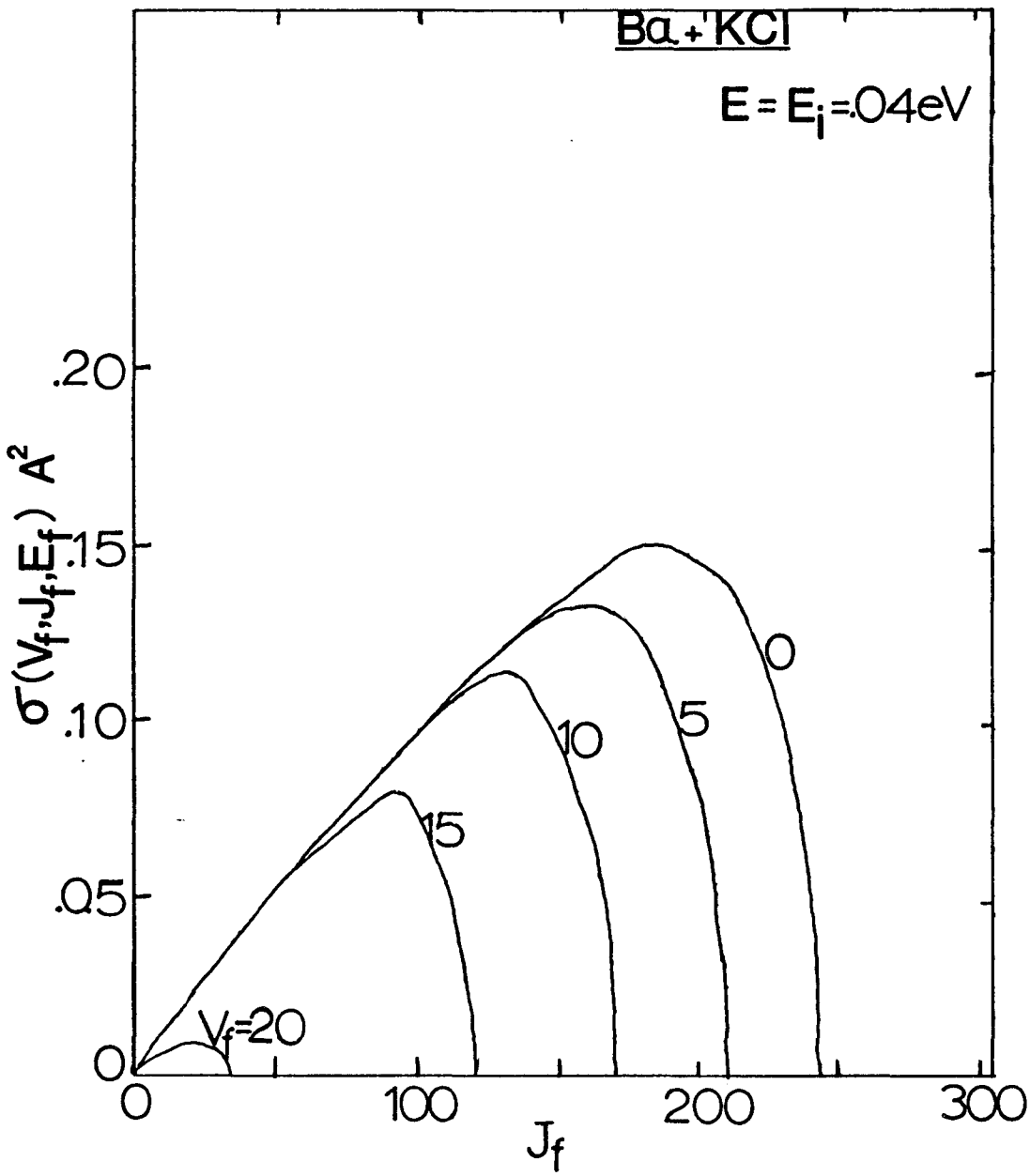

Fig. 11. Effect of final rotational energy on the cross section for the Ba + KCl reaction.

barrier,

$$V(r)_{eff} = - C/r^6 + Eb^2/r^2$$

the attractive term being the long range dipole-induced dipole interaction. The condition

$$E_i = \max V(r)_{eff}$$

leads to

$$b_o = (27\ C/4E_i)^{1/6}.$$

In order to compute the reactive cross section, one can use the following result (19):

$$\sigma_r = \pi b_o^2\ (N_r/(N_r+N_{nr}). \qquad (4.14)$$

The total reactive cross sections were calculated using the above equation for the Ba + KCl system. The results obtained by such calculations agree quite well with those obtained by the more laborious calculations done by summing over all angular momentum, final vibrational, and rotational states. Results are tabulated in Table 4. We have calculated the cross sections for the reactions of barium with KI, CsCl, and CsI on the basis of the simplified model. Results are shown in Table 5.

Table 4. Reactive Cross Section for the Ba + KCl Reaction Calculated on the Simplified Statistical Model

E_i(eV)	b_o(Å)	$N_r/(N_r + N_{nr})$	σ_r from Eq. (4.14) (Å^2)	σ_r from Eq. (4.13) (Å^2)
0.04	8.780	0.995	240.97	230.81
0.06	8.208	0.992	209.96	201.28
0.085	7.742	0.988	186.04	178.37
0.15	7.047	0.973	151.80	146.09
0.20	6.716	0.956	135.46	131.70
0.30	6.274	0.925	114.39	112.17
0.40	5.981	0.896	100.69	98.93
1.02	5.117	0.767	63.09	60.59

Table 5. Reactive Cross Section for the Reactions at E_i = 0.085 eV

System	$C(\times 10^{60})$ (erg-cm^6)	b_o (Å)	σ_r (Å^2)
Ba + KI	5250	8.0	196
Ba + KCl	4340	7.7	186
Ba + CsI	6360	8.3	198
Ba + CsCl	4560	7.8	180

CHAPTER 5

DIFFERENTIAL CROSS SECTION

General Formulation of the Statistical Theory

The differential cross section for the formation of a final state, f, from an initial state, i, in the CM is related through the T-matrix by the relationship (26)

$$d\sigma = \frac{8\pi^4\hbar^2}{\mu_i E_i} |\langle b\ E_b\hat{n}_b|T|a\ E_a\hat{n}_a\rangle|^2\ \delta(E_b-E_a)d\Omega, \qquad (5.1)$$

where a is the channel index for the incoming state and b is the index for the outgoing channel; a and b consist of all quantum numbers defining a single state; E_a and E_b are the total initial and final energies; $\hat{n}_a$ and $\hat{n}_b$ are unit vectors in the initial and final directions of motion, respectively. E_i is the initial translational energy and μ_i is the initial reduced mass of the system.

By expanding $\hat{n}_a$ and $\hat{n}_b$ in terms of the eigenfunctions of angular momentum, Equation (5.1) can be written as

$$d\sigma = \frac{8\pi^4\hbar^2}{\mu_i E_i} \Big| \sum_{\ell_f=0}^{\infty} \sum_{m_f=-\ell_f}^{+\ell_f} \sum_{\ell_i=0}^{\infty} \sum_{m_i=-\ell_i}^{+\ell_i} \langle \hat{n}_b|\ell_f m_f\rangle$$

$$\times \langle \ell_f m_f E_b b|T|\ell_i m_i E_a a\rangle$$

$$\cdot \langle \ell_i m_i|\hat{n}_a\rangle|^2 \delta(E_b-E_a)d\Omega. \qquad (5.2)$$

Choosing $\hat{n}_a$ to lie along Z-axis, we can write

$$\langle \ell_i m_i | \hat{n}_a \rangle = [\frac{(2\ell_i+1)}{4\pi}]^{\frac{1}{2}} \delta_{om} \tag{5.3a}$$

and

$$\langle \hat{n}_b | \ell_f m_f \rangle = Y^{m_f}_{\ell_f}(\theta, \Phi). \tag{5.3b}$$

Substituting these values in Equation (5.2), we get

$$d\sigma = \frac{2\pi^3 \hbar^2}{\mu_i E_i} \Big|_{\ell_f, m_f} \sum_{\ell_i} (2\ell_i+1)^{\frac{1}{2}} Y^{m_f}_{\ell_f}(\theta, \Phi)$$

$$\cdot \langle \ell_f m_f E_b b | T | \ell_i 0 E_a a \rangle |^2 \delta(E_b - E_a) d\Omega. \tag{5.4}$$

To evaluate this equation explicitly, one requires the knowledge of the magnitude and phase of each non-zero matrix element. If the system is strongly coupled, the phases will be large and will vary very rapidly with small variations in total energy. It can be assumed that this variation is rapid enough such that the random phase approximation is justified. In this case, only the diagonal elements in Equation (5.4) survive, and we can approximate the square of the sum in Equation (5.4) by the sum of the squares,

$$d\sigma \approx (\frac{2\pi^3 \hbar^2}{\mu_i E_i}) \sum_{\ell_f, m_f} \sum_{\ell_i} (2\ell_i+1) |Y^{m_f}_{\ell_f}(\theta, \Phi)|^2$$

$$\cdot |\langle \ell_f m_f E_b b | T | \ell_i 0 E_a a \rangle|^2 \delta(E_b - E_a) d\Omega. \tag{5.5}$$

The scattering matrix S and matrix elements of operator T are related by the relationship

$$S^{E\ell}_{ba} - \delta_{ba} = -2\pi i \langle b|T_\ell|a\rangle.$$

Using this relationship, we can rewrite Equation (5.5) in terms of S-matrix as

$$d\sigma = \left(\frac{\pi\hbar^2}{2\mu_i E_i}\right)\left[\sum_{\ell_f,m_f}\ \sum_{\ell_i}(2\ell_i+1)\left|Y^{m_f}_{\ell_f}(\theta,\Phi)\right|^2\right.$$

$$\left.\cdot\ \left|\langle S_{ba}-\delta_{ba}\rangle\right|^2\right]\delta(E_b-E_a)d\Omega, \qquad (5.6)$$

where $S_{ba} = \langle \ell_f m_f E_b b|S|\ell_i 0\ E_a a\rangle$.

This may be writtin in terms of the total cross section for reaction between well specified states as

$$d\sigma(\Omega,b|a,E) = \sum_{\ell_f,m_f}\ \left|Y^{m_f}_{\ell_f}(\theta,\Phi)\right|^2$$

$$\cdot\ \sigma(\ell_f,m_f b|a,E)d\Omega, \qquad (5.7)$$

where cross section $\sigma(\ell_f m_f b|a,E)$ is given by

$$\sigma(\ell_f m_f b|a,E) = \left(\frac{\pi\hbar^2}{2\mu_i E_i}\right)\left[\sum_{\ell_i}(2\ell_i+1)\left|\langle S_{ba}-\delta_{ba}\rangle\right|^2\right]. \qquad (5.8)$$

Equation (5.7) gives the differential cross section $d\sigma$ at a given angle in the center of mass for a specified internal state. The total intensity of the products at a given angle in the center of mass can be obtained by summing over the internal states of the product, b.

$$I_{total}\ (\Omega|a,E) = \sum_{b} d\sigma(\Omega,b|a,E).$$

In Equation (5.8) the sum over ℓ_i runs over all states, the S-matrix element will be zero unless conservation conditions are satisfied, and initial and final states can be connected by the same intermediate complex. Moreover, the S-matrix element connects the initial channel a, the reactants with specified internal states, to the final channel b, the products with specified internal states. In other words, if we use the language of the statistical theory, these matrix elements are supposed to be calculable as products of the cross section for formation of a strong coupling complex of angular momentum $\mathcal{J},\mathcal{J}_z$ and the probability of its decomposition into products with specified internal states. The sum over all intermediate complexes accessible to both reactants and products then gives the cross section $\sigma(\ell_f m_f b|a,E)$ in Equation (5.8). Thus we can write

$$\sigma(\ell_f m_f b|a,E) = \sum_{\mathcal{J},\mathcal{J}_z} P(\ell_f m_f b|\mathcal{J},\mathcal{J}_z,E) \cdot \sigma(\mathcal{J},\mathcal{J}_z|a,E), \qquad (5.9)$$

where P is the probability of decomposition of the intermediate complex, and $\sigma(\mathcal{J},\mathcal{J}_z|a,E)$ is the cross section for the formation of the complex. We assume further that all accessible states are equally likely to occur, i.e.,

$$P(\ell_f m_f b | \mathcal{J}, \mathcal{J}_z, E) = \frac{1}{N(\mathcal{J},E)} \times q(\ell_f m_f b | \mathcal{J}, \mathcal{J}_z, E), \tag{5.10}$$

where function q is defined as

$$q(\alpha|\beta) = 1 \text{ if state } \alpha \text{ is accessible from state } \beta,$$
$$= 0 \text{ otherwise.} \tag{5.11}$$

N is the total number of states accessible from the complex,

$$N(\mathcal{J},E) = \sum_{b,\ell_f,m_f} q(\ell_f m_f b | \mathcal{J}, \mathcal{J}_z, E), \tag{5.12}$$

where the sum runs over all internal states of reactants and products. $N(\mathcal{J},E)$ does not depend on $\mathcal{J}_z$ since the number of states available for the decomposition of the complex can not, in field free space, depend on the orientation of the complex. Figure 6 indicates the region of allowed $(J\ell)$ space for a given $\mathcal{J}$ and E.

Consider the second factor in Equation (5.9)—the cross section $\sigma(\mathcal{J},\mathcal{J}_z|a,E)$ for the formation of intermediate complex from reactants with specified internal states. This is given by

$$\sigma(\mathcal{J},\mathcal{J}_z|a,E) = \left(\frac{\pi\hbar^2}{2\mu_i E_i}\right) \sum_{\ell_i} (2\ell_i+1) \cdot \frac{q(\mathcal{J},\mathcal{J}_z|\ell_i,0,a,E)}{n(\ell_i,0,a,E)}, \tag{5.13}$$

where $n(\ell_i,0,a,E)$ is a normalizing constant which is the total number of states of the complex (defined by $\mathcal{J},\mathcal{J}_z$) formed from the state $|\ell_i,0,a,E\rangle$. Thus,

$$n(\ell_i,0,a\ E) = \sum_{\mathcal{J},\mathcal{J}_z} q(\mathcal{J},\mathcal{J}_z|\ell_i,0,a,E),$$

where q is defined in Equation (5.11). The criteria which define whether a given state of reactants or products is accessible from a specified state $(\mathcal{J},\mathcal{J}_z)$ of the complex, or vice versa, are given by

1. The total angular momentum $\mathcal{J}$ and its zth component $\mathcal{J}_z$ must be conserved, i.e.,

$$|J+\ell| \geq \mathcal{J} \geq \max \begin{cases} |J-\ell| \\ |\mathcal{J}_z| \end{cases} \tag{5.14}$$

and

$$\mathcal{J}_z = \ell_z + J_z,$$

where J is the rotational angular momentum of the diatomic molecule, J_z its zth component, and ℓ is the orbital angular momentum. The above conditions must be satisfied for both reactants as well as products.

2. The translational energy of the system be such that it can cross over the potential energy barrier. The potential V(r) for a neutral-neutral system is expressed as, say for reactant channel,

$$V_a(r) = -\frac{C_a}{r^6} + \frac{\ell_i(\ell_i+1)\hbar^2}{2\mu_i r^2}. \tag{5.15}$$

The first term on the right side gives the contributions from dipole-induced dipole attraction, and dispersion; the

second term is due to orbital angular momentum. The requirement that translation energy, E_i, must exceed the maximum of this potential yields

$$\ell_i(\ell_i+1)\hbar^2 \leq 6\ \mu_i\ C_a^{1/3}(E_i/2)^{2/3}. \tag{5.16a}$$

Similarly, one can write for the product channel,

$$\ell_f(\ell_f+1)\hbar^2 \leq 6\ \mu_f\ C_b^{1/3}(E_f/2)^{2/3}, \tag{5.16b}$$

where the translational energy, E_{tr}, is given by

$$E_{tr} = E - \frac{J(J+1)\hbar^2}{2\ \mu_o\ r_o^2} - E_{vib} - Q. \tag{5.17}$$

In the above expression Q is the exothermicity of the reaction (for reforming reactants, Q = 0). μ_o is the reduced mass, r_o is the inter-nuclear separation, and E_{vib} is the vibrational energy of the diatomic molecule. Thus Thus for a fixed ℓ_i, J_i, and J_{iz} Equation (5.13) becomes

$$\sigma(\mathcal{J},\mathcal{J}_z|a,E) = \left(\frac{\pi\hbar^2}{2\mu_i E_i}\right) \sum_{\ell_i=\ell_{min}(\mathcal{J},a)}^{\ell_{max}(\mathcal{J},a)} (2\ell_i+1) \cdot \frac{\delta(J_{iz}-\mathcal{J}_z)}{n(\ell_i,0,a,E)}, \tag{5.18}$$

where limits on ℓ_i are obtained from the two criteria discussed above and are given by

$$\ell_{max}(\mathcal{J},a) = \min \begin{cases} L_{max}(a,E) \\ |\mathcal{J}+J_i| \end{cases} \tag{5.19}$$

and

$$\ell_{min}(\mathcal{J},a) = |\mathcal{J} - J_i|.$$

When $J_i = 0$, the sum over ℓ_i in Equation (5.18) reduces to a single term and limits reduce to

$$\ell_{max}(\mathcal{J},a) = \min \{ {}^{L_{max}(a,E)}_{\mathcal{J}}$$

and

$$\ell_{min}(\mathcal{J},a) = \mathcal{J}.$$

$L_{max}(a,E)$ is given by Equation (5.16a). Under these conditions $\ell_i = \ell_{min} = \ell_{max} = L_{max} = \mathcal{J}$ and Equation (5.18) becomes

$$\sigma(\mathcal{J},\mathcal{J}_z|a,E) = \left(\frac{\pi\hbar^2}{2\mu_i E_i}\right) (2 L_{max} + 1).$$

$n(\ell_i,0,a,E)$ in Equation (5.18) is given by

$$n(\ell_i,0,a,E) = \mathcal{J}_{max} - \mathcal{J}_{min}$$

or

$$n(\ell_i,0,J_i,v_i,E) = |\ell_i+J_i| - \max \{ {}^{|\ell_i-J_i|}_{|J_{iz}|} + 1.$$

+ 1 is included in order to satisfy the boundary condition, i.e., when $J_i = 0$, $n(\ell_i,0,J_i,v_i,E) = 1$, and Equation (5.18) can be written in simplified form as

$$\sigma(\mathcal{J},\mathcal{J}_z|a,E) = \left(\frac{\pi\hbar^2}{2\mu_i E_i}\right) \sum_{\ell_{min}(\mathcal{J},a)}^{\ell_{max}(\mathcal{J},a)} \frac{(2\ell_i + 1)}{(|\ell_i+J_i| - \max\{ {}^{|\ell_i-J_i|}_{|J_{iz}|} + 1}.$$

(5.20)

We note from the above equations that the cross section for the formation of a complex of given $\mathcal{J}_z$ is determined not by the entire range of $\mathcal{J}$ but by the range of J_{iz}, i.e., in the complex the entire zth component of the angular momentum is determined by the zth component of the initial rotation of the diatomic. Since

$$\mathcal{J}_z = J_{iz} + \ell_{iz} \qquad (\ell_{iz} = 0)$$

$$\therefore \mathcal{J}_z = J_{iz}$$

The cross section for decomposition into state $|b,\ell_f,m_f\rangle$ is not independent of m_f. This, of course, leads to the final distributions which are symmetric about $\pi/2$ but not isotropic in the center of mass.

We are interested in the calculation of $\sigma(v_f,J_f,J_{fz} \longleftarrow v_i,J_i,J_{iz})$, the cross section which depends only on v, J, and J_z. For this Equation (5.10) can be rewritten as

$$\sigma(v_f,J_f,J_{fz} \longleftarrow v_i,J_i,J_{iz}) = \sum_{\ell_f} \sum_{m_f} \sum_{\mathcal{J}} P(\ell_f,m_f,v_f,J_f,J_{fz} \cdot |\mathcal{J},\mathcal{J}_z,E) \cdot \sigma(\mathcal{J},\mathcal{J}_z|v_i,J_i,J_{iz},E)$$

$$= \sum_{\mathcal{J}} \sum_{\ell_{fmin}}^{\ell_{fmax}} \sum_{m_f} \frac{\sigma(\mathcal{J},\mathcal{J}_z|v_i,J_i,J_{iz},E)}{N(\mathcal{J},E)}, \quad (5.21)$$

where limits on $\mathcal{J}$ are:

$$\mathcal{J}_{min} = 0$$

$$\mathcal{J}_{max} = J_i + L_{max}(a,E);$$

limits on m_f are:

$$\mathcal{J}_z = J_{iz} + \ell_{iz} = J_{fz} + \ell_{fz} = J_{fz} + m_f,$$

$$(\text{since } \ell_{iz} = m_i = 0;\ \ell_{fz} = m_f),$$

$$\therefore\ m_f = J_{iz} - J_{fz}.$$

For a given value of J_{iz} and J_{fz}, m_f^{Σ} reduces to a single term, and can be used to define limits on ℓ_f.

By combining Equations (5.20) and (5.21), we get

$$\sigma(v_f,J_f,J_{fz} \leftarrow v_i,J_i,J_{iz}) = \sum_{\mathcal{J}} \ell_f^{\Sigma} \frac{1}{N(\mathcal{J},E)} \cdot \left(\frac{\pi\hbar^2}{2\mu_i E_i}\right) \cdot \ell_i^{\Sigma} \frac{(2\ell_i + 1)}{(|\ell_i+J_i|-\max\{^{|\ell_i-J_i|}_{|J_{iz}|} + 1},$$

and differential cross section $d\sigma(\theta)$ can be expressed as

$$d\sigma_{v_f J_f J_{fz} \leftarrow v_i J_i J_{iz}}(\theta) = \left(\frac{\pi\hbar^2}{2\mu_i E_i}\right) \sum_{\mathcal{J}} \frac{1}{N(\mathcal{J},E)} \cdot \ell_i^{\Sigma} \frac{(2\ell_i+1)}{(|\ell_i+J_i|-\max\{^{|\ell_i-J_i|}_{|J_{iz}|} + 1} \ell_f^{\Sigma} |Y^{m_f}_{\ell_f}|^2. \quad (5.22)$$

This is the most significant expression which will be used for the calculation of the differential cross section. The differential cross section dependent only on J_f, the rotational angular momentum of final diatomic molecule, can be written as

$$d\sigma(J_f,\theta) = \frac{1}{(2J_i+1)} \sum_{v_f,J_{fz}} d\sigma_{v_f,J_f,J_{fz} \leftarrow v_i,J_i,J_{iz}}(\theta) \tag{5.23}$$

and

$$d\sigma(E_f,\theta) = d\sigma(J_f,\theta)\,\frac{dJ_f}{dE_f}$$

where E_f is final translational energy. From Equation (5.17)

$$\frac{dJ_f}{dE_f} = \frac{2\,\mu_o r_o^2}{(2J_f+1)\hbar^2} = \frac{I_f}{(2J_f+1)\hbar^2}$$

where I_f is the moment of inertia of the final diatomic molecule.

$$\therefore\ d\sigma(E_f,\theta) = d\sigma(J_f,\theta)\,\frac{I_f}{(2J_f+1)\hbar^2}\ . \tag{5.24}$$

Spherical Harmonics: $Y_\ell^m(\theta,\Phi)$

The exact quantum mechanical expression for evaluating spherical harmonics is given by (27)

$$Y_\ell^m(\theta,\Phi) = (-)^m(i)^\ell\left[\frac{(2\ell+1)}{4\pi}\cdot\frac{(\ell-m)!}{(\ell+m)!}\right]^{\frac{1}{2}}\exp(im\Phi)\cdot P_\ell^m(\cos\theta) \tag{5.25}$$

where $P_\ell^m(\cos\theta)$, the associated legendre polynomial, is given by

$$P_\ell^m(\cos\theta) = (-)^{\ell+m}\frac{(\ell+m)!}{2^\ell\,\ell!(\ell-m)!}(\sin\theta)^{-m}\cdot\left(\frac{d}{d\cos\theta}\right)^{\ell-m}(\sin\theta)^{2\ell}.$$

If Equation (5.25) is used for the calculation of spherical harmonics, the limits on ℓ and m while summing the expression for differential cross section will be as follows.

Limit on ℓ:

$$\ell_{fmax} = \min \begin{cases} L_{max}(b,E) \\ |\mathcal{J}+J_f| \end{cases}$$

$$\ell_{fmin} = |\mathcal{J}-J_f| \qquad (5.26)$$

Limit on m:

since $\mathcal{J}_z = \ell_{iz}+J_{iz} = \ell_{fz}+J_{fz}$

or $\mathcal{J}_z = J_{iz} = m_f+J_{fz}$ (as $\ell_{iz} = m_i = 0$ and $\ell_{fz} = m_f$

or $m_f = J_{iz}-J_{fz}$ (5.27)

J_{fz} can take values from $+J_f$ to $-J_f$. For a given value of J_{iz}, m_f can take values from $J_{iz}-J_f$ to $J_{iz}+J_f$. Moreover m_f can also take values from $-\ell_f$ to $+\ell_f$.

Limits on m_f are given by

$$(m_f)_{max} = \min \begin{cases} J_{iz}+J_f \\ +\ell_f \end{cases}$$

$$(m_f)_{min} = \max \begin{cases} J_{iz}-J_f \\ -\ell_f \end{cases} .$$

But this quantum mechanical expression (Equation 5.25) for the calculation of spherical harmonics is not very handy when one sums over all ℓ's and m's using Gaussian quadrature

technique. For this we have used a classical expression which was derived by the WKB method. According to that, $Y_\ell^m(\theta,\Phi)$ can be given by (28)

$$Y_\ell^m(\theta,\Phi) \cong \pi^{-1}\exp(im\Phi)(1-\mu^2-z^2)^{-\frac{1}{4}} \cdot \left[\cos\left[(\ell+\tfrac{1}{2})\int_0^z (1-x^2)^{-1}(1-\mu^2-x^2)^{\frac{1}{2}}dx - (\ell+m)\frac{\pi}{2}\right]\right] \tag{5.28}$$

where $\mu=\frac{m}{\ell}$, $z=\cos\theta$, and $\ell>>1$. In $\Phi = 0$ plane, Equation (5.28) becomes

$$Y_\ell^m(\theta,0) \cong \frac{1}{\pi}\frac{\cos\left[(\ell+\tfrac{1}{2})\int_0^z (1-x^2)^{-1}(1-\mu^2-x^2)^{\frac{1}{2}}dx-(\ell+m)\frac{\pi}{2}\right]}{(1-\mu^2-z^2)^{\frac{1}{4}}}$$

or

$$|Y_\ell^m(\theta,0)|^2 \cong \frac{1}{\pi^2}\frac{\cos^2\left[(\ell+\tfrac{1}{2})\int_0^z (1-x^2)^{-1}(1-\mu^2-x^2)^{\frac{1}{2}}dx-(\ell+m)\frac{\pi}{2}\right]}{(1-\mu^2-z^2)^{\frac{1}{2}}} \tag{5.29}$$

Replacing the square of cosine term by its average value $\frac{1}{2}$, Equation (5.29) becomes

$$|Y_\ell^m(\theta,0)|^2 \simeq \frac{1}{2\pi^2}\frac{1}{(1-\mu^2-z^2)^{\frac{1}{2}}} \simeq \frac{1}{2\pi^2}\frac{1}{(1-(m/\ell)^2-\cos^2\theta)^{\frac{1}{2}}} \tag{5.30}$$

If the above classical expressions are used to calculate spherical harmonics, limits on ℓ and m while summing will be as follows.

Limits on ℓ:

From Equation (5.30) we get

$$1 - \frac{m^2}{\ell^2} - \cos^2\theta > 0$$

or $$\ell^2(1-\cos^2\theta) > m^2$$

or $$\ell > \frac{m}{(1-\cos^2\theta)^{\frac{1}{2}}} ;$$

i.e., $$\ell_{min} = m/(1-\cos^2\theta)^{\frac{1}{2}} = m \text{ cosec } \theta$$

and $$\ell_{max} = \min \{ L_{max}(b,E) \; , \; |\mathcal{J}+J_f| \} .$$

Limits on m:

Limits on m_f can be obtained from Equation (5.27) as

$$m_f = J_{iz} - J_{fz}$$

which yields for a given value of J_{iz}

$$(m_f)_{min} = J_{iz} - J_f$$

$$(m_f)_{max} = J_{iz} + J_f .$$

Moreover,

$$\mathcal{J} \geq |\ell_f - J_f|$$

or $$\ell_f \leq \mathcal{J} + J_f$$

and $$\ell_f > \frac{m_f}{(1-\cos^2\theta)^{\frac{1}{2}}} ;$$

so one can write

$$|\mathcal{J}+J_f|^2 \geq \ell_f^2 \geq \frac{m_f^2}{(1-\cos^2\theta)}$$

$$\text{or} \quad m_f \leq (\mathcal{J}+J_f)(1-\cos^2\theta)^{\frac{1}{2}}$$

$$\text{or} \quad m_f \leq |\mathcal{J}+J_f| \sin\theta$$

$$(m_f)_{max} = \min \begin{Bmatrix} (\mathcal{J}+J_f)\sin\theta \\ (J_{iz}+J_f) \end{Bmatrix} .$$

Similarly,

$$\mathcal{J} \geq |\ell_f - J_f|$$

$$\ell_f \leq (\mathcal{J} + J_f)$$

$$\text{or} \quad m_f > -(\mathcal{J} + J_f) \sin\theta$$

$$\therefore (m_f)_{min} = \max \begin{Bmatrix} -(\mathcal{J}+J_f)\sin\theta \\ J_{iz} - J_f \end{Bmatrix} .$$

In order to check the accuracy of Equation (5.30), which has been used in our calculations, a sample run was made for the calculation of

$$\sum_{\ell,m} |Y_\ell^m(\theta,0)|^2$$

by using (a) Equation (5.25), the exact quantum mechanical expression, and (b) Equations (5.29) and (5.30) for a case where $L_{max}(a,E) = 100$, $J_f = 50$, $J_{iz} = 10$, $\mathcal{J} = 50$, and $\theta = 30^o$. The values obtained are 770.37, 721.02, and 719.39 respectively, which looks quite good as the calculations done with Equation (5.30) were quite fast and saved a lot of computer time. Moreover the replacement of the square

of cosine term by its average value ($\frac{1}{2}$) does not affect our results as shown by above calculation.

Now the final expression for the differential cross section $d\sigma(J_b,\theta)$ can be written as

$$d\sigma(J_f,\theta) = \left[\frac{\pi\hbar^2}{2\mu_i E_i}\frac{1}{(2J_i+1)}\right]\sum_{\mathcal{J}}\frac{1}{N(\mathcal{J},E)}\sum_{J_{iz}}\sum_{\ell_i}(2\ell_i+1)$$

$$\cdot\ \frac{1}{(|\ell_i+J_i|-\max\{^{|\ell_i-J_i|}_{|J_{iz}|}+1)}\sum_{m_f}\sum_{\ell_f}|Y^{m_f}_{\ell_f}(\theta,0)|^2 \qquad (5.31)$$

and $d\sigma(E_f,\theta)$ as

$$d\sigma(E_f,\theta) = \left[\left[\frac{\pi\hbar^2}{2\mu_i E_i}\frac{1}{(2J_i+1)}\right]\sum_{\mathcal{J}}\frac{1}{N(\mathcal{J},E)}\sum_{J_{iz}}\sum_{\ell_i}(2\ell_i+1)\right.$$

$$\left.\cdot\ \frac{1}{(|\ell_i+J_i|-\max\{^{|\ell_i-J_i|}_{|J_{iz}|}+1)}\sum_{m_f}\sum_{\ell_f}|Y^{m_f}_{\ell_f}(\theta,0)|^2\right]\frac{I_f}{(2J_f+1)\hbar^2}\cdot \qquad (5.32)$$

Equation (5.32) will give differential cross section as a function of E_f, the relative final translational energy and θ, the angle at which products scatter after the reaction in the center of mass. In order to compare the results obtained by this theory with the experimental results obtained in the laboratory, the angular distribution as predicted by this theory in the laboratory is required. A detailed discussion on CM $\longrightarrow$ LAB conversion can be seen

elsewhere (13), but the main relationship is given by

$$I_{LAB}\ (v,\Theta) = (\frac{v}{u})^2\ I_{CM}(u,\theta),$$

where v is the LAB velocity and u is the velocity of the product in the CM. For this conversion we need $d\sigma(u,\theta)$, which is given by

$$d\sigma(u,\theta) = d\sigma(E_f,\theta) \cdot (\frac{\partial E_f}{\partial u}) \qquad (5.33)$$

since $E_f = \frac{1}{2}\mu_f V_f^2$ and $\mu_f V_f = M\ u$ (in CM),

$$\therefore\ E_f = \frac{1}{2}\ \mu_f\ (\frac{M\ u}{\mu_f})^2\ .$$

On differentiating E_f with respect to u, we get

$$\frac{\partial E_f}{\partial u} = \frac{M^2}{\mu_f}\ u,$$

where V_f is the final relative velocity, μ_f is the reduced mass of final atom-diatomic system, u is the velocity in the CM, M is the mass of the product, and Θ is the angle in the LAB system where the products scatter after the reaction. Equation (5.33) can be written as

$$d\sigma(u,\theta) = d\sigma(E_f,\theta)\ (\frac{M^2\ u}{\mu_f}). \qquad (5.34)$$

Calculations were done by the procedure discussed in Chapter 4. $d\sigma(E_f,\theta)$ were calculated at four angles: 10^o, 30^o, 45^o, and 80^o. The plots of $d\sigma(E_f,\theta)$ against E_f were found to be quite smooth curves.

In order to use $d\sigma(E_f,\theta)$ in the CM $\rightarrow$ LAB transformation program, we need a mathematical expression which can generate these curves at all angles, i.e., a distribution function is required in E_f or u as a function of θ. For this we assume a two dimensional linear extrapolation in θ and E_f as

$$d\sigma(E_f,\theta) = \frac{(E_f-E_f2)\ (\theta-\theta2)}{(E_f1-E_f2)(\theta1-\theta2)}\ d\sigma(E_f1,\theta1)$$

$$+ \frac{(E_f1-E_f)(\theta-\theta2)}{(E_f1-E_f2)(\theta1-\theta2)}\ d\sigma(E_f2,\theta1)$$

$$+ \frac{(E_f-E_f2)(\theta1-\theta)}{(E_f1-E_f2)(\theta1-\theta2)}\ d\sigma(E_f1,\theta2)$$

$$+ \frac{(E_f1-E_f)(\theta1-\theta)}{(E_f1-E_f2)(\theta1-\theta2)}\ d\sigma(E_f2,\theta2)$$

where values of E_f and θ lie between (E_f1 and E_f2) and ($\theta1$ and $\theta2$).

The calculation for the differential cross-section $d\sigma(E_f,\theta)$ has been done for four systems, namely reactions of barium with chlorides and iodides of potassium and cesium. The values of the physical quantities used in these calculations are listed in Tables 6 and 7.

Results

From Equation (5.17) we see that for a given E, the total energy and v_f, the final vibrational quantum number, the final translational energy E_f is directly related to the final rotational quantum number J_f. The differential

Table 6. Values of Physical Constants

	r_e Å	D_o kcals	d_2 D	E as used in London Formula eV	$\alpha(Å^3)$
Ba				4.036[c]	34.0
K				1.61	45.2(29)
Cs				1.45(31)	63.3(30)
Ba^+					2.70
K^+					0.9
Cs^+					2.5
Cl^-					3.0
I^-					7.0
KI	3.0478(22)	78.5	11.05	6.041[b]	5.567
CsCl	2.91	105.5	10.38	6.17[b]	4.5
BaCl	2.588	115.0	9.21	7.75[b]	4.70[a]
CsI	3.32	81.5	12.1	5.660[b]	7.167[a]
BaI	3.0	88.0	11.25	7.098[b]	7.367

[a]Estimated as ($\alpha_{MX} = \alpha_{M^+} + \frac{2}{3} \alpha_{X^-}$).

[b]Estimated as E_{MX} = (I.P. of M + $\frac{1}{2}$ dissociation energy of MX).

[c]For a $6S^2 \rightarrow 6S\ 7P$ resonance line.

Table 7. Vibrational Frequency

	ω_e cm^{-1}	$\omega_e x_e$ cm^{-1}
KI	186.53	0.574
CsCl	214.2	0.74
CsI	119.2	0.254
BaI	154.0(32)	0.31[a]
BaCl	279.3	0.89

[a]Our estimate.

cross section $d\sigma(E_f, v_f, \theta)$ or $d\sigma(J_f, v_f, \theta)$ for a given value of v_f and θ is plotted against E_f for the four systems in Figs. 12, 13, 14, and 15. One can see that as the vibrational quantum number v_f increases, the area under the curve decreases. This appears reasonable since an increase in vibrational energy decreases the translational energy of the products and, therefore, the cross section. The differential cross section $d\sigma(E_f, \theta)$ is obtained by summing of $d\sigma(E_f, v_f, \theta)$ over all possible v_f and is plotted against E_f for different values of θ in Figs. 16, 17, 18, and 19. The data on these figures are used to obtain the LAB distribution of the product atom or diatomic. The LAB distributions are shown in Figs. 20, 21 22, 23, and 24. Notice that each distribution is characterized by two peaks. Computer program used is listed in Appendix B.

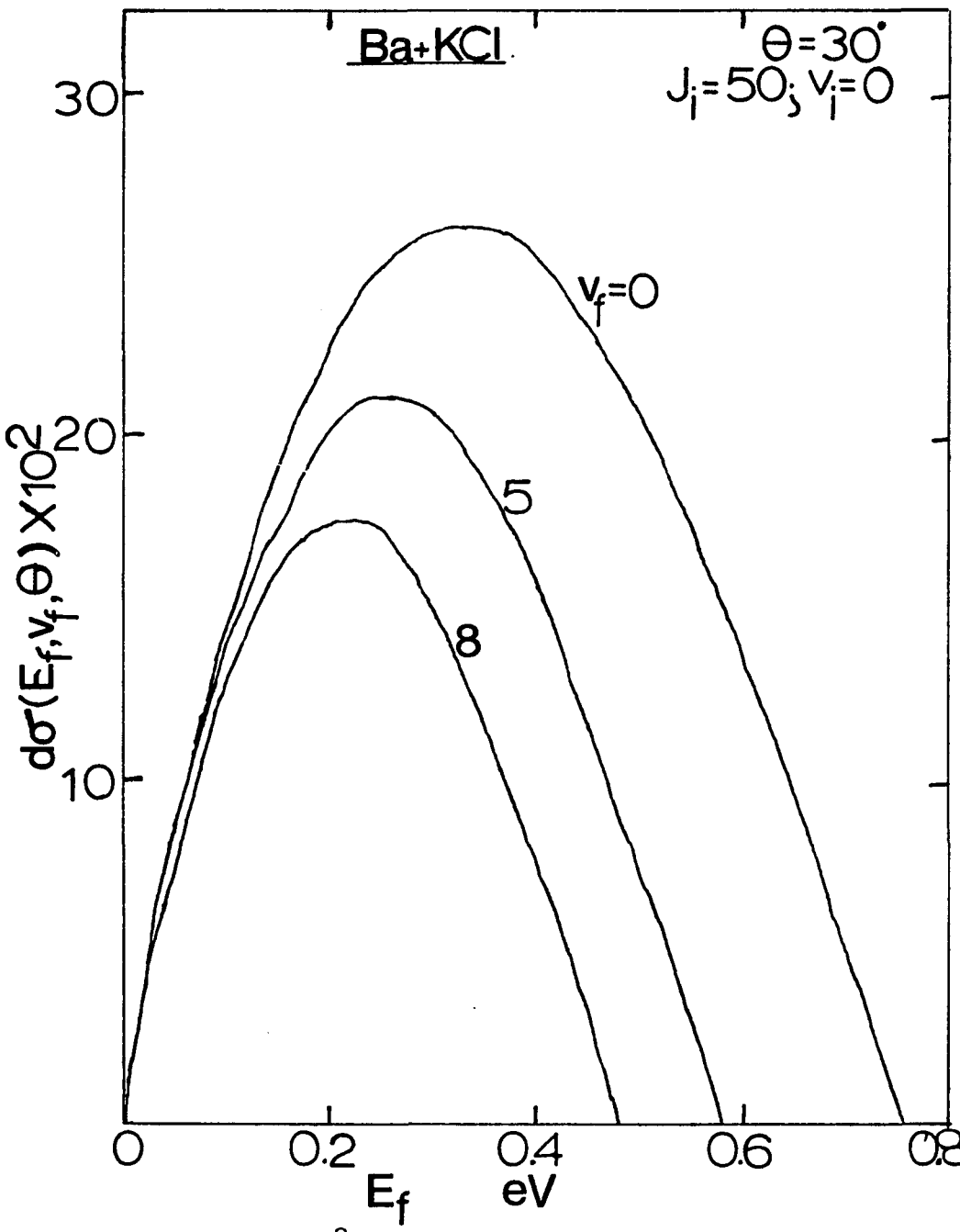

Fig. 12. $d\sigma(E_f, v_f, \theta)(\text{Å}^2/\text{str})$ plotted against E_f, the final relative translational energy for v_f = 0, 5, and 8 for the Ba + KCl reaction.

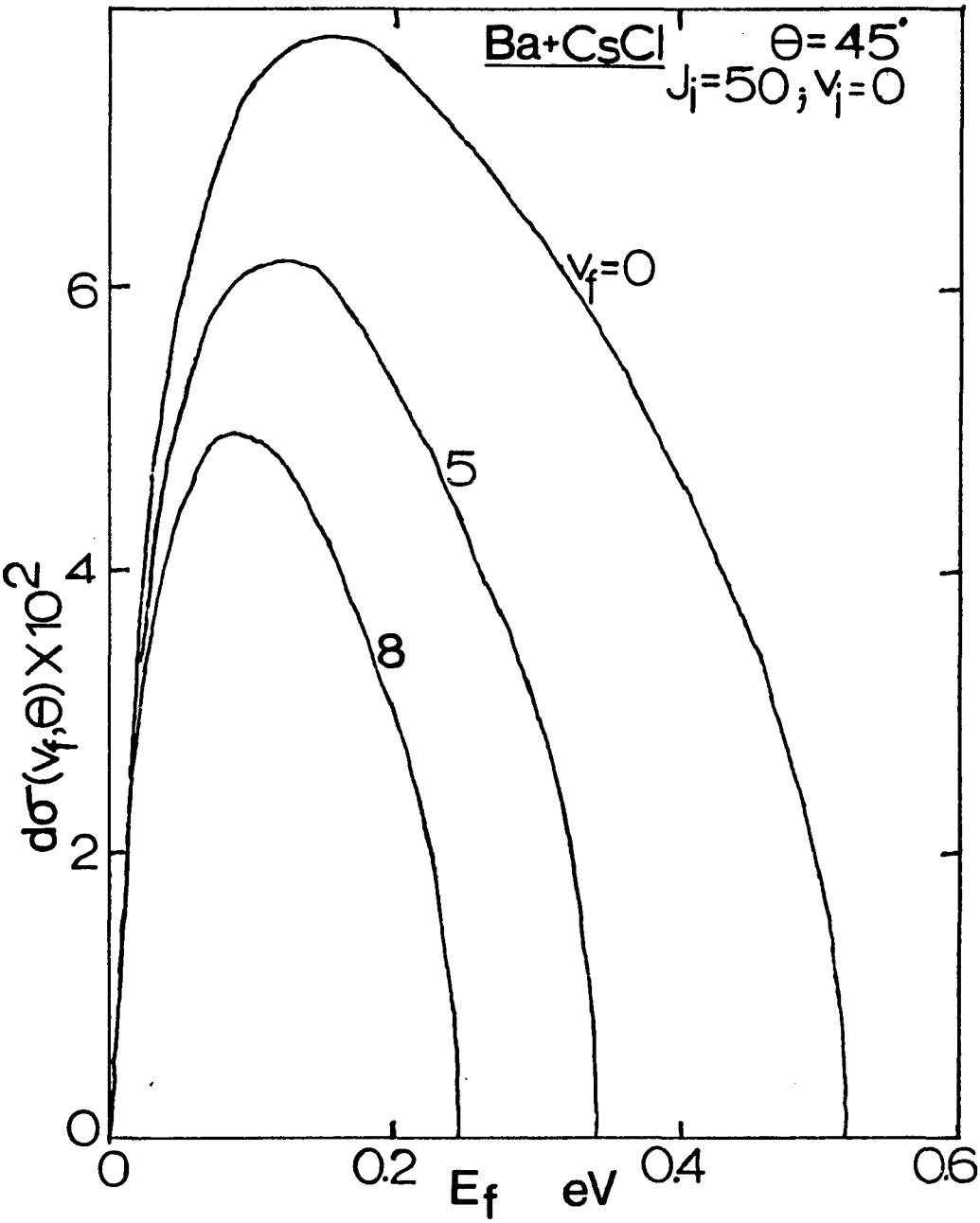

Fig. 13. $d\sigma(E_f, v_f, \theta)(\text{Å}^2/\text{str})$ plotted against E_f, the final relative translational energy for v_f = 0, 5, and 8 for the Ba + CsCl reaction.

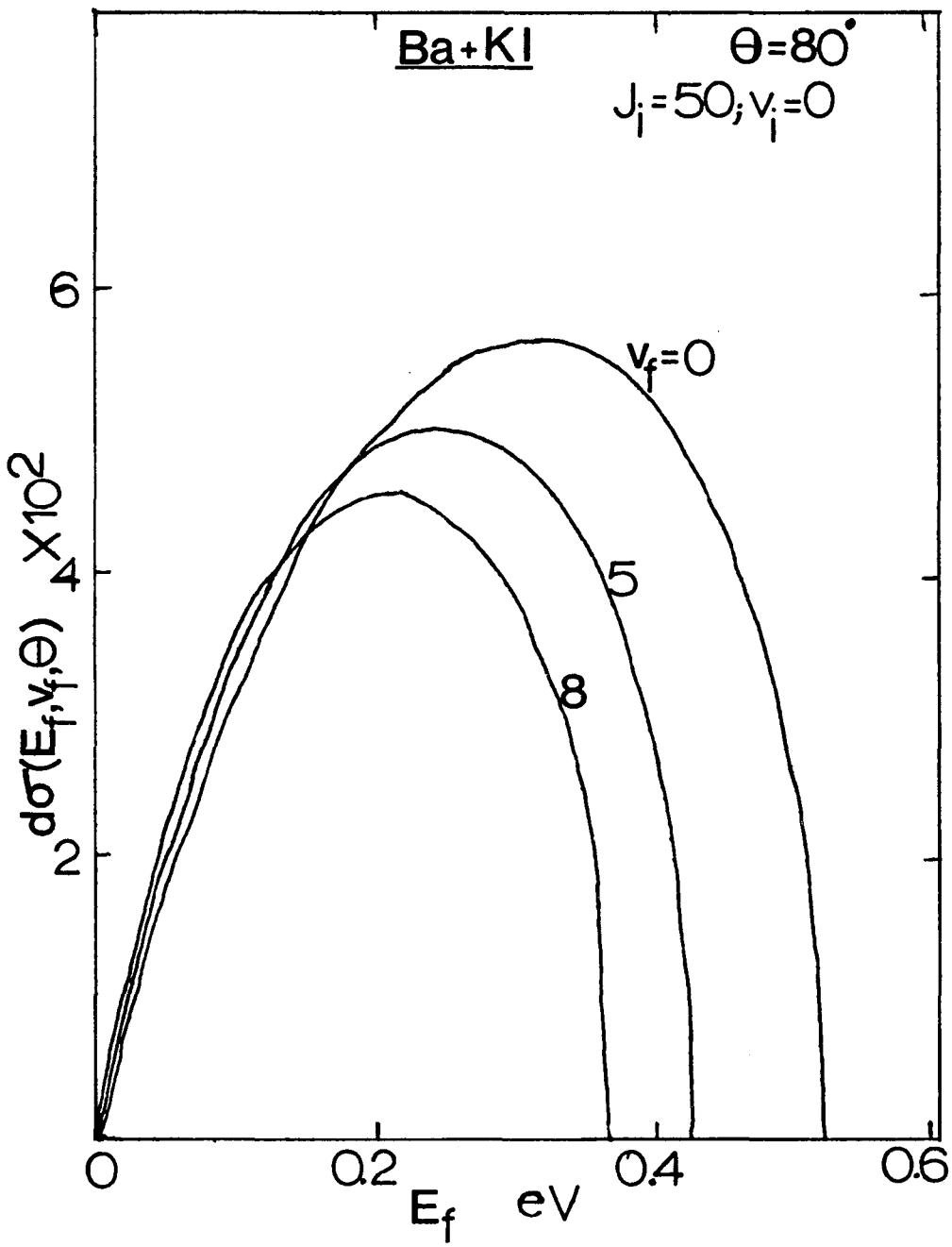

Fig. 14. $d\sigma(E_f, v_f, \theta)(\text{Å}^2/\text{str})$ plotted against E_f, the final relative translational energy for v_f = 0, 5, and 8 for the Ba + KI reaction.

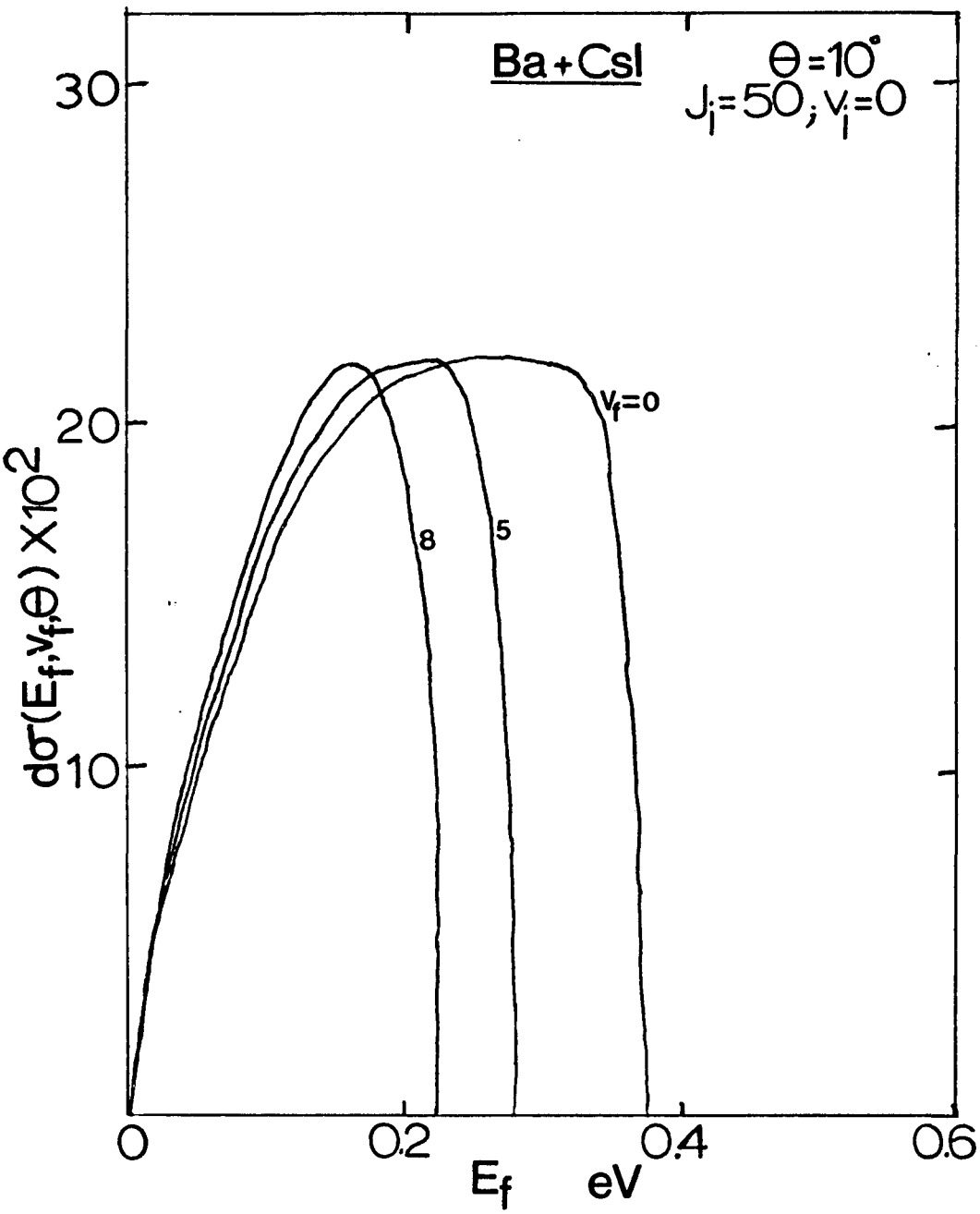

Fig. 15. $d\sigma(E_f, v_f, \theta)(\text{Å}^2/\text{str})$ plotted against E_f, the final relative translational energy for v_f = 0, 5, and 8 for the Ba + CsI reaction.

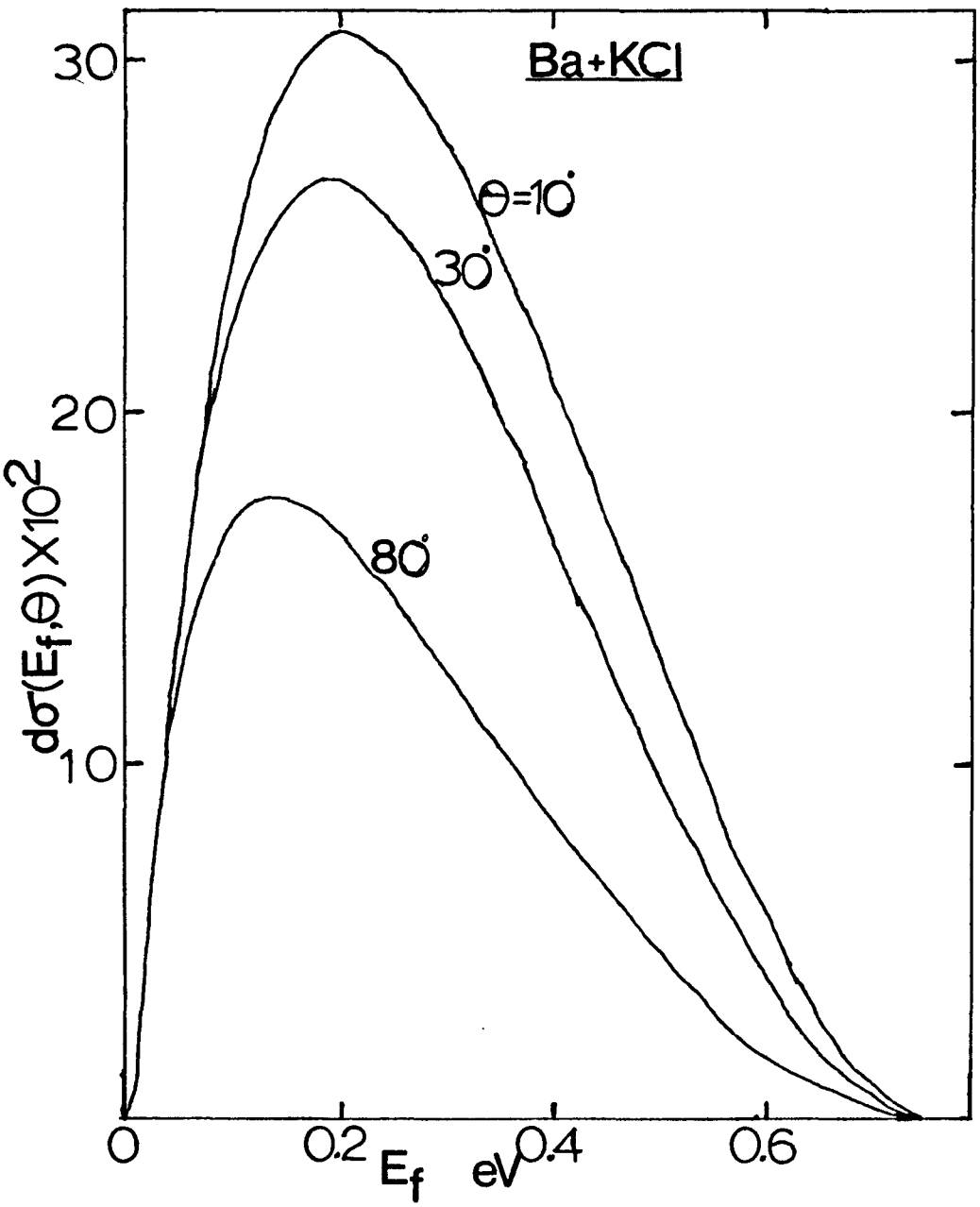

Fig. 16. $d\sigma(E_f,\theta)(\text{Å}^2/\text{str})$ plotted against E_f, the final relative translational energy at angles $\theta = 10^\circ$, 30°, and 80° for the Ba + KCl reaction.

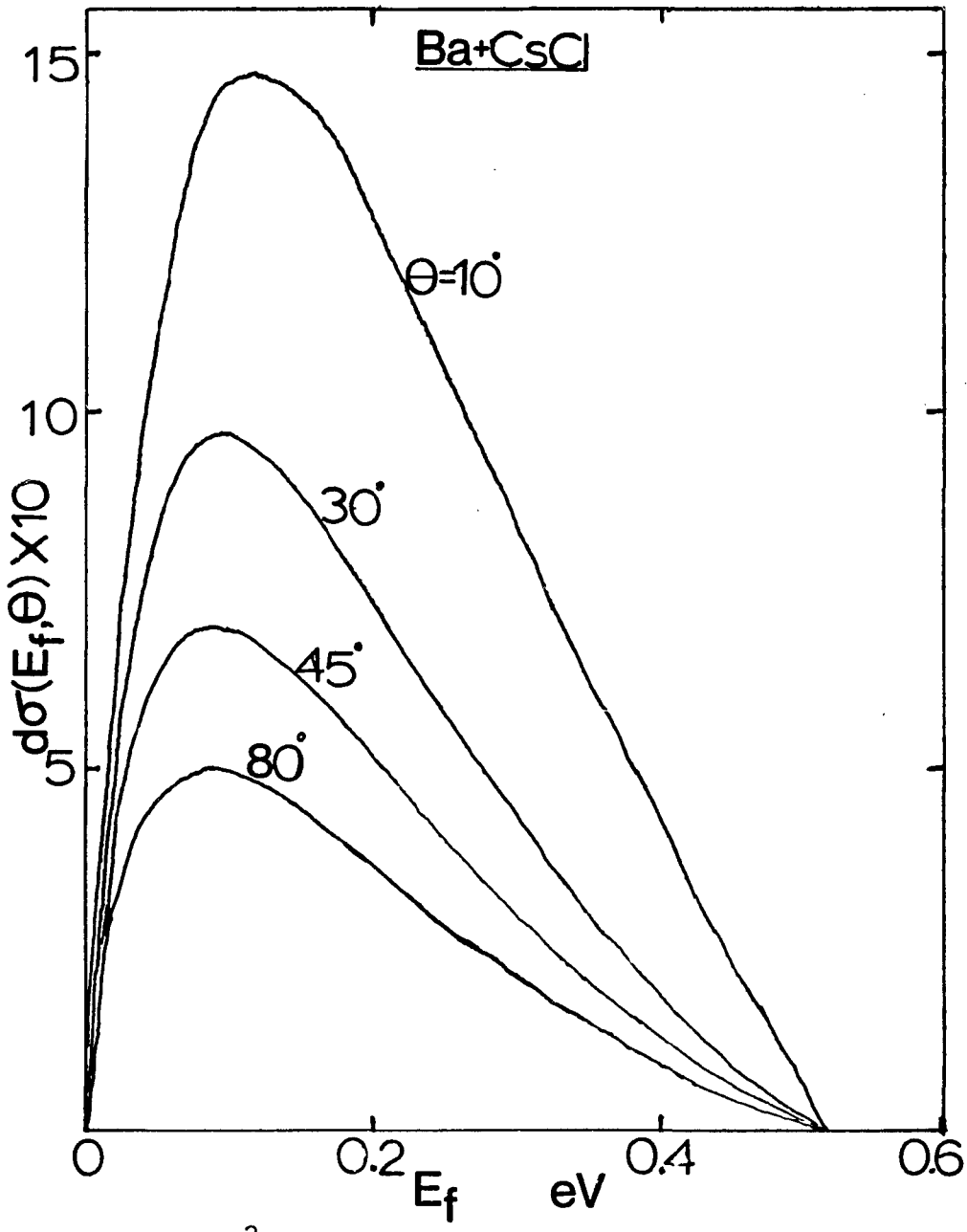

Fig. 17. $d\sigma(E_f,\theta)(\text{Å}^2/\text{str})$ plotted against E_f, the final relative translational energy at angles $\theta = 10^\circ$, 30°, 45°, and 80° for the Ba + CsCl reaction.

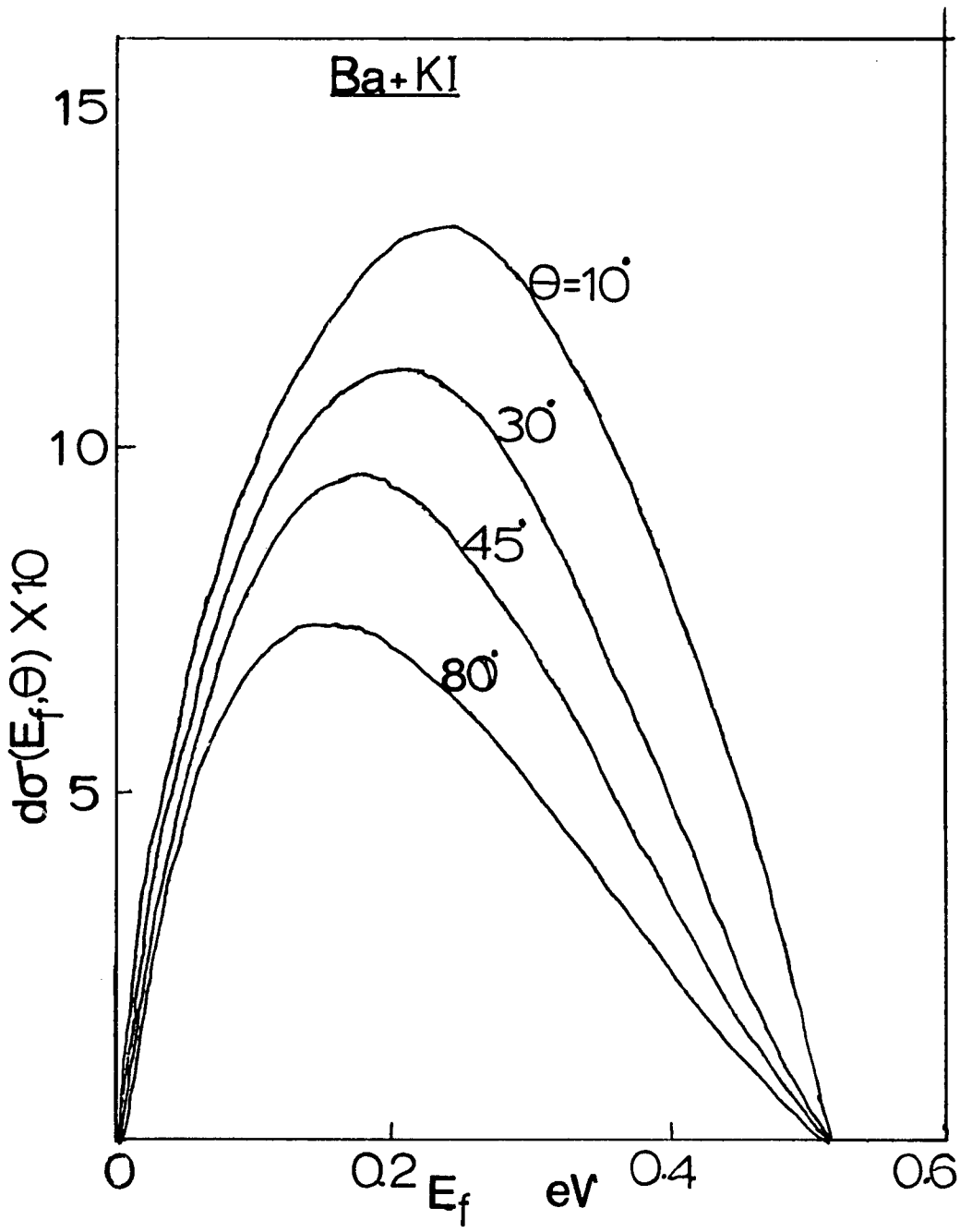

Fig. 18. $d\sigma(E_f,\theta)(\text{Å}^2/\text{str})$ plotted against E_f, the final relative translational energy at angles $\theta = 10^\circ$, 30°, 45°, and 80° for the Ba + KI reaction.

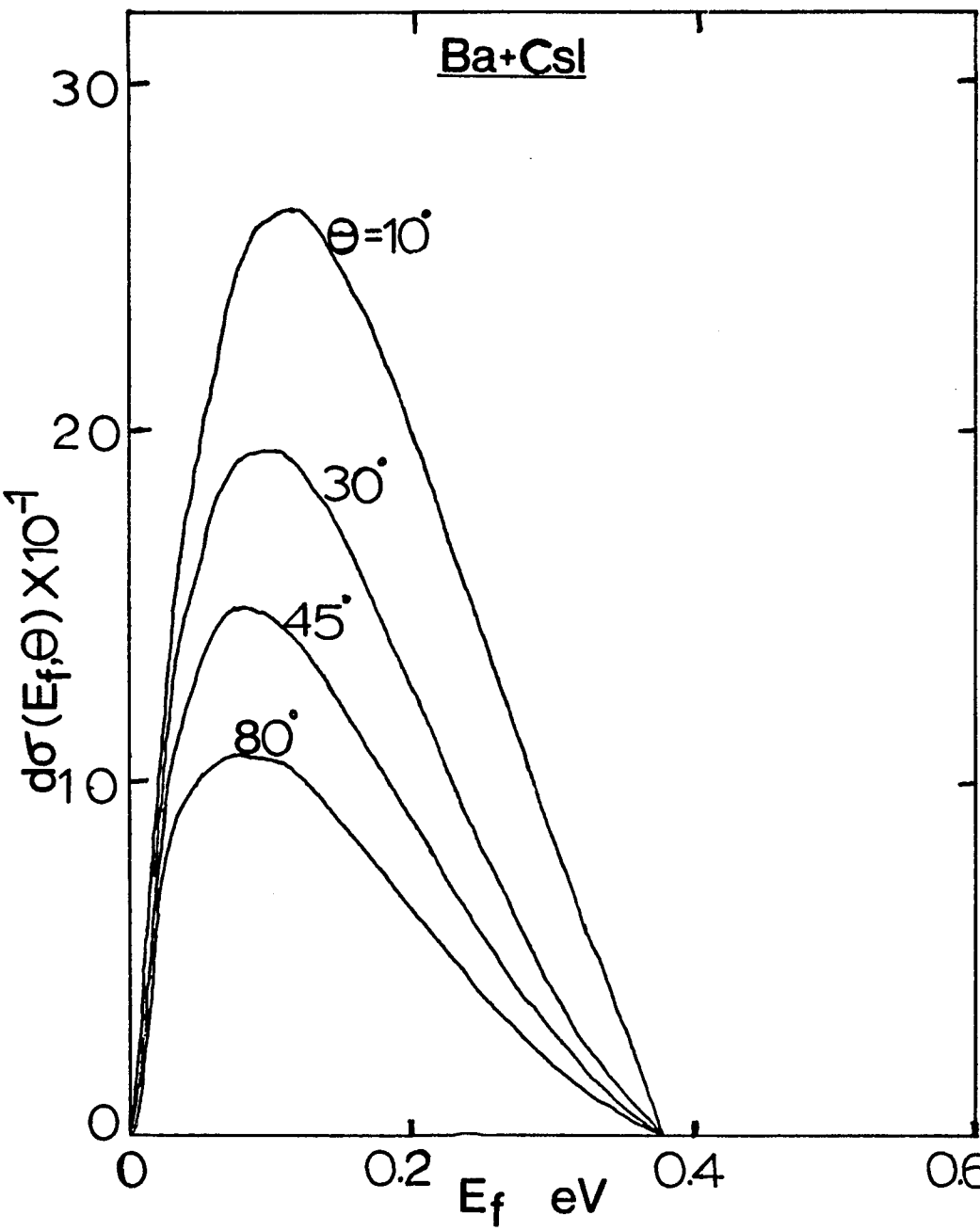

Fig. 19. $d\sigma(E_f,\theta)(\text{Å}^2/\text{str})$ plotted against E_f, the final relative translational energy at angles $\theta = 10^\circ$, 30°, 45°, and 80° for the Ba + CsI reaction.

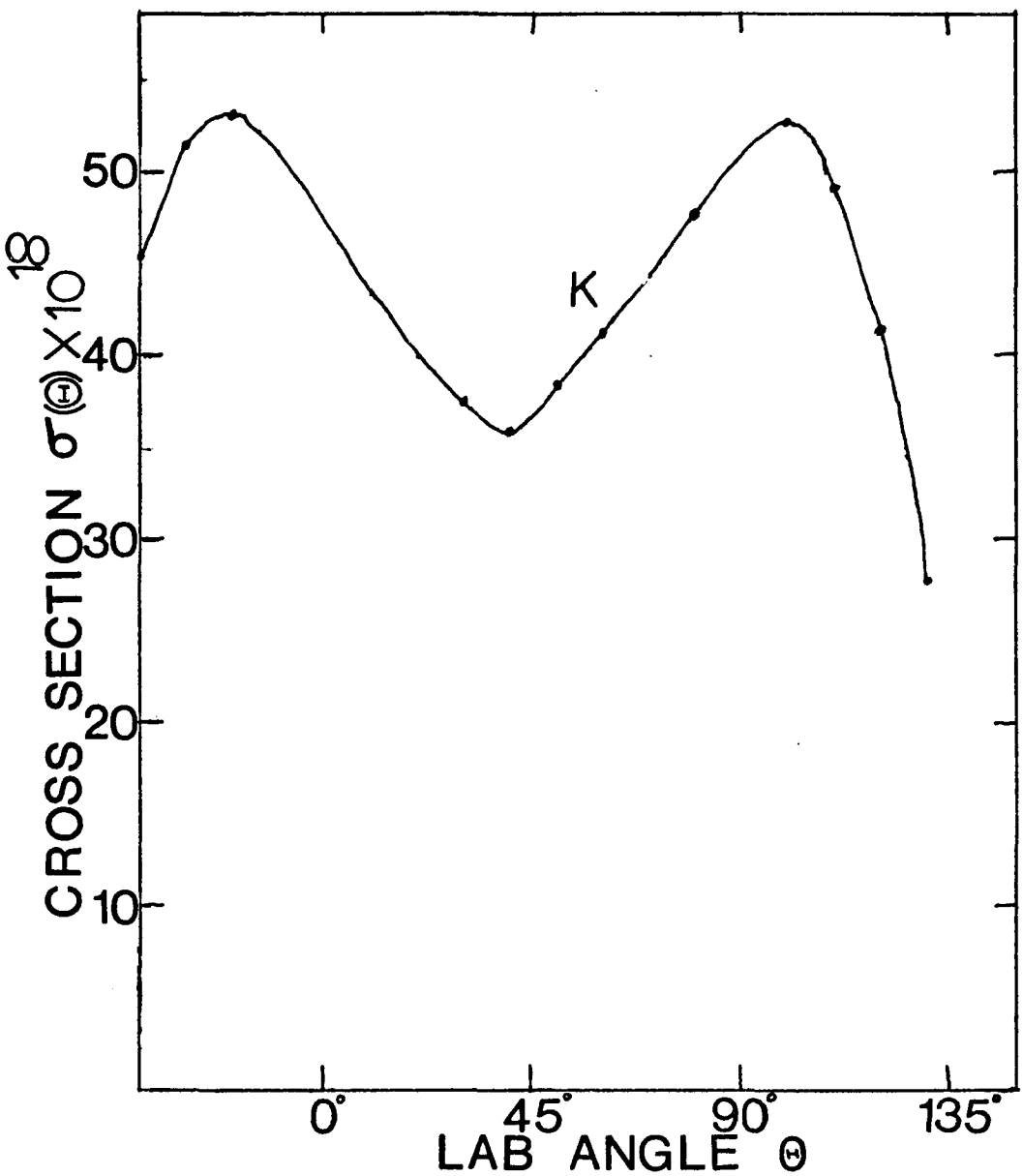

Fig. 20. Laboratory distribution of K (expressed in cm^2/str) in Ba + KCl → BaCl + K reaction -- E_i = 0.085 eV; v_i = 0; J_i = 50.

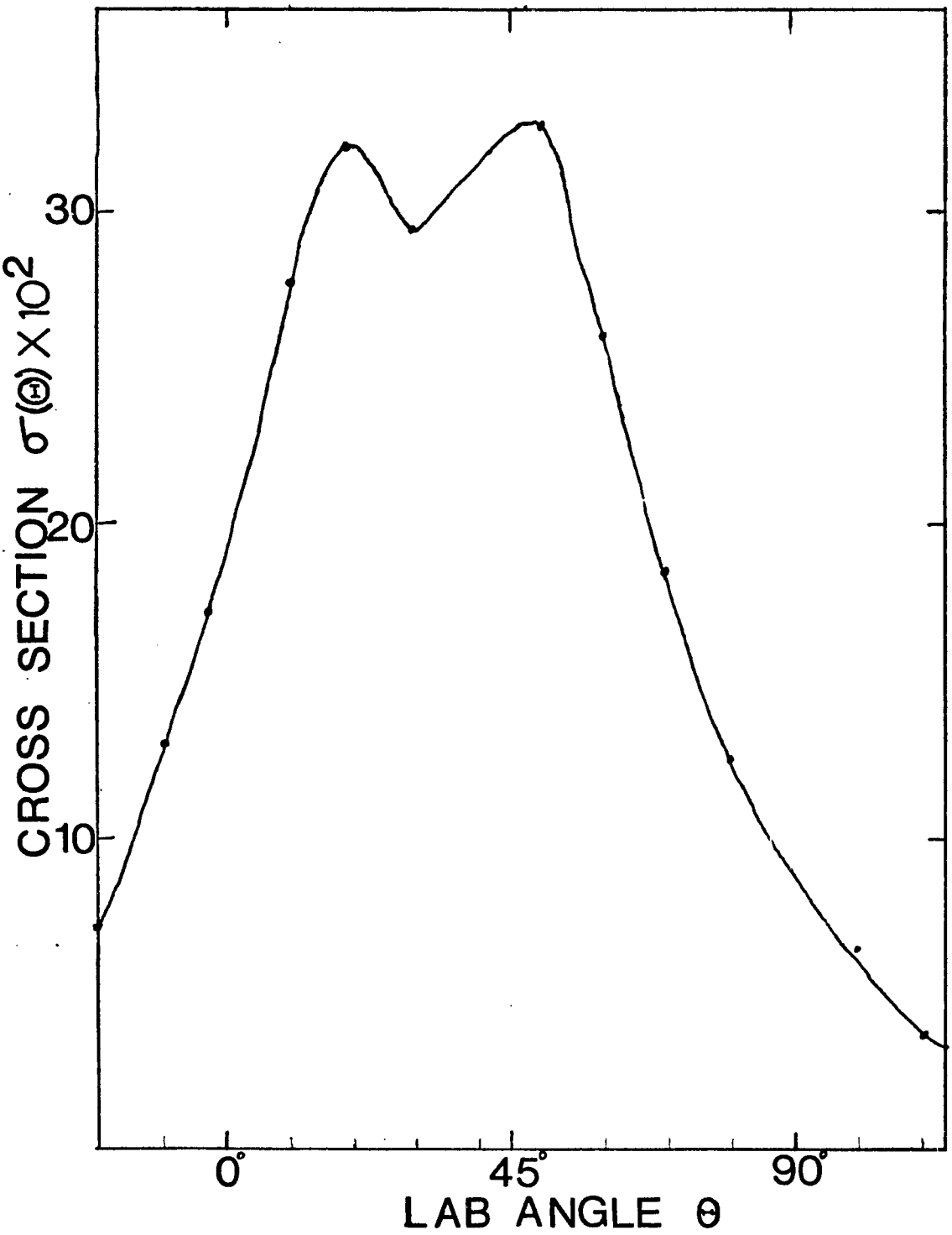

Fig. 21. Laboratory distribution of BaCl (expressed in $\mathring{A}^2$/str) in Ba + KCl → BaCl + K reaction -- E_i = 0.085 eV; v_i = 0; J_i = 50.

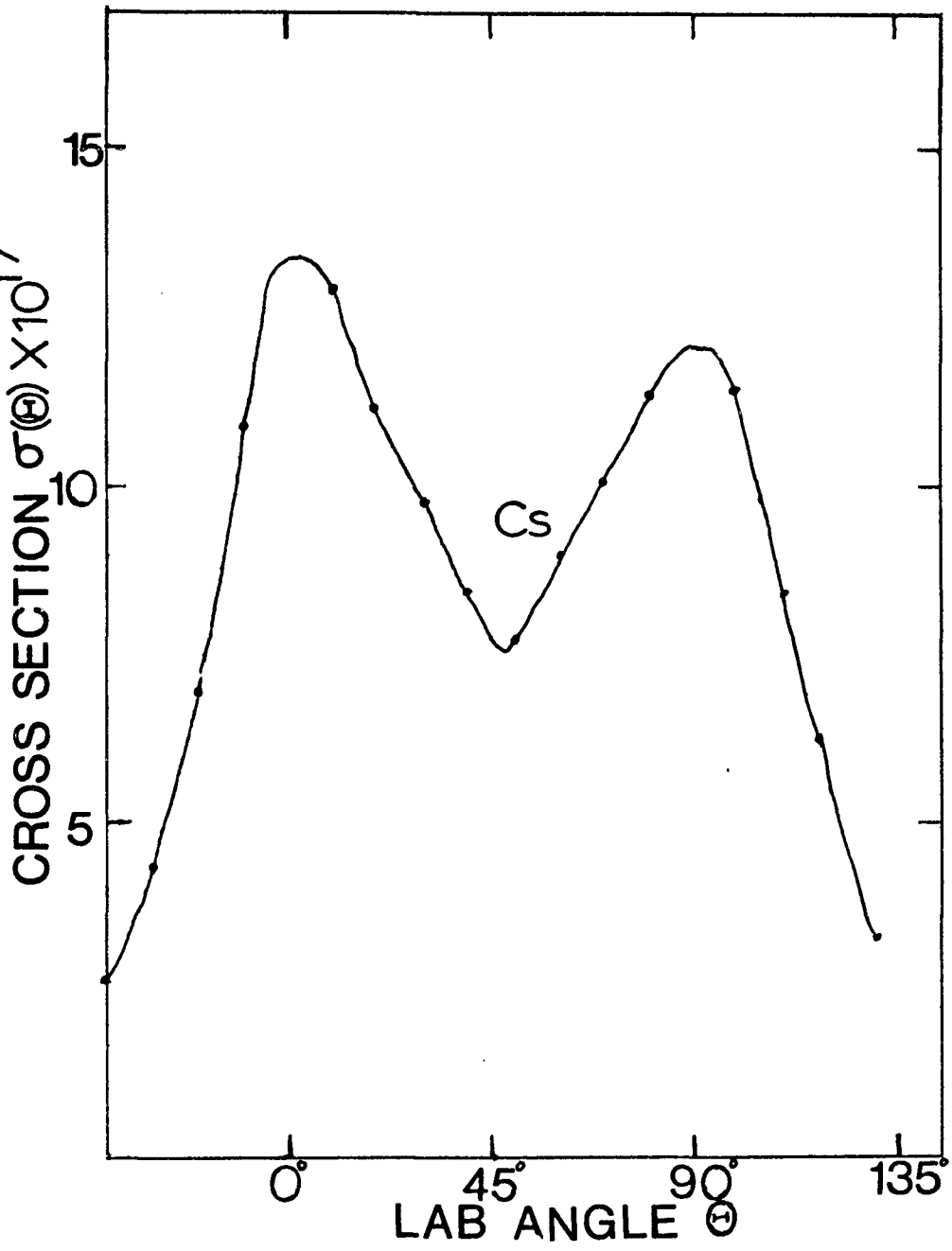

Fig. 22. Laboratory distribution of Cs (expressed in cm^2/str) in Ba + CsCl $\rightarrow$ BaCl + Cs reaction -- E_i = 0.085 eV; v_i = 0; J_i = 50.

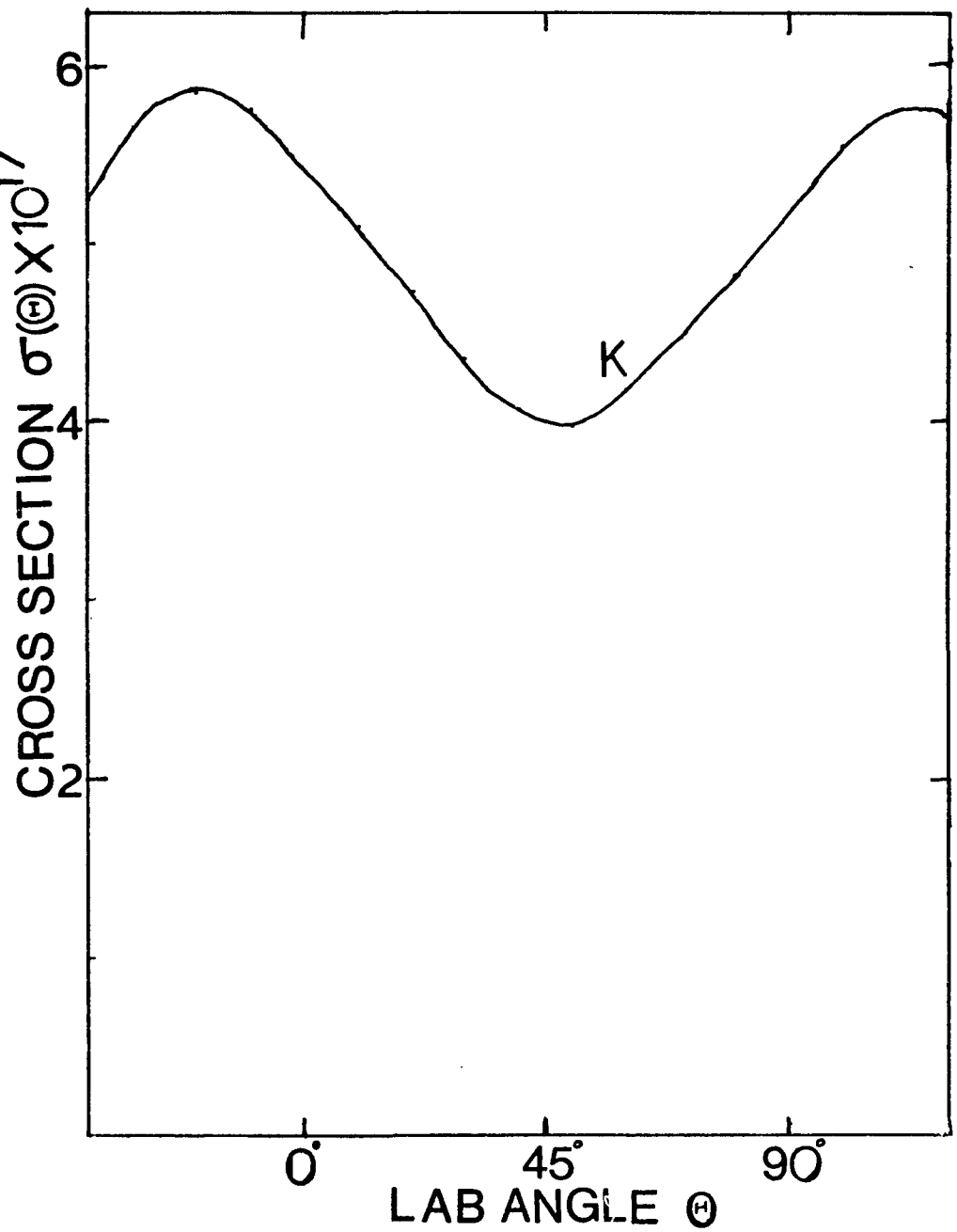

Fig. 23. Laboratory distribution of K (expressed in cm^2/str) in Ba + KI → BaI + K reaction -- E_i = 0.085 eV; v_i = 0; J_i = 50.

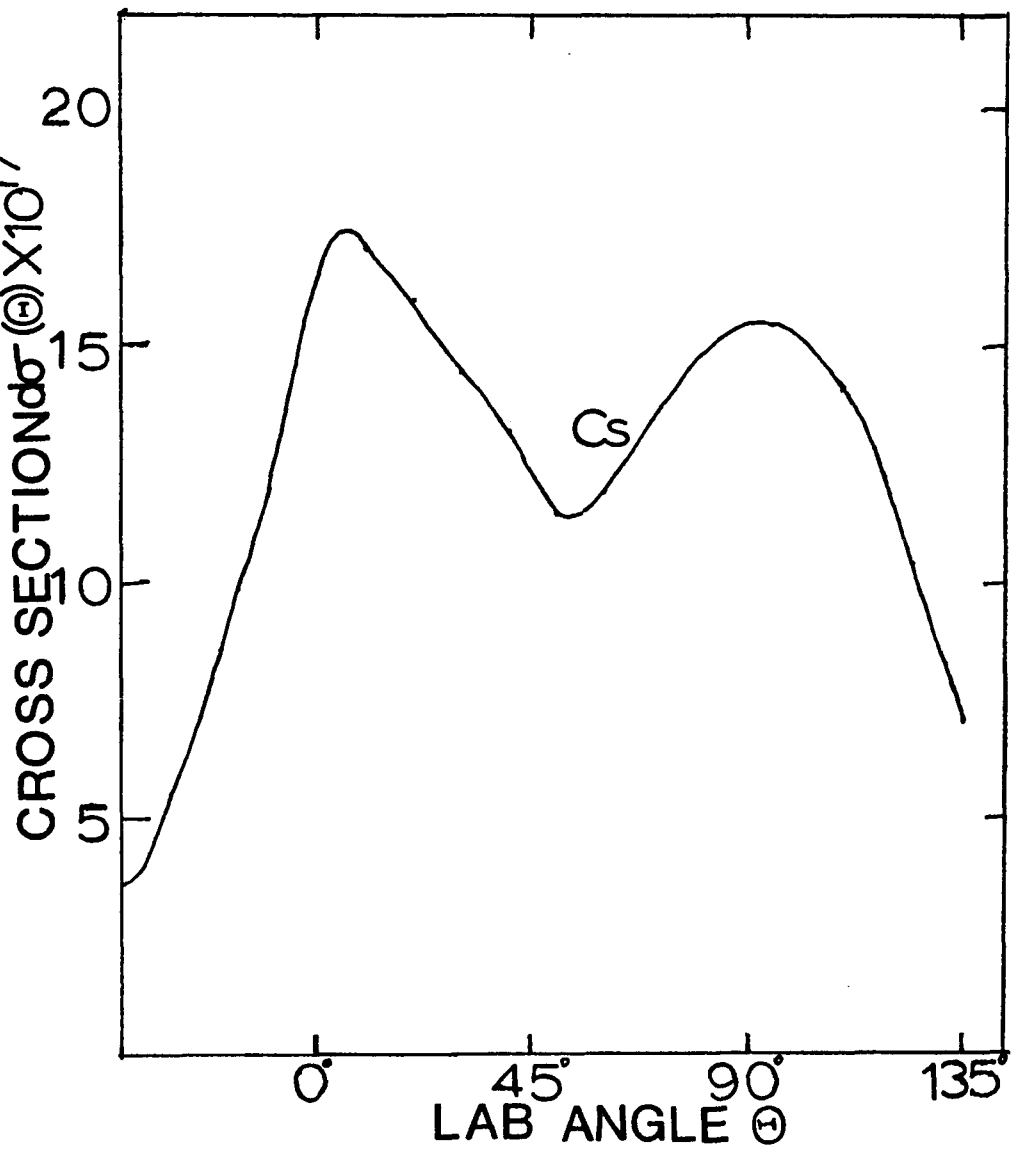

Fig. 24. Laboratory distribution of Cs (expressed in cm^2/str) in Ba + CsI → BaI + Cs reaction -- E_i = 0.085 eV; v_i = 0; J_i = 50.

CHAPTER 6

CONCLUSIONS

The purpose of this work has been to study the crossed molecular beam reactions whose exothermicities lie in the intermediate range. For this, the reactions of barium with the chlorides and iodides of potassium and cesium have been studied.

Angular distribution data, experimentally obtained for the reactions of barium with potassium chloride, cesium chloride, and potassium iodide, have provided a better understanding of these reactions. Experimental results indicate that these reactions belong to the osculating category, which means that the lifetime of the intermediate complex formed in these reactions must be in the region of 2-3 rotational periods as has been observed in similar reactions. Moreover, the lifetime of these complexes follow the order

$$[BaKCl]^{\dagger} > [BaCsCl]^{\dagger} > [BaKI]^{\dagger}$$

as has been determined by the best fit of parameters in an assumed CM function.

Theoretical studies on these reactions have also been carried out in order to estimate the total cross section and expected angular distribution. For this we

have used the statistical theory suggested by Pechukas et al. (10) and White and Light (11). This theory has predicted a fairly accurate angular distribution of products for reactions which proceed via long-lived complexes. We have used this theory to test whether it is possible to extend it to predict results for osculating reactions.

For the calculation of cross sections, we have followed the procedure suggested by Pechukas et al. (10). The numbers obtained for the cross sections appear reasonable.

For the calculation of the angular distributions we have essentially followed their theory but have used a somewhat different approach. The places where we have incorporated the simplifications are:

1. They have obtained the differential cross section as a function of final orbital angular momentum, ℓ_f, and its zth component, m_f, $d\sigma(\ell_f, m_f)$ and have used this function in the transformation of data from the center of mass coordinate to the laboratory coordinate. We have done this part in a simple way by obtaining differential cross sections as a function of final rotational quantum number, J_f, or as a function of the relative translational energy of the products, E_f. This is a better function because we can measure or select these quantities in

an experiment. Moreover, the function $d\sigma(E_f,\theta)$ can be used easily in the center of mass $\longrightarrow$ laboratory program.

2. We have used a classical expression for the calculation of spherical harmonics which gives fairly accurate results at large values of ℓ.

We have tried to explore this theory in more detail than White and Light (11), and have developed a computer program to calculate differential cross sections in the center of mass.

The angular distributions obtained from this theory do not agree with the experimental data. This is not due to the changes made in the calculation procedure by us, but due to the assumptions made in the theory itself. One of the limitations of this theory is that it will always predict a center of mass distribution symmetric about $\pi/2$. This is due to the random phase approximation which made the differential cross section directly proportional to $|Y_\ell^m(\theta,\Phi)|^2$ and which will always lead to a symmetric distribution about $\pi/2$. This approximation was made to solve the problems which arise in evaluating the off-diagonal terms in the T-matrix.

Though this theory was not very successful for the prediction of angular distributions, it may be able to predict the energy distribution of products at a given

angle. In order to test this possibility the products must be analyzed with a velocity selector. Further, velocity analyzed data will give insight into the partitioning of total available energy in the products. We have not pursued that aspect in this investigation.

APPENDIX A

CALCULATION OF POLARIZABILITY

There are a number of simple formulas (33) available for the calculation of the polarizability of atoms or ions, but these are restricted to the closed shell structure, e.g., Na^+, He, Ar, K^+, etc., and when applied to the case of $Ba^+(6S^1)$, lead to absurd results. The method used here is based on the concept of a quantum effect. In an electric field F an atom or ion becomes polarized, the center of charge of the electrons being shifted with respect to that of the nucleus. The electric moment of the induced dipole is αF, where α is the polarizability of the atom or ion. The polarization energy is $-\frac{1}{2}\alpha F^2$.

In the Ba atom (------$6S^2$), the valence core (Ba^+) is polarized in the field $-(\frac{e}{r^2})$ of the valence electron. Thus the polarization energy is equal to $-\frac{1}{2}\alpha(-\frac{e}{r^2})^2$, and the energy needed to remove the electron to infinity, W, is given by (34)

$$W = -\frac{z^2e^2}{2a_o(n-\Delta)^2} = -\frac{z^2e^2}{2a_o n^2} - \frac{\alpha e^2}{2}\left(\overline{\frac{1}{r^4}}\right) \qquad (A.1)$$

where Δ is the quantum defect. Rewriting Equation (A.1):

$$W = -\frac{z^2 e^2}{2a_o n^2 (1-\frac{\Delta}{n})^2} = -\frac{z^2 e^2}{2a_o n^2} - \frac{\alpha e^2}{2}\left(\overline{\frac{1}{r^4}}\right)$$

or

$$-\frac{z^2 e^2}{2a_o n^2}(1-\frac{\Delta}{n})^{-2} = -\frac{z^2 e^2}{2a_o n^2} - \frac{\alpha e^2}{2}\left(\overline{\frac{1}{r^4}}\right).$$

As $\frac{\Delta}{n} < 1$, higher powers of $\frac{\Delta}{n}$ in the expansion will be $<< 1$ and can be neglected:

$$-\frac{z^2 e^2}{2a_o n^2}(1+\frac{2\Delta}{n}) = -\frac{z^2 e^2}{2a_o n^2} - \frac{\alpha e^2}{2}\left(\overline{\frac{1}{r^4}}\right),$$

or

$$\Delta = \frac{\alpha a_o n^3}{2\ z^2}\left(\overline{\frac{1}{r^4}}\right). \qquad \text{(A.2)}$$

Since quantum mechanical average

$$\left(\overline{\frac{1}{r^4}}\right)\ \left[\left\langle\frac{1}{r^4}\right\rangle = \int\frac{1}{r^4}\ \Psi\Psi^* d\tau\right]$$

is given by (34, p. 32)

$$\left(\overline{\frac{1}{r^4}}\right) = \frac{\frac{3}{2}\ z^4\left[1-\frac{\ell(\ell+1)}{3n^2}\right]}{a_o^4 n^3\ (\ell+\frac{3}{2})(\ell+1)(\ell+\frac{1}{2})(\ell-\frac{1}{2})\ell}\ . \qquad \text{(A.3)}$$

Substituting this value of $\left(\overline{\frac{1}{r^4}}\right)$ in Equation (A.2) we get

$$\Delta = \frac{3\alpha z^2\ \left[1-\frac{\ell(\ell+1)}{3n^2}\right]}{4\ a_o^3\ (\ell-\frac{1}{2})\ell(\ell+\frac{1}{2})(\ell+1)(\ell+\frac{3}{2})}$$

or

$$\alpha = \frac{4\, a_o^3\, \Delta\ell(\ell-\frac{1}{2})(\ell+\frac{1}{2})(\ell+1)(\ell+\frac{3}{2})}{3\, z^2[1-\frac{\ell(\ell+1)}{3n^2}]} \quad . \qquad (A.4)$$

In order to calculate the polarizability: (a) calculate Δ with Equation (A.1) using known values of W from spectra; (b) the value of Δ calculated from step (a) may be used to calculate α with the help of Equation (A.4) since all other parameters are known.

The only limitation with this method is that one can not calculate for S-electrons (ℓ=0), for which Equation (A.4) gives $\alpha = 0$.

For barium atom (see Table 8), sample calculation for Δ ($6S^2 \rightarrow 6S^1$):

$$W = \frac{z^2e^2}{2a_o(n-\Delta)^2} \quad .$$

In this case, z = 1, e = 4.8×10^{-10}esu, $a_o = 0.528 \times 10^{-8}$cm W = 8.304×10^{-12}ergs, n = 6. Substituting these values in the above equations, we get

$$(n-\Delta)^2 = 2.6274$$

$$n - \Delta = 1.62$$

$$\Delta = 4.38.$$

The quantum defect Δ calculated by this method agrees very well with the values reported in the literature (31, p. 182) as shown in Table 9.

Table 8. Transition Energies for Ba Atom

Initial Configuration	Final Configuration	Energy Required*	W (for a $6S^1$ Configuration) x 10^{12} ergs
$6S^2(^1S)$	$6S^1(^1P_o)$	5.19 ev	8.304
$6S^2$	$6S^16P^1(^1P_o)$	5537.01 A	4.714
$6S^2$	$6S^17P^1(^1P_o)$	3072.47 A	1.839
$6S^2$	$6S^18P^1(^1P_o)$	2786.10 A	1.176

*Ref. (35).

Table 9. Quantum Defect for Ba^+

Configuration	Calculated Δ	n*	$\Delta = (n - n^*)$
6S	4.38	1.615	4.385
6P	3.85	2.139	3.861
7P	3.556	3.402	3.598
8P	3.69	4.67	3.33

The values of polarizability as calculated using Equation (A.4) are given in Table 10. Mean value of α for $Ba^+ = 2.697 \times 10^{-24} cm^3$, which appears to be reasonable as the reported values for the polarizability of the Ba atom and Ba^{++} ion are $34 \times 10^{-24} cm^3$ (36) and $1.7 \times 10^{-24} cm^3$ (37) respectively.

Table 10. Polarizability of Ba^+

Initial Configuration	Final Configuration	Δ	$\alpha \times 10^{24}$
$6s^2$	$6s^1$	4.38	--
$6s^2$	$6s^1 6p^1$	3.85	2.90 cm^3
$6s^2$	$6s^1 7p^1$	3.556	2.65 cm^3
$6s^2$	$6s^1 8p^1$	3.69	2.74 cm^3
		3.33(31, p. 182)	2.467 cm^3

APPENDIX B

LISTING OF THE COMPUTER PROGRAM USED IN THE CALCULATION OF ANGULAR DISTRIBUTION OF PRODUCTS

```
PROGRAM STMOD      73/73   OPT=1                              FTN 4.0+P357

      PROGRAM STMOD (INPUT,OUTPUT,PUNCH)
C    CALCULATION USING STAT MODEL ( A+BC =DE+F )
C      G=MASS,R=INTERATOMIC DISTANCE(A),W=VIB.FREQ.(1/CM)
C      DEL=EXOTHERMICITY(EV),Q=I.P.OR RES.ENERGY(EV)
C      PO=POLARIZABILITY(A3),DIP=DIPOLEMOMENT(D)
       COMMON  /LEG/XEQ(73),WEQ(73)
       COMMON  G1,G2,GP,E1,C1,C2,DELT,W1,W2,W3,W4,R1,R2,AI,AN,GI
       COMMON  FACT,FACT1,FACT2
       COMMON  I1,I2,ET
       DIMENSION  SUMAK(8),SUMBK(8),TH(15)
       DIMENSION   SIGTH2(100),SIGTH1(100)
       REAL  LMXF,LF1,LF2,LF11,LF12
       REAL  I1,I2,JI
       REAL  MB1,MB2
       REAL  JIZ,LA2,LA1,LMXI,JFZ,LIM
       REAL JIZ1,JIZ2
       FACT=1.054E-27
       AI=1.0E-08
       FACT1 =1.9863E-16
       AN=6.02252E+23
       FACT2=1.6E-12
    77 READ 10,GA,GB,GC,GD,GE,GF,R1,R2
       READ 20,W1,W2,W3,W4,E,DEL
       READ 30,QA,QBC,QDE,QF
       READ 40,POA,POBC,PODE,POF,DIPBC,DIPDE
    10 FORMAT(8F10.4)
    20 FORMAT (6F10.4)
    30 FORMAT (4F10.4)
    40 FORMAT (6F10.4)
       E1 =E*FACT2
       EI =23.06*E
       DELT =DEL *FACT2
       G1 =GA*(GC+GB)/(GA+GB+GC)
       G2 =GF*(GD+GE)/(GD+GE+GF)
       GP =GD*GE/(GD+GE)
       GI =GB*GC/(GB+GC)
       I2 =(GP/AN)*(R2*AI)**2
       I1 =(GI/AN)*(R1*AI)**2
       U =0.0
       T1 =0.5*W1-0.25*W2
       EU =(U+0.5)*W1-((U+0.5)**2)*W2-T1
       EU =EU*FACT1
       JI =50.
       ET =E1+EU+JI*(JI+1)*FACT*FACT/(2.0*I1)
       CA=1.5*QA*QBC/(QA+QBC)*FACT2*POA*POBC*AI**6
       CB =POA*(DIPBC)**2*1.0E-60
       C1 =CA+CB
       CA1 =1.5*QF*QDE/(QDE+QF)*FACT2*POF*PODE*AI**6
       CB1 =POF*(DIPDE**2)*1.0E-60
       C2 =CA1+CB1
       TLM1=(6.0*G1/AN*(C1**(1.0/3.0))*(0.5*E1)**(2.0/3.0))
       LMXI=SQRT(TLM1)/(FACT)
       PRINT 1500
 1500 FORMAT(22H    8A+CSI STAT CALC.       )
       PRINT  1501
 1501 FORMAT(XXXXXX3HG1=6X3HG2=6X3HGP=6X3HGI=10X5HLMXI=)
       PRINT 15,G1,G2,GP,GI,LMXI
```

```
      PROGRAM STMOD       73/73   OPT=1                          FTN 4.0+P357

        15 FORMAT(4F10.4,F15.4)
           PRINT 1021
      1021 FORMAT(XXXXXXXXX3HC1=9X3HC2=)
           PRINT 221,C1,C2
       221 FORMAT(2E15.4)
           AK1 =0.0
           AK2 =LMXI+JI
           NEQ =6
           NEQ0 =(NEQ*(NEQ-1))/2
           IF (DELT.NE.0.0)  GO TO  85
           PRINT 1600
      1600 FORMAT(30H  NO REACTION (BA+CSI=BA+CSI)          )
           DO 70   IEQ=1,NEQ
           NEQI =NEQ0+IEQ
           AK =0.5*(AK2-AK1)*XEQ(NEQI)+0.5*(AK2+AK1)
           SUMAK (IEQ)=SUMI1(AK,E2,VX)
        70 CONTINUE
           IF (DELT.EQ.0.0) GO TO  77
        85 NEQ =6
           NEQ0 =(NEQ*(NEQ-1))/2
           PRINT 1601
      1601 FORMAT(27H  REACTION (BA+CSI=BAI+CS)  )
           DO 87  IEQ=1,NEQ
           NEQI =NEQ0+IEQ
           AK =0.5*(AK2-AK1)*XEQ(NEQI)+0.5*(AK2+AK1)
           SUMBK (IEQ)=SUMI1(AK,E2,VX)
        87 CONTINUE
           DATA(SIGTH2(I),I=1,29)/0.0,0.0,0.0,0.0,0.0,0.0,0.0,0.0,0.0,0.0,0.0,0.0,0.0,0.0
          1,0.0,0.0,0.0,0.0,0.0,0.0,0.0,0.0,0.0,0.0,0.0,0.0,0.0,0.0,0.0,0.0,0.0,0.0,0.0,0
          2.0,0.0,0.0,0.0,0.0,0.0,0.0/
           V =0.0
           T2 =0.5*W3-0.25*W4
        18 EV =(V+0.5)*W3-((V+0.5)**2)*W4-T2
           EV =EV*FACT1
           EC =ET-EV+DELT
           PRINT 11,EC
        11 FORMAT (XX3HEC=,E10.4)
           IJ =1
           E2 =0.025
           E2 =E2*FACT2
        16 ETT=(ET-E2-EV+DELT  )*2.0*I2/(FACT*FACT)
           IF (ETT.LE.0.0) GO TO 443
           JF =(-1.0+SQRT(1.0+4.0*ETT))*0.5
           IF(JF.EQ.0)  JF=1
           TLM2 =(6.0*G2/AN*(C2**(1.0/3.0))*(0.5*E2)**(2.0/3.0))
           LMXF =SQRT(TLM2)/FACT
           PI =3.14159
           TH1 = 80.0
           THETA =3.14159/180.0*TH1
           Z =COS(THETA)
           SUM =0.0
           NEQ =6
           NEQ0 =(NEQ*(NEQ-1))/2
           DO 80   JEQ=1,NEQ
           NEQJ =NEQ0+JEQ
           AK =0.5*(AK2-AK1)*XEQ(NEQJ)+0.5*(AK2+AK1)
           JIZ1 =-JI
```

```
      PROGRAM STMOD      73/73   OPT=1                              FTN 4.0+P357

115               JIZ2 =JI
                  SIGJZ =0.0
                  NIQ =6
                  NIQ0 =(NIQ*(NIQ-1))/2
                  DO  44 JIQ =1,NIQ
120               JIQJ =NIQ0+JIQ
                  JIZ =0.5*(JIZ2-JIZ1)*XEQ(JIQJ)+0.5*(JIZ2+JIZ1)
                  IF(JI.EQ.0.0) JIZ=0.0
                  AMB2 =(AK+JF)*SQRT(1.0-Z*Z)
                  IF(AMB2.GT.(JIZ+JF)) AMB2 =JIZ+JF
125               AMB1 =JIZ-JF
                  IF(ABS(JIZ-JF).GT.((AK+JF)*SQRT(1.-Z*Z)))AMB1=-(AK+JF)*
                 1SQRT(1.-Z*Z)
                  IF((JIZ-JF).GT.0.0) AMB1 =JIZ-JF
                  JQ =6
130               JQ0 =(JQ*(JQ-1))/2
                  SIGMB =0.0
                  DO  81  KQ=1,JQ
                  JQJ =JQ0+KQ
                  AMB =0.5*(AMB2-AMB1)*XEQ(JQJ)+0.5*(AMB2+AMB1)
135               AMB =ABS(AMB)
                  LF11 =AMB/SQRT(1.0-Z*Z)
                  IF(JF.EQ.0) GO TO 46
                  LF12 =ABS(AK-JF)
                  LF1 =LF11
140               IF(LF11.LT.LF12)  LF1 =LF12
                  LF2 =LMXF
                  IF(LMXF.GT.(AK+JF)) LF2=AK+JF
                  IF(LF2.LT.LF1)  GO TO 49
                  NCQ =6
145               NCQ0 =(NCQ*(NCQ-1))/2
                  SIGLB =0.0
                  DO  43  KCQ =1,NCQ
                  NCQK =NCQ0+KCQ
                  ALB =0.5*(LF2-LF1)*XEQ(NCQK)+0.5*(LF2+LF1)
150               YLM =1.0/(2.0*PI*PI*SQRT(1.0-(AMB/ALB)**2-Z*Z))
               43 SIGLB =SIGLB+YLM*WEQ(NCQK)
                  SIGLB =SIGLB*(LF2-LF1)/2.0
               49 IF(LF2.LT.LF1) SIGLB=0.0
                  SIGMB =SIGMB+SIGLB*WEQ(JQJ)
155            81 CONTINUE
                  IF(AMB1.GT.AMB2)  SIGMB=0.0
                  SIGMB =SIGMB*(AMB2-AMB1)/2.0
               47 LAQ =6
                  LA1 =ABS(AK-JI)
160               LA2 =LMXI
                  IF(LMXI.GT.(AK+JI)) LA2=AK+JI
                  SUMLA =0.0
                  LAQ0 =(LAQ*(LAQ-1))/2
                  DO 86 LQ=1,LAQ
165               LAQK =LAQ0+LQ
                  ALI =0.5*(LA2-LA1)*XEQ(LAQK)+0.5*(LA2+LA1)
                  LIM =ABS(ALI-JI)
                  JIZ =ABS(JIZ)
                  IF(JIZ.GT.LIM) LIM=JIZ
170               SMLA =(2.0*ALI+1.0)/(ALI+JI-LIM+1.)
               86 SUMLA =SUMLA+SMLA*WEQ(LAQK)
```

```
      PROGRAM STMOD      73/73   OPT=1                              FTN 4.0+P357

                  SUMLA =SUMLA*(LA2-LA1)/2.0
                  IF(JI.EQ.0.0) SUMLA =2.0*AK+1.0
                  SIGMB =SIGMB*SUMLA
175            44 SIGJZ =SIGJZ+SIGMB*WEQ(JIQJ)
                  SIGJZ =SIGJZ*(JIZ2-JIZ1)/2.0
                  SIGJZ =SIGJZ/(SUMAK(JEQ)+SUMBK(JEQ))
               80 SUM =SUM+SIGJZ*WEQ(NEQJ)
                  SIGTH =SUM*(AK2-AK1)/2.0
180               CONT =FACT*FACT/(8.0*G1*E1)*AN
                  SIGTH =CONT*SIGTH/(2.0*JI+1.0)
                  AJAC =2.0*I2/(FACT*FACT*(2.0*JF+1))
                  SIGTH =SIGTH*AJAC *4.0*PI
                  IF(V.EQ.0.0)  GO  TO  45
185               IF(V.EQ.1.0)  GO  TO  45
                  IF(V.EQ.5.0)  GO  TO  45
                  IF(V.EQ.8.0)  GO  TO  45
                  IF(V.EQ.15.0) GO  TO  45
               48 SIGTH1(IJ) =SIGTH
190               II =IJ
                  SIGTH2(II) =SIGTH1(IJ)+SIGTH2(II)
                  IJ =IJ+1
                  E2 =E2+0.025*FACT2
                  IF(E2.GT.EC)  GO  TO  17
195               GO TO 16
               17 V =V+1.0
                  PRINT 42,(SIGTH2(I),I=1,29)
               42 FORMAT(6E12.5)
                  GO TO  18
200            45 PRINT 1042,SIGTH,TH1,V,JF,JI,U,E2
             1042 FORMAT(XXXX6HSIGTH=,E12.5,5X4HTH1=,F5.1,6X2HV=,F4.1,5X3HJF=,
                 1I5,5X3HJI=,F4.1,5X2HU=,F5.1,4X3HE2=,E10.4)
                  GO  TO  48
               46 ALB =AK
205               AMB =JIZ
                  LF11 =AMB/SQRT(1.0-Z*Z)
                  IF(ALB.LT.LF11)  GO TO 149
                  YLM =1.0/(2.0*PI*PI*SQRT(1.0-(AMB/ALB)**2-Z*Z))
                  SIGLB =YLM
210               SIGMB =SIGLB
                  GO TO  47
              149 SIGLB =0.0
                  SIGMB =SIGLB
                  GO TO  47
215           443 PRINT 444 ,(SIGTH2(II) , II=1,29 )
              444 FORMAT(E15.4)
                  PUNCH 445, (SIGTH2(II), II=1,29)
              445 FORMAT ( E10.4)
                  END
```

```
FUNCTION SUMT1      73/73   OPT=1                                FTN 4.0+P357

                    FUNCTION   SUMT1(AK,E2,VX)
                    COMMON  /LEG/XEQ(78),WEQ(78)
                    COMMON  G1,G2,GP,E1,C1,C2,DELT,W1,W2,W3,W4,R1,R2,AI,AN,GI
                    COMMON  FACT,FACT1,FACT2
 5                  COMMON  I1,I2,ET
                    REAL  LO,JO,I2
                    TLO =SQRT(6.0*G2/AN)*(C2**(1.0/6.0))*(0.5)**(1.0/3.0)
                    TLL =TLO/FACT
                    AON =(TLL*TLL*TLL)
10                  TJO =SQRT(2.0*I2)
                    TJJ =TJO/FACT
                    ANR =(TJJ*TJJ)
                    AX =1.5*ANR/AON
                    ALX =(-1.0+SQRT(1.0+4.0*AX*AK))/(2.0*AX)
15                  AJX =AK-ALX
                    EX =(ALX*ALX*ALX)/AON+(AJX*AJX)/ANR
                    ERF =0.0
                    ET1 =ERF-ET-DELT+EX
                    A =W4*FACT1
20                  B =(W4-W3)*FACT1
                    C =-ET1
                    X1 =SQRT(B*B-4.0*A*C)
                    VX =(-B-X1)/(2.0*A)
                    PRINT 1030
25            1030  FORMAT(XXXXX3HVX=10X3HAK=)
                    PRINT  82,VX,AK
                82  FORMAT(F10.4,F15.4)
                    NEQ =6
                    NEQ0 =(NEQ*(NEQ-1))/2
30                  IF (VX.LE.NEQ) GO TO  511
                    VM =VX
                    V1 =-0.5
                    SUMT1 =0.0
                    DO 83   KEQ=1,NEQ
35                  NEQK =NEQ0+KEQ
                    V =0.5*(VM-V1)*XEQ(NEQK)+0.5*(VM+V1)
                    T2 =0.5*W3-0.25*W4
                    EV =(V+0.5)*W3-((V+0.5)**2)*W4-T2
                    EV =EV*FACT1
40                  E2 =ET+DELT-EV
                    LO =SQRT(6.0*G2/AN)*(C2**(1.0/6.0))*(0.5*E2)**(1.0/3.0)
                    ALO=LO/FACT
                    JO =SQRT(2.0*I2*E2)
                    AJO =JO/FACT
45                  PRINT  1011
              1011  FORMAT(XX4HALO=11X4HAJO=11X3HAK=10X2HV=)
                    PRINT 125,ALO,AJO,AK,V
               125  FORMAT(3F15.4,F10.4)
                    AAL2 =AL2(ALO,AJO,AK)
50                  AAL1=AL1(ALO,AJO,AK)
                    SUM =0.0
                    DO 220  IEQ =1,NEQ
                    NEQI =NEQ0+IEQ
                    AL =0.5*(AAL2-AAL1)*XEQ(NEQI)+0.5*(AAL2+AAL1)
55                  AAJ =AJ(AL,ALO,AJO,AK)
               220  SUM =SUM+AAJ*WEQ(NEQI)
                    SUM =-SUM*(AAL2-AAL1)/2.0
```

```
      FUNCTION SUMT1       73/73   OPT=1                              FTN 4.0+P357

                      PRINT  1012
                 1012 FORMAT (XX5HAAL1=10X5HAAL2=10X4HSUM=)
   60                 PRINT 115,AAL1,AAL2,SUM
                  115 FORMAT(2F15.4,E15.6)
                   83 SUMT1 =SUMT1+SUM*WEQ(NEQK)
                      SUMT1=SUMT1*(VM-V1)/2.0
                      PRINT  1014
   65                 1014 FORMAT(XXX6HSUMT1=)
                      PRINT  121,SUMT1
                  121 FORMAT(E15.6)
                      RETURN
                  511 V =0.0
   70                 SUMT1 =0.0
                      T2 =0.5*W3-0.25*W4
                   51 EV =(V+0.5)*W3-((V+0.5)**2)*W4-T2
                      EV =EV*FACT1
                      E2 =ET+DELT-EV
   75                 IF(E2.LE.0.0)  RETURN
                      LO =SQRT(6.0*G2/AN)*(C2**(1.0/6.0))*(0.5*E2)**(1.0/3.0)
                      ALO=LO/FACT
                      JO =SQRT(2.0*I2*E2)
                      AJO=JO/FACT
   80                 AAL2 =AL2(ALO,AJO,AK)
                      AAL1=AL1(ALO,AJO,AK)
                      SUM =0.0
                      DO 330  IEQ =1,NEQ
                      NEQI =NEQ0+IEQ
   85                 AL =0.5*(AAL2-AAL1)*XEQ(NEQI)+0.5*(AAL2+AAL1)
                      AAJ =AJ(AL,ALO,AJO,AK)
                  330 SUM =SUM+AAJ*WEQ(NEQI)
                      SUM=-SUM*(AAL2-AAL1)/2.0
                      PRINT  2011
   90                 2011 FORMAT(XX4HALO=11X4HAJO=11X3HAK=18X2HV=)
                      PRINT 325,ALO,AJO,AK,V
                  325 FORMAT(3F15.4,F10.4)
                      PRINT  2012
                 2012 FORMAT (XX5HAAL1=10X5HAAL2=10X4HSUM=)
   95                 PRINT 315,AAL1,AAL2,SUM
                  315 FORMAT(2F15.4,E15.6)
                      SUMT1 =SUMT1+SUM
                      PRINT  2014
                 2014 FORMAT(XXX6HSUMT1=)
  100                 PRINT  321,SUMT1
                  321 FORMAT(E15.6)
                      V =V+1.0
                      IF (V.GT.VX)  RETURN
                      GO TO 51
  105                 END
```

```
FUNCTION AJ          73/73   OPT=1                          FTN 4.0+P357

                FUNCTION   AJ(AL,ALO,AJO,AK)
                A =1.0/(ALO*ALO*ALO)
                B =1.0/(AJO*AJO)
                A1 =3.0*AL*AL-2.8284*B*AL/A+4.2426*AL*AK+2.0*B*AK/A+
 5             11.5*AK*AK
                A2 =3.0*AL+3.0*AK/1.4142+1.4142*B/A
                AO =AL*AL*AL+(3.0*AK/1.4142+1.4142*B/A)*AL*AL+(1.5*AK*AK-2.0
               1*B*AK/A)*AL+(AK*AK*AK/2.8284+B*AK*AK/(1.4142*A)-2.8284/A)
                R =(A1*A2-3.0*AO)/6.0-A2*A2*A2/27.0
10              Q =A1/3.0-A2*A2/9.0
                T =Q*Q*Q+R*R
                IF(T.GT.0.0) GO TO 101
                T1 = SQRT(-T)
                D =SQRT(R*R+T1*T1)
15              THETA =ACOS(R/D)
                Z1 =2.0*D**(1.0/3.0)*COS(THETA/3.0)-A2/3.0
                AJ =Z1
                RETURN
              101 T1 =SQRT(T)
20              S1 = (R+T1)**(1.0/3.0)
                IF(R.LT.T1)  GO TO  30
                S2 = (R-T1)**(1.0/3.0)
               31 Z1 =(S1+S2)-A2/3.0
                AJ =Z1
25              RETURN
               30 S2 = -(T1-R)**(1.0/3.0)
                GO TO 31
                END
```

```
FUNCTION AL1        73/73   OPT=1                                FTN 4.0+P357

                    FUNCTION  AL1(ALO,AJO,AK)
                    IF (AK.LE.ALO) GO TO 25
                    A =1.0/(ALO*ALO*ALO)
                    B =1.0/(AJO*AJO)
 5                  A1 =1.5*AK*AK-2.0*B*AK/A
                    A2 =3.0*AK/1.4142+1.4142*B/A
                    A0 =AK*AK*AK/2.8284+B*AK*AK/(1.4142*A)-2.8284/A
                    R =(A1*A2-3.0*A0)/6.0-A2*A2*A2/27.0
                    Q =A1/3.0-A2*A2/9.0
10                  T =Q*Q*Q+R*R
                    T1 =SQRT(-T)
                    D =SQRT(R*R+T1*T1)
                    THETA =ACOS(R/D)
                    Z1 =2.0*D**(1.0/3.0)*COS(THETA/3.0)-A2/3.0
15                  GO TO 55
                 25 Z1 =AK/1.4142
                 55 AL1 =Z1
                    RETURN
                    END
```

```
FUNCTION AL2        73/73   OPT=1                                FTN 4.0+P357

                    FUNCTION  AL2(ALO,AJO,AK)
                    IF (AK.LE.AJO) GO TO 45
                    A =1.0/(ALO*ALO*ALO)
                    B =1.0/(AJO*AJO)
 5                  A1 =1.5*AK*AK-2.0*B*AK/A
                    A2 =3.0*AK/1.4142+1.4142*B/A
                    AO =AK*AK*AK/2.8284+B*AK*AK/(1.4142*A)-2.8284/A
                    R =(A1*A2-3.0*AO)/6.0-A2*A2*A2/27.0
                    Q =A1/3.0-A2*A2/9.0
10                  T =Q*Q*Q+R*R
                    T1 =SQRT(-T)
                    D =SQRT(R*R+T1*T1)
                    THETA =ACOS(R/D)
                    Z3 =-D**(1.0/3.0)*COS(THETA/3.0)-A2/3.0+1.732*SIN(THETA/
15                 13.0)*D**(1.0/3.0)
                    GO TO 65
                 45 Z3 =-AK/1.4142
                 65 AL2 =Z3
                    RETURN
20                  END
```

```
BLOCK DATA LEG        73/73   OPT=1                          FTN 4.0+P357

                      BLOCK DATA LEG
                      COMMON /LEG/X,W
                      DIMENSION X(78),W(78)
                      DATA (X(I),I=1,1)/0.0/
 5                    DATA (W(I),I=1,1)/2.0/
                      DATA (X(I),I=2,3)/-0.57735026918963,0.57735026918963/
                      DATA (W(I),I=2,3)/1.0,1.0/
                      DATA (X(I),I=4,6)/-0.77459666924148,0.0,0.77459666924148/
                      DATA (W(I),I=4,6)/0.55555555555556,0.88888888888889,
10                   1 0.55555555555556/
                      DATA (X(I),I=7,10)/-0.86113631159405,-0.33998104358486,
                     1 0.33998104358486,0.86113631159405/
                      DATA (W(I),I=7,10)/0.34785484513745,0.65214515486255,
                     1 0.65214515486255,0.34785484513745/
15                    DATA (X(I),I=11,15)/-0.90617984593866,-0.53846931010568,0.0,
                     1 0.53846931010568,0.90617984593866/
                      DATA (W(I),I=11,15)/0.23692688505619,0.47862867049937,
                     1 0.56888888888889,0.47862867049937,0.23692688505619/
                      DATA (X(I),I=16,21)/-0.93246951420315,-0.66120938646626,
20                   1 -0.23861918608320,0.23861918608320,0.66120938646626,
                     2 0.93246951420315/
                      DATA (W(I),I=16,21)/0.17132449237917,0.36076157304814,
                     1 0.46791393457269,0.46791393457269,0.36076157304814,
                     2 0.17132449237917/
25                    DATA (X(I),I=22,28)/-0.94910791234276,-0.74153118559939,
                     1 -0.40584515137740,0.0,0.40584515137740,0.74153118559939,
                     2 0.94910791234276/
                      DATA (W(I),I=22,28)/0.12948496616887,0.27970539148928,
                     1 0.38183005050512,0.41795918367347,0.38183005050512,
30                   2 0.27970539148928,0.12948496616887/
                      DATA (X(I),I=29,36)/-0.96028985649754,-0.79666647741363,
                     1 -0.52553240991633,-0.18343464249565,0.18343464249565,
                     2 0.52553240991633,0.79666647741363,0.96028985649754/
                      DATA (W(I),I=29,36)/0.10122853629038,0.22238103445337,
35                   1 0.31370664587789,0.36268378337836,0.36268378337836,
                     2 0.31370664587789,0.22238103445337,0.10122853629038/
                      END
```

```
PROGRAM CMLAB      73/73   OPT=1                              FTN 4.0+P357

      PROGRAM CMLAB (INPUT,OUTPUT)
C     ANGLES  ARE  IN  DEGREES.
C     UNITS OF VELOCITY ARE 10**4 CM/SEC
C     UNITS  OF ENERGY  ARE  KCAL/MOLE
C     CM-LAB   TRANSFORMATION
      DIMENSION P(400),THL(100)
      DIMENSION FABG(400),CX(400),CY(400),E(400),COSTV(400)
      DIMENSION SINTV(400)
      DIMENSION VAPAR(5),VBPAR(5),UPAR(5),THPAR(6)
      COMMON  XEP(31),XTH(4),XCS(31,4)
      Y=.017453292
      R=0.0019872
  100 READ 1000
      READ 1001,IPUNCH
      READ 1001,NVA,NVB,NGAM,GA,GB,GAMMA,HWIDB
      IF((NVA.EQ.0).AND.(NVB.EQ.0).AND.(NGAM.EQ.0)) CALL EXIT
      G=GA+GB
      NGRID=NVA*NVB*NGAM
      READ 1002,(VAPAR(I),I=1,5)
      READ 1002,(VBPAR(I),I=1,5)
      CALL CNEWT(NVA,NVB,VAPAR,VBPAR,GA,GB,NGAM,GAMMA,HWIDB,
     1FABG,CX,CY,E,COSTV,SINTV)
      READ 1001,NTHL,NPHIL,NV,GC,DELTDO,XXV,T
      RT=R*T
      EPFACT =SQRT(G*GC/(G-GC))*4.8E-19
      GPFAC =0.00119503*G*GC/(G-GC)
      READ 1003,(THL(I),I=1,NTHL)
      PRINT 1000
      PRINT 1020
      PRINT 1001,NVA,NVB,NGAM,GA,GB,GAMMA,HWIDB
      PRINT 1012,(VAPAR(I),I=1,5)
      PRINT 1022,(VBPAR(I),I=1,5)
      PRINT 1021
      PRINT 1001,NTHL,NPHIL,NV,GC,DELTDO,XXV,T
 1000 FORMAT(55H
     1)
 1001 FORMAT(3I5,5X,5F10.4)
 1002 FORMAT(8F10.5)
 1003 FORMAT(16F5.0)
 1012 FORMAT( 5H0VAPAR,5F10.5)
 1022 FORMAT(6H VBPAR,5F10.5)
 1020 FORMAT( 5H0 NVA2X3HNVB1X4HNGAM9X2HGA5X2HGB7X5HGAMMA5X5HHWIDB
 1021 FORMAT(5H0NTHL1X5HNPHIL2X2HNV9X2HGC6X6HDELTD07X3HXXV7X1HT)
      CALL  INN
      DO 30 ITHL=1,NTHL
      TL=THL(ITHL)*Y
      CT=COS(TL)
      ST=SIN(TL)
      FLX=0.
      DO 20 IV=1,NV
      VL=FLOAT(IV)*XXV
      VX=VL*CT
      VY=VL*ST
      F=0.0
      DO 10 IJK=1,NGRID
      UX=VX-CX(IJK)
      UY=VY-CY(IJK)
```

```
      PROGRAM CMLAB      73/73   OPT=1                          FTN 4.0+P357

                  U=SQRT(UX*UX+UY*UY)
                  THCM=ATAN2(ABS(UX*SINTV(IJK)+UY*COSTV(IJK)),
60                1 UX*COSTV(IJK)-UY*SINTV(IJK))/Y
                  EP =GPFAC*U**2
                10 F=F+FABG(IJK)*(VL/U)**2*CS(E(IJK),EP,THCM)*EPFACT*SQRT(EP)
                  FLX=FLX+F*XXV
                20 P(IV)=F
65                PRINT 1010,THL(ITHL),FLX
              1010 FORMAT(5H THL=,F6.1,+X5HFLUX=,1PE11.4)
                  PRINT 1011,(P(I),I=1,NV)
              1011 FORMAT(XX8E10.3)
                  IF(IPUNCH.EQ.0) GO TO 30
70                PRINT 1010,THL(ITHL),FLX
                  PRINT 1011,(P(J),J=1,NV)
                30 CONTINUE
                  GO TO 100
                  END
```

```
SUBROUTINE CNEWT      73/73   OPT=1                                FTN 4.0+P357

                      SUBROUTINE CNEWT(NVA,NVB,VAPAR,VBPAR,GA,GB,NGAM,GAMMA ,
                     1HWIDB,FABG,CX,CY,E,COSTV,SINTV)
                      DIMENSION FABG(400),CX(400),CY(400),E(400),COSTV(400)
                      DIMENSION SINTV(400)
 5                    DIMENSION VA(10),VB(10),FA(10),FB(10),GAM(3),FG(3)
                      DIMENSION VAPAR(5),VBPAR(5)
                      Y=.017453292
                      G=GA+GB
                      GFAC=.00119503*GA*GB/G
10                    NH=NGAM/2+1
                      FNH=NH
                      DO 1 K=1,NGAM
                      GAM(K)=GAMMA+FLOAT(K-NH)*HWIDB/FNH
                      FG(K)=1.0
15                  1 IF(HWIDB.NE.0.0) FG(K)=1.0-ABS(GAM(K)-GAMMA)/HWIDB
                      FNH=(NVA+1)/2
                      DO 2 I=1,NVA
                      VA(I)=VAPAR(1)*FLOAT(I)/FNH
                    2 FA(I)=UDIST(VA(I),VAPAR)
20                    FNH=(NVB+1)/2
                      DO 3 J=1,NVB
                      VB(J)=VBPAR(1)*FLOAT(J)/FNH
                    3 FB(J)=UDIST(VB(J),VBPAR)
                      SUM=0.0
25                    IJK=0
                      DO 4 K=1,NGAM
                      GMK=GAM(K)*Y
                      CG=COS(GMK)
                      SG=SIN(GMK)
30                    FGK=FG(K)
                      DO 4 I=1,NVA
                      V1=VA(I)
                      FAI=FA(I)
                      DO 4 J=1,NVB
35                    V2=VB(J)
                      IJK=IJK+1
                      V=SQRT(V1**2+V2**2-2.*V1*V2*CG)
                      E(IJK)=GFAC*V**2
                      FABG(IJK)=V*FAI*FB(J)*FGK
40                    CX(IJK)=(GA*V1+GB*V2*CG)/G
                      CY(IJK)=GB*V2*SG/G
                      COSTV(IJK)=(V1**2+V**2-V2**2)/(2.*V1*V)
                      SINTV(IJK)=V2/V*SG
                    4 SUM=SUM+FABG(IJK)
45                    NGRID=NVA*NVB*NGAM
                      DO 5 IJK=1,NGRID
                    5 FABG(IJK)=FABG(IJK)/SUM
                      RETURN
                      END
```

```
    FUNCTION UDIST      73/73   OPT=1                          FTN 4.0+P357

                      FUNCTION UDIST(U,PAR)
                      DIMENSION PAR(5)
                      R=U/PAR(1)
                      IF(R.GT.1.0) GO TO 10
 5                    A=PAR(2)
                      B=PAR(3)
                   20 UDIST=R**A*EXP((1.0-R**B)*A/B)
                      RETURN
                   10 A=PAR(4)
10                    B=PAR(5)
                      GO TO 20
                      END
```

```
FUNCTION CS          73/73   OPT=1                              FTN 4.0+P357

                    FUNCTION   CS(E,EP,THCM)
                    COMMON  XEP(31),XTH(4),XCS(31,4)
                    TH =THCM
                    E2 =EP/23.060
 5                  IF(TH.GT.90.0) TH=(180.0-TH)
                    DO 10    I =2,16
                    IEP =I
                    IF(E2.LT.XEP(I))  GO  TO  12
                 10 CONTINUE
10                  CS =0.0
                    RETURN
                 12 DO  20  J=2,4
                    JTH =J
                    IF(TH.LT.XTH(J))  GO TO 22
15               20 CONTINUE
                 22 CONTINUE
                    NT2 =JTH
                    NT1 =JTH-1
                    NE2 =IEP
20                  NE1 =IEP-1
                    CS =0.0
                    CS =CS+XCS(NE1,NT1)*(XEP(NE2)-E2)*(XTH(NT2)-TH)/((XEP(NE2)
                   1-XEP(NE1))*(XTH(NT2)-XTH(NT1)))
                    CS =CS+XCS(NE1,NT2)*(XEP(NE2)-E2)*(XTH(NT1)-TH)/((XEP(NE2)
25                 1-XEP(NE1))*(XTH(NT1)-XTH(NT2)))
                    CS =CS+XCS(NE2,NT1)*(XEP(NE1)-E2)*(XTH(NT2)-TH)/((XEP(NE1)
                   1-XEP(NE2))*(XTH(NT2)-XTH(NT1)))
                    CS =CS+XCS(NE2,NT2)*(XEP(NE1)-E2)*(XTH(NT1)-TH)/((XEP(NE1)
                   1-XEP(NE2))*(XTH(NT1)-XTH(NT2)))
30                  RETURN
                    END
```

```
SUBROUTINE INN        73/73   OPT=1                          FTN 4.0+P357

                      SUBROUTINE   INN
                      COMMON  XEP(31),XTH(4),XCS(31,4)
                      READ 1001, ((XCS(I,J),I=1,16),J=1,4)
                 1001 FORMAT(E10.4)
 5                    DO  20  I = 1,15
                      XEP(I) =(I-1)*0.025
                   20 CONTINUE
                      XEP(16) = 0.372
                      DO 15 J=1,4
10                    XCS(1,J)=0.0
                   15 XCS(16,J) =0.0
                      XEP(1)= 0.0
                      XTH(1) =10.0
                      XTH(2)=30.0
15                    XTH(3) =45.0
                      XTH(4) =80.0
                      RETURN
                      END
```

REFERENCES

1. Datz, S., and E. H. Taylor, J. Chem. Phys. 39, 1896 (1963).

2. Polanyi, M., Atomic reactions (Williams and Norgate, London, 1932).

3. Polanyi, J. C., Appl. Opt. Suppl. 2, 81 (1965).

4. Evans, M. G., and M. Polanyi, Trans. Faraday Soc. 35, 178 (1939).

5. Struve, W. S., T. Kitagawa, and D. R. Herschbach, J. Chem. Phys. 54, 2759 (1971).

6. Kassel, L. S., The Kinetics of Homogeneous Gas Reactions (The Chemical Catalog Co., New York, 1932), p. 36.

7. Herschbach, D. R., Advances in Chemical Physics 10, 319 (1966).

8. Fisk, G. A., J. D. McDonald, and D. R. Herschbach, Disc. Faraday Soc. 44, 228 (1967).

9. Kwei, G. H., A. B. Lees, and J. A. Silver, J. Chem. Phys. 55, 456 (1971).

10. Pechukas, P., J. C. Light, and C. Rankin, J. Chem. Phys. 44, 794 (1966).

11. White, R. A., and J. C. Light, J. Chem. Phys. 55, 379 (1971).

12. Touw, T. R., and J. W. Trishka, J. Appl. Phys. 34, 3635 (1963).

13. Entemann, E. A., Ph.D. Thesis, Harvard University, 1967.

14. Morse, F. A., and R. B. Bernstein, J. Chem. Phys. 37, 2019 (1962).

15. Warnock, T. T., and R. B. Bernstein, J. Chem. Phys. 49, 1878 (1968).

16. Siska, P. E., Ph.D. Thesis, Harvard University, 1969.

17. Miller, W. B., S. A. Saffron, and D. R. Herschbach, Disc. Faraday Soc. 44, 108 (1967).

18. Herschbach, D. R., Disc. Faraday Soc. 33, 149 (1962).

19. Miller, W. H., J. Chem. Phys. 52, 543 (1969).

20. Landau, L., and E. M. Lifshitz, Quantum Mechanics (Addison-Wesley Publishing Company, Inc., Reading, Massachusetts, 1958), p. 118.

21. Hirschfelder, J. O., C. F. Curtiss, and R. B. Bird, Molecular Theory of Gases and Liquids (John Wiley and Sons, Inc., New York, 1954), p. 963.

22. Maltz, Charles, Chemical Physics Letters 9, 707 (1969).

23. Herschbach, D. R., and V. W. Laurie, Tables of Vibrational Force Constants, University of California, UCRL-9694, July 1961, p. III-3.

24. Herzberg, G. Spectra of Diatomic Molecules (D. Van Nostrand Company, Inc., New York, 1950, 2nd ed.), p. 544.

25. Handbook of Mathematical Functions, Ed. M. Abramowitz and I. A. Stegun, NBS Applied Mathematics Series, December 1965, p. 887.

26. Davydov, A. S., Quantum Mechanics (NEO Press, Ann Arbor, Michigan, n.d.), p. 422.

27. Newton, R. G., Scattering Theory of Waves and Particles (McGraw-Hill, New York, 1966), p. 30.

28. Brusaard, P. J., and H. A. Tolhoek, Physica XXIII, 955 (1957).

29. Hall, W. D., and J. C. Zorn, Bull. Am. Phys. Soc. 12, 131 (1967).

30. Sternheimer, R. M., Phys. Rev. 183(1), 192 (1969).

31. Kuhn, H. G., Atomic Spectra (Longmans, Second ed., 1969), p. 157.

32. Krasnov, K. S., and N. V. Karaseva, Opt. and Spec. 19(1), 14 (1965).

33. Heinrichs, J., J. Chem. Phys. 52, 6316 (1970).

34. Pauling, L., and S. Goudsmit, The Structure of Line Spectra (McGraw-Hill, New York, 1930), p. 45.

35. Friedrich, H., and E. Trefftz, J. Quant. Spec. and Rad. Trans. 9, 333 (1969).

36. Shabanova, L. N., Opt. and Spec. 27, 205 (1969).

37. Dalgarno, A., Adnan. Phys. 11, 281 (1962).